



Published in final edited form as:

J Med Chem. 2023 February 09; 66(3): 1809–1834. doi:10.1021/acs.jmedchem.2c01624.

Dopamine D₃/D₂ Receptor Ligands Based on Cariprazine for the Treatment of Psychostimulant Use Disorders that May be Dual Diagnosed with Affective Disorders

Emma S. Gogarnoiu^{†,¶}, Caleb D. Vogt^{†,¶}, Julie Sanchez^{‡,§,¶}, Alessandro Bonifazi[†], Elizabeth Saab[†], Anver Basha Shaik[†], Omar Soler-Cedeño[†], Guo-Hua Bi[†], Benjamin Klein[†], Zheng-Xiong Xi[†], J. Robert Lane^{‡,§}, Amy Hauck Newman^{†,*}

[†]Medicinal Chemistry Section, Molecular Targets and Medications Discovery Branch, National Institute on Drug Abuse – Intramural Research Program, National Institutes of Health, 333 Cassell Drive, Baltimore, Maryland 21224, United States

[‡]Division of Physiology, Pharmacology and Neuroscience, School of Life Sciences, Queen's Medical Centre, University of Nottingham, Nottingham NG7 2UH, United Kingdom

[§]Centre of Membrane Protein and Receptors, Universities of Birmingham and Nottingham, Midlands NG2 7AG, United Kingdom

Abstract

Highly selective dopamine D₃ receptor (D₃R) partial agonists/antagonists have been developed for the treatment of psychostimulant use disorders (PSUD). However, none have reached the clinic due to insufficient potency/efficacy or potential cardiotoxicity. Cariprazine, an FDA approved drug for the treatment of schizophrenia and bipolar disorder, is a high affinity D₃R partial agonist ($K_i = 0.22$ nM) with 3.6-fold selectivity over the homologous dopamine D₂ receptor (D₂R). We hypothesized that compounds that are moderately D₃R/D₂R selective partial agonists/antagonists, may be effective for treatment of PSUD. By systematically modifying the parent molecule, we discovered partial agonists/antagonists, as measured in BRET-based assays, with high D₃R affinities ($K_i = 0.14$ –50 nM) and moderate selectivity (<100-fold) over D₂R. Cariprazine and two lead analogues, **13a** and **13e**, decreased cocaine self-administration (FR2; 1–10 mg/kg, i.p.) in rats, suggesting that partial agonists/antagonists with modest D₃R/D₂R-selectivity may be effective in treating PSUD and potentially comorbidities with other affective disorders.

Graphical Abstract

*Corresponding Authors: Amy Hauck Newman: anewman@intra.nida.nih.gov.

[¶]Equal contributors

Authors Contributions

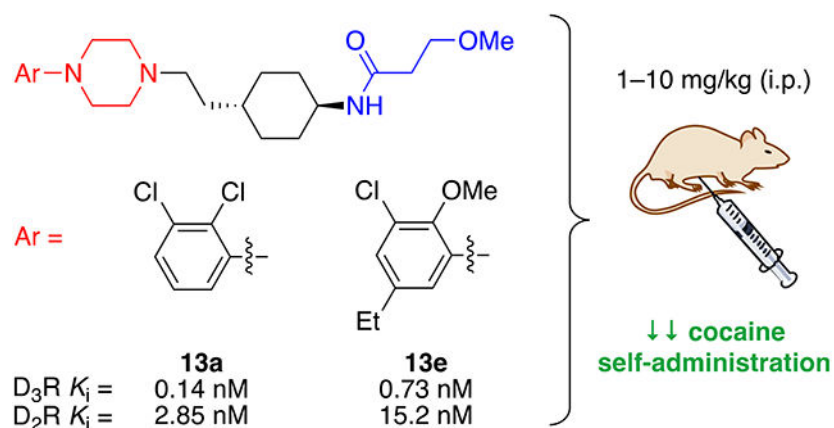
A.H.N., E.S.G., and C.D.V. wrote the manuscript with input of all the authors; A.B., A.B.S., Z.-X.X., J.R.L., and A.H.N. designed and supervised the experiments and data analysis; E.S.G., C.D.V., and A.B.S. synthesized and characterized compounds; A.B. and E.S. determined binding affinities; J.S. performed the functional assays; O.S.-C., G.-H.B. and B.K. performed the behavioral studies.

The Supporting Information is available free of charge on the ACS Publications website.

Supplementary Tables and representative HPLC traces (pdf)

SMILES strings (excel)

The authors declare no competing financial interest.



Keywords

Dopamine D₃ receptors; Dopamine D₂ receptors; bitopic ligands; substance use disorders; psychostimulant use disorder; cocaine; affective disorders; schizophrenia; bipolar disorder; cariprazine; self-administration; reward

INTRODUCTION

In the midst of the COVID-19 pandemic, drug overdose fatalities soared to >100,000 in 2021.¹ While opioids are involved with a majority of these deaths, polysubstance use is another contributing factor, leading to increases in morbidity that poses further challenges for prevention and treatment.² To further complicate matters, substance use disorders (SUDs) frequently occur with affective disorders, including anxiety, major depressive disorder, and bipolar disorder. Such dual disorders have also increased during the COVID-19 pandemic^{3–5} and are particularly difficult to treat when comorbid with psychostimulant use disorder (PSUD),^{6, 7} for which there is currently no FDA-approved pharmacotherapeutic.

Development of highly selective dopamine D₃ receptor (D₃R) partial agonists/antagonists for the treatment of SUD has been of great interest due to their ability to attenuate drug reinforcement as well as inhibit cue- and stress-induced reinstatement for psychostimulants and opioids in animal models.^{8–11} D₃R-selective antagonists, specifically, have been shown to block the expression of cocaine- or heroin-induced conditioned place preference and inhibit the rewarding effects of these drugs.^{12–14} In addition to promising preclinical work, gaining D₃R selectivity over the dopamine D₂ receptor (D₂R) may avoid the extrapyramidal side effects, weight gain, metabolic disorders, and motor coordination deficits associated with D₂R antagonism.^{15–20} To this end, highly selective compounds (Figure 1), such as SB277011A (>100-fold),²¹ PG01037 (>100-fold),²² (±)-VK4-116 (1,700-fold),^{23, 24} (±)-ABS-1-113 (>300-fold),²⁵ and BP1.4979 (~200-fold),²⁶ have been discovered in spite of the ~80% homology between the D₂R and D₃R subtypes.^{27–29}

While highly D₃R-preferential antagonists and low-efficacy partial agonists demonstrate potential as treatments for SUD,²⁹ there are two challenges that still need to be addressed. The first is that these compounds generally show favorable results in animal

models of opioid use disorder but are often not as effective in mitigating cocaine or methamphetamine self-administration, especially at low fixed-ratio schedules (e.g., FR1 or FR2) of reinforcement.^{18, 29} Secondly, relatively high doses (e.g., 10–56 mg/kg, i.p.) are required to observe reductions in drug-seeking behaviors despite having very high affinities (K_i values in the low nM to pM range) for the desired target, D₃R. These challenges have led us to reconsider whether some D₂R agonist activity would improve both the efficacy and potency of our compounds. Bearing in mind that high affinity D₂R antagonists would likely cause negative side effects, including neuroleptic dysphoria³⁰ (especially in a patient population with SUD), we sought to design molecules with D₃R and D₂R agonist activities and binding selectivities in the 10- to 100-fold range. Ultimately, the goal of this study was to identify a pharmacological profile that would not only have promise for treating patients with PSUD but might also be efficacious in patients with dual diagnoses.

Of note, there is one D₃R-preferential agonist that is in clinical use for the treatment of schizophrenia and more recently, bipolar disorder. Cariprazine (see Figure 1), formerly described in the literature as RGH188, is a high affinity D₂R/D₃R agonist with preference for the D₃R (3- to 10-fold).^{31–34} Most D₂-like antipsychotics on the market generally reduce positive symptoms (e.g., delusions, disorganized speech, and hallucinations) of schizophrenia and manic episodes of bipolar disorder but are not effective at ameliorating the spectrum of other debilitating symptoms.³⁴ However, cariprazine appears to be unique in that it also improves the negative (e.g., anhedonia, social and emotional withdrawal) and cognitive symptoms (e.g., attention deficit and executive function impairment) while significantly decreasing global illness severity of schizophrenia.³⁴ Cariprazine can effectively treat the manic and mixed episodes without induction of depression in bipolar 1 disorder (BD-I).^{35, 36} Most patients with BD-I take atypical antipsychotics in combination with an antidepressant to treat both poles of the disorder.³⁶ It is believed that these therapeutic benefits are associated with cariprazine's profile as a relatively modest D₃R preferential agonist.^{34, 37, 38}

Herein, we report the design of cariprazine-based analogues resulting in a wide range of D₃R/D₂R selectivities while maintaining high (low nM to pM) binding affinities at D₃R. These ligands are considered bitopic, meaning they include a primary pharmacophore (PP), which binds to the orthosteric binding site, that is then linked to a secondary pharmacophore (SP), which binds to D₃R-unique secondary binding pocket (see Figure 1).³⁹ By changing the PP, SP, and linker portions of various bitopic ligands, we have previously altered their D₃R/D₂R selectivities and functional efficacies.^{17, 40–42} Recent work by Keser and coworkers, in particular, suggests that adjustments to the aliphatic SP of cariprazine have the potential to “tune” efficacy by repositioning the molecule in the orthosteric binding site through its interactions with the secondary binding pocket.^{43, 44} Further investigation of this hypothesis with additional aliphatic SPs will be of interest to support these findings. Hence, using the bitopic ligand design, we explored different modifications to the 2,3-dichlorophenylpiperazine (PP), *trans*-1,4-cyclohexane ring system (linker), and *N,N*-dimethylurea (SP) of cariprazine. Analogues were tested for D₂R and D₃R binding affinities in transfected HEK293 cells, and a subset was selected for functional bioluminescence resonance energy transfer (BRET) assays to assess their intrinsic efficacy. Based on the results of these experiments and additional off-target studies, two analogues

(**13a** and **13e**) along with cariprazine were evaluated for effectiveness in reducing cocaine self-administration in rats.

RESULTS AND DISCUSSION

Chemistry

We modified the PP and SP of cariprazine following the synthetic routes outlined in Scheme 1. Initially, 2-(*trans*-4-((*tert*-butoxycarbonyl)amino)cyclohexyl)acetic acid (**1**) was reduced with borane-dimethyl sulfide (BMS) complex, and the resulting alcohol (**2**) was converted to aldehyde **3** via Swern oxidation. In the next step, primary pharmacophores were installed by reductive amination using various aryl piperazines (**4a-e**).⁴² Deprotection of these intermediates with trifluoroacetic acid (TFA) gave amines **5a-e**, which were then functionalized with different SPs. To that end, cariprazine and substituted ureas **6b-7e** were prepared from either *N,N*-dimethyl- or *N*-methylcarbonyl chloride. Other urea-containing analogues were accessed by treating a selection of the aforementioned amines (**5a**, **5b**, and **5e**) with potassium cyanate under acidic conditions (**8a** and **8e**) or phosgene followed by 5,6,7,8-tetrahydro-1,6-naphthyridine (**9a** and **9b**).⁴⁵ Lastly, amides **10a-13e** were synthesized from a variety of carboxylic acids with either 1-ethyl-3-(3-dimethylaminopropyl)carbodiimide•HCl (EDCI) or *O*-(1*H*-6-chlorobenzotriazole-1-yl)-1,1,3,3-tetramethyluronium hexafluorophosphate (HCTU) serving as the coupling reagent.

Manipulations to the linker between the primary and secondary pharmacophores of cariprazine were additionally explored. As shown in Scheme 2, the cyclohexylamine was replaced with a piperidine ring using one of two aldehydes. The first (**17a**) retained the two-carbon chain found in cariprazine and was prepared from *tert*-butyl 4-oxopiperidine-1-carboxylate (**14**). Briefly, a Horner–Wadsworth–Emmons reaction furnished α,β -unsaturated ester **15**, which was sequentially reduced by hydrogenation over palladium on carbon (**16**) and DIBALH to afford **17a**. The second aldehyde (**17b**), possessing an extended carbon chain, was obtained using a Swern oxidation on commercially available *tert*-butyl 4-(3-hydroxypropyl)piperidine-1-carboxylate (**18**). With these materials in hand, we followed the same steps described in Scheme 1 to prepare analogues **21a-22b** (i.e., reductive amination, Boc-deprotection of **19a** and **19b**, followed by functionalization of amines **20a** and **20b**).

Expanding on the previous set of compounds, we also introduced a hydroxyl group onto the linker, while simultaneously adjusting the ring size (Scheme 3). In this case, cariprazine analogues were constructed from building blocks **26a** and **26b**, which were accessed using a parallel sequence of transformations. Specifically, a three-carbon chain was introduced onto *tert*-butyl 3-oxopyrrolidine-1-carboxylate (**23a**) and *tert*-butyl 4-oxopiperidine-1-carboxylate (**23b**) through separate Grignard reactions with allyl magnesium bromide. The terminal alkenes of **24a** and **24b** were then subjected to hydroboration–oxidation reactions, and the corresponding alcohols (**25a** and **25b**) were converted to hemiacetals **26a** and **26b**. Like before (see Schemes 1 and 2), the synthesis of analogues **29a-30b** proceeded through intermediates **27a-28b**.

Binding affinities of cariprazine and its analogues at D₂R and D₃R

To investigate the structure-activity relationships (SAR) of our cariprazine analogues, we determined their affinities at D₂R and D₃R. Competitive binding experiments using membrane preparations from stably transfected HEK293 cells expressing human D_{2L} and D₃ receptors were performed with [³H]*N*-methylspiperone serving as the radioligand.⁴⁶ The *K_i* value for each compound is presented in Tables 1 and 2 along with the corresponding multiparameter optimization (MPO) scores, which are a prediction of brain penetrability.⁴⁷ ⁴⁸ For our purposes, derivatives with MPO scores >3 were considered as potentially drug-like.

In the first series of compounds, we focused on modifying the SP (blue) of cariprazine (Table 1, **4a**, cariprazine, and **7a-13a**). Compared to the parent compound, similar D₃R binding affinities and selectivities were observed for the primary metabolites, **7a** and **8a**.⁴⁹ When the *N,N*-dimethylamino group of the SP was replaced with different heterocycles (**9a-12a**), D₃R affinity was retained (*K_i* = 0.31–0.66 nM), while selectivity over D₂R increased from 5- to 44-fold. Importantly, the analogue inspired by BPI.4979 (**13a**) exhibited similar affinity (*K_i* = 0.14 nM) but better selectivity (20-fold) for D₃R than cariprazine, while simultaneously maintaining a desirable MPO score (3.6).

The next several series of compounds explored different PPs (red) in varying combinations with the aforementioned SPs. As shown in Table 1, the 2,3-dichlorophenyl was substituted with a 2-chloro-3-ethylphenyl (**6b**, **7b**, and **9b-13b**) derived from our previously reported D₃R agonists.^{23, 25} Although high D₃R affinities were achieved (*K_i* = 0.18–1.31 nM), none of these analogues were substantially more selective than cariprazine, and most had poor MPO scores (<3). Conversely, the 2-fluoro-3-methoxyphenyl analogue (**6c**) noticeably decreased D₃R and D₂R affinities (*K_i* = 9.4 and 134 nM, respectively). Of note, compound **13c** showed much greater D₃R/D₂R selectivity than any of the analogues in this series, which was a bit surprising. We have previously reported that D₂R agonists are sensitive to the radioligand they are displacing and typically show much lower affinities when tested against a D₂-like antagonist (e.g., [³H]-*N*-methylspiperone).^{51, 52} We considered that the 2-fluoro-3-methoxy-substituted phenyl piperazine PP might be conferring agonist actions and thus binding affinities using the D₂-like agonist [³H]7-OH-DPAT were tested (Supporting Information, Table S1). Indeed, we discovered that D₃R selectivities were much lower in this binding assay (D₂R *K_i*/D₃R *K_i* = 0.9 and 15 for **6c** and **13c**, respectively), suggesting these analogues were agonists at D₂R and possibly D₃R. The 2-fluoro-3-methoxy-containing PP also caused a loss in affinity when the *N,N*-dimethylurea was replaced with the 3-methoxypropanamide (**13c**), and further analogues were not pursued. The 2-trifluoromethyl substituted pyridine analogues (**6d**, **11d**, and **13d**) showed promising increases in D₃R selectivity. Specifically, SPs with the 4-quinoline (**11d**) and 3-methoxypropanamide (**13d**) showed a 160- and 120-fold D₃R/D₂R selectivity, respectively. However, replacing the 2,3-dichlorophenyl substituent with the 3-chloro-5-ethyl-2-methoxyphenyl group (**4e**, **6e-8e**, **10e**, and **13e**) discovered in the highly D₃R-selective VK4-116²³ resulted in D₃R affinities and selectivities over D₂R that were only modestly different from the parent compound, unless the SP contained an indole (**10e**). Nevertheless, the 3-methoxypropanamide SP in this

series gave compound **13e** with a 21-fold D₃R/D₂R selectivity, subnanomolar affinity for D₃R ($K_i = 0.73$ nM), and potentially drug-like MPO score (3.3).

For the last series of analogues, the terminal urea of cariprazine was incorporated into the *trans*-1,4-cyclohexane ring system of the linker. As shown in Table 2, analogues **21a** and **22a** retained the two-carbon chain between the 6-membered ring and the PP, which resulted in ~20-fold D₃R selectivity over D₂R regardless of the SP. When the linking chain was increased by an additional methylene group, the D₃R binding affinity for **21b**, which is a constitutional isomer of cariprazine, was reduced by ~9-fold compared to the parent drug. Interestingly, only the 3-methoxypropanamide containing analogue (**22b**) retained the ~20-fold D₃R selectivity. If a hydroxyl group was appended to the linking chain between the PP and SP (**29a**, **30a**, **29b**, and **30b**), the MPO scores noticeably improved to 5, but the D₃R affinities were substantially reduced ($K_i = 18.7$ – 50.7 nM). The D₃R/D₂R selectivities for these analogues were also undesirable (<10-fold), so the synthesis of additional analogues containing this hydroxyl group was not pursued further.

Characterization of selected compounds in assays of D₂R and D₃R activation

With the binding studies and SAR established, we then characterized the abilities of 14 selected ligands to signal through both D₂R and D₃R along with quinpirole and dopamine as reference agonists and haloperidol as a reference antagonist.

To measure D₂R activation, we used two BRET assays. The first consisted of a relatively amplified and sensitive G protein activation (GPA) assay that measures G $\beta\gamma$ release from G α_{oA} , which allows detection of signals from less efficacious agonists (Table 3, Figure 2A, C and E). The second measured recruitment of a truncated, soluble ‘mini’ Gi-protein fused with a Venus fluorescent protein (mGsi-Venus) to a D_{2L}R fused with a nanoluciferase (D_{2L}R-Nluc). This less amplified, proximal assay allows us to distinguish between full agonists and more efficacious agonists (miniG assay, Table 3, Figure 2B, D and F) that gave a maximal response relative to the reference agonist quinpirole in the GPA assay.^{53–55}

As expected, the reference agonist quinpirole displayed 43-fold lower potency in the miniG assay as compared to the GPA assay consistent with a lower degree of signal amplification. Quinpirole and dopamine displayed equivalent maximal responses in the miniG assay (Table 3). All ligands tested retained D₂R agonism to various levels of intrinsic efficacy. The 2,3-dichlorophenyl compounds (cariprazine and **13a**) are D₂R agonists (Figure 2B, E_{max} value of 22.5% and 18.4% of the dopamine maximal response respectively in miniGsi recruitment assay) but displayed a maximal effect similar to quinpirole in the GPA assay. The 2-chloro-3-ethylphenyl compounds (**11b** and **13b**) are weak agonists at D₂R displaying lower efficacy than cariprazine with submaximal responses in the GPA assay (41% and 75% of quinpirole response, respectively) and no detectable effect in the miniG assay.^{40, 42} The 2-fluoro-3-methoxyphenyl compounds (**6c** and **13c**) displayed a maximal effect similar to that of dopamine and quinpirole in both assays indicating they are full D₂R agonists. Indeed, these data corroborated the binding data obtained using [³H]7-OH-DPAT as the radioligand, as described above (see Table S1). The 2-trifluoromethyl substituted pyridine compounds (**11d** and **13d**) were both weak agonists displaying lower efficacy

than cariprazine in both assays. The 3-chloro-5-ethyl-2-methoxyphenyl compounds (**6e**, **7e**, and **13e**) were also weak agonists displaying lower maximal effects than both quinpirole and cariprazine, but with higher potency than the 2-trifluoromethyl substituted pyridine compounds. Finally the modified linker compounds (**21a**, **22a**, and **22b**) all behaved as weak agonists in the miniG assay, displaying slightly higher (**21a**, 38% of dopamine E_{max}), similar (**22a**, 25%), and lower (**22b**, 15%) efficacy as compared to cariprazine (23%). Thus, apart from the compounds with the 2-fluoro-3-methoxyphenyl PP, all compounds exhibited weak agonism at the D_2R like cariprazine but with subtle differences in maximal effects across the compound set. As we have previously suggested,⁴¹ the efficacies of D_2R and D_3R compounds can be modified through modifications to PP, linker, and SP. As there is a range of potencies and efficacies in this series of analogues, we now have the tools necessary to determine the optimal pharmacological profile, including binding affinities, selectivities and functional efficacies at both D_2R and D_3R .

All 14 selected compounds were then tested for D_3R signaling profiles with the aim of selecting agonists or antagonists. The same GPA assay overexpressing $G\alpha_{oA}$ was used to investigate D_3R agonism as the D_3R has been shown to selectively couple to this G protein α subunit (Table 4, Figure 3A, C and E).⁵⁶ The 2,3-dichlorophenyl compounds (cariprazine and **13a**) both behaved as D_3R agonists in this assay with similar maximal effects (45% and 49% of quinpirole maximal effect), suggesting that this GPA assay would be suitable to detect D_3R agonism with a similar or lower level than that of cariprazine. The 2-fluoro-3-methoxyphenyl compounds did not display the desired weak agonist/antagonist properties at the D_3R but instead behaved as full agonists at D_3R in this assay, consistent with their action at the D_2R . The modified linker compounds were all D_3R agonists with **21a** exhibiting the strongest response with a higher efficacy than cariprazine (Figure 3E, E_{max} value of 73.2 %). Finally, no agonist response was detected for the 2-chloro-3-ethylphenyl (**11b** and **13b**), the 2-trifluoromethyl substituted pyridine (**11d** and **13d**), and the 3-chloro-5-ethyl-2-methoxyphenyl compounds (**6e**, **7e**, and **13e**).

To quantify D_3R antagonism, a competitive assay was used where test compounds were added together with an EC_{50} concentration of quinpirole to assess their ability to displace and antagonize the agonist response (Table 4, Figures 3B, 3D, and 3F). Haloperidol was used as a reference D_3R antagonist. Compounds that signaled as robust D_3R agonists (**6c**, **13c**, and **21a**) were not tested as antagonists. Out of the 11 remaining compounds, all showed some antagonist activity, with the agonists acting to reduce the quinpirole response down to their level of agonism (around 25% for cariprazine and **13a**, around 30% for **22a** and **22b**). The most potent antagonists were **13b**, **13d**, and **13a**, showing similar potencies to haloperidol. In addition, **13a** showed a very similar signaling profile to cariprazine (weak agonist with similar efficacy at both the D_2R and D_3R) but with improved selectivity for D_3R . Thus, this compound, like **13e**, is a agonist at D_2R (with 2-fold lower maximal effect than cariprazine) in the miniG assay but acted as a D_3R antagonist.

Off-target data for cariprazine and related derivatives

Eleven compounds with a range of selectivities for D_3R over D_2R (between 7.1- to 370-fold) were then evaluated for off-target binding affinities (Table 5) and functional potencies/

efficacies (Supporting Information, Tables S2–S5) against cariprazine. All tested analogues were selective for D₃R over other dopamine receptors (i.e., D₁R and D₄R), exhibiting markedly lower affinities for these two subtypes (K_i 3 μ M and 200 nM, respectively). Like cariprazine, several derivatives (e.g., **13a**, **13b**, and **13d**) exhibited high binding affinities for the 5-HT_{1A} receptor (K_i <10 nM), which is a key target in the treatment of schizophrenia.^{57, 58} Interestingly, 5-HT_{1A} affinity decreased by 18-fold between **13a** and **13e** (K_i = 6.0 vs. 108 nM, respectively) when the classic 2,3-dichlorophenyl containing PP was replaced by a 3-chloro-5-ethyl-2-methoxyphenyl group. In general, compounds were far more selective for D₃R over 5-HT_{2A} and 5-HT_{2C} (216- and 253-fold, respectively). The only exceptions to this trend were **11b** and **13b**, which were not pursued further. The full subset of cariprazine analogues also displayed high affinities for 5-HT_{2B} (K_i 34.2 nM). Although activation of this serotonin receptor subtype has been associated with cardiotoxic effects,⁵⁹ all tested compounds behaved as 5-HT_{2B} antagonists in the functional assays, including cariprazine itself (see Table S5). Therefore, none of our analogues are expected to induce cardiotoxicity from 5-HT_{2B} stimulation.

Effects of cariprazine and selected analogues on cocaine self-administration in rats

Cariprazine was tested in a rat model of cocaine self-administration under a fixed-ratio 2 (FR2, i.e., two-active lever presses lead to one cocaine infusion) schedule of reinforcement. Figure 4A shows dose-dependent biphasic effects of cariprazine on cocaine self-administration, specifically an increase at a very low dose (0.3 mg/kg) and a decrease at the higher doses (1, 3 mg/kg). One-way ANOVA with repeated measures (RM) over drug doses revealed a significant treatment main effect (Figure 4A, $F_{(3, 24)} = 9.616$, $p < 0.001$). Dunnett's post-hoc tests indicated a significant reduction in the number of cocaine infusions only after 3 mg/kg cariprazine administration compared to the vehicle control group ($q' = 3.497$, $p = 0.005$). In contrast, cariprazine failed to alter the number of inactive lever presses (Figure 4B, $F_{(3, 24)} = 1.362$, $p > 0.05$), suggesting that cariprazine did not produce sedation or locomotor impairment. Figure 4C shows the representative records of cocaine self-administration before and after the different doses of cariprazine administration, illustrating that at low doses (0.3mg/kg, i.p.), cariprazine produced an increase in drug taking, as previously reported,⁶⁰ which is possibly a compensatory response to a reduction in cocaine reward. However, at high doses (1, 3 mg/kg), cariprazine caused a typical extinction-like pattern of cocaine self-administration (i.e., an initial burst-like increase in drug intake followed by cessation of cocaine intake), indicating a robust reduction in cocaine reward after high dose cariprazine administration. In total, this classical pattern of drug self-administration suggests that cariprazine pretreatment produces a dose-dependent reduction in cocaine's reinforcing effects (efficacy).

Based on D₃R binding affinities and selectivity profiles, as well as favorable MPO scores (>3) and agonist/antagonist profiles at both D₃R and D₂R, we selected **13a** and **13e** for behavioral testing in comparison to the parent compound. Similar to cariprazine (Figure 4), **13a** also produced a dose-dependent biphasic effect on cocaine self-administration. That is, at 0.3 mg/kg, **13a** produced a significant increase, while at higher doses (1, 3 mg/kg) it produced a dose-dependent reduction in the number of cocaine infusions (Figure 5A, $F_{(3, 24)} = 23.822$, $p < 0.001$; Dunnett's post-hoc, $q' = 2.556$, $p = 0.045$ at 0.3 mg/kg; $q' = 2.873$, p

= 0.022, at 1 mg/kg; $q' = 5.395$, $p < 0.001$, at 3 mg/kg). Like cariprazine, **13a** pretreatment also failed to affect the number of inactive lever presses (Figure 5B; $F_{(3, 24)} = 2.708$, $p > 0.05$).

Next, we tested **13e** and found that higher doses (10 mg/kg) of **13e** are required to inhibit cocaine self-administration under FR2 reinforcement, in rats (Figure 6). One-way ANOVA revealed a significant treatment main effect on cocaine infusions (Figure 6A, $F_{(4, 43)} = 4.130$, $p = 0.006$; Dunnett's post-hoc, $q' = 3.283$, $p = 0.007$, at 10 mg/kg compared to vehicle). As observed with cariprazine and **13a**, there was no effect on the number of inactive lever presses (Figure 6B; $F_{(4, 43)} = 0.736$, $p > 0.05$).

There are three important findings in this behavioral test. First, cariprazine and its analogs appear to be more potent than highly selective D₃R antagonists in reducing cocaine self-administration under low-cost high-payoff (FR2) reinforcement conditions. In particular, considerably lower doses (0.3, 1, 3 mg/kg) of cariprazine and **13a** are required to alter cocaine self-administration. Second, cariprazine and **13a** produced unique biphasic effects on cocaine self-administration—increasing the number of cocaine infusions at low doses and decreasing drug intake at higher doses. These biphasic effects are usually seen after pretreatment with non-selective dopamine receptor antagonists, such as pimozide and (+)-butaclamol.⁶¹ In contrast, highly selective D₃R antagonists usually produced a monophasic reduction in cocaine or opioid self-administration, and higher doses (10–30 mg/kg) are required to inhibit cocaine or oxycodone self-administration.^{8, 24} The increase in cocaine self-administration after low doses of cariprazine and **13a** is a compensatory response to reduced cocaine reward, as the pattern of cocaine self-administration is comparable to the responses produced by lower doses of cocaine - evenly distributed drug intake with shorter infusion intervals.^{61, 62} Thus, the increased behavioral performance reveals a reduction in cocaine's rewarding effects. Congruently, at higher doses, cariprazine, **13a** and **13e** all produced a classical extinction-like pattern of cocaine self-administration—initial burst-like increase in drug infusions followed by cessation of drug taking.

Taken together, these data show that cariprazine and its two analogs, **13a** and **13e**, produce a dose-dependent reduction in cocaine reward, which is consistent with their pharmacological profiles as D₃R agonists/antagonists with moderate D₃R/D₂R selectivities (cariprazine, 3.6-fold; **13a/13e**, ~20-fold). We note that **13a** displays similar pharmacological potency to cariprazine in attenuating cocaine reward, while **13e** displays slightly lower potency as a higher dose (10 mg/kg) of **13e** is required to inhibit cocaine self-administration. This behavioral potency difference is in line with their receptor binding profiles. Whereas **13a** has a similar binding affinity to D₂R and D₃R as cariprazine (Table 1), **13e** displays ~5-fold lower affinities for D₂R and D₃R compared to **13a** (Table 3). Similarly, *in vitro* functional assays indicate that the EC₅₀ value of **13e** in activating D₂R is ~10-fold higher than that of **13a**. This is consistent with the effective dose of **13e** (10 mg/kg, Figure 6) in attenuating cocaine self-administration that is also ~3-fold higher than that of **13a** (3 mg/kg, Figure 5).

CONCLUSIONS

We have hypothesized that compounds that are moderately D₃R/D₂R selective and are partial agonists, especially at D₂R may be more effective than highly D₃R selective antagonists for treatment of PSUD. Previously, highly selective D₃R partial agonists/antagonists have been shown to block the reinforcing effects of opioids, such as oxycodone,^{24, 63, 64} but are often less effective for psychostimulants, such as cocaine or methamphetamine,^{18, 65} especially when the drug is readily available (low fixed ratio schedule of reinforcement e.g., FR1 or FR2). Nevertheless, compounds that are D₂R antagonists are generally not well tolerated in this patient population.³⁰ To test this hypothesis, we designed a series of compounds, based on cariprazine, with varying selectivities and functional efficacies at D₂R and D₃R, depending on their PP, SP, and/or linker. By systematically modifying each piece of the parent molecule, we have discovered compounds with high D₃R affinities ($K_i < 1$ nM) and improved selectivities (~20-fold) over D₂R that have the desired D₂R partial agonist functional efficacies and are either low efficacy partial agonists or antagonists at D₃R, as measured in BRET-based assays for each receptor subtype. We have obtained off target activities (D₁R, D₄R, 5HT_{1A}, 5HT_{2A}, 5HT_{2B}, and 5HT_{2C}) on a subset of these compounds that had desirable D₃R/D₂R selectivity profiles as well as MPO scores (>3) that further demonstrated D₃R-selectivity.

Based on all the *in vitro* data obtained, we selected **13a** and **13e** as our initial lead compounds, which were tested side-by-side with cariprazine in a rat model of cocaine self-administration. The two new compounds had higher but still moderate D₃R/D₂R selectivities (~20-fold) as compared to cariprazine (3.6-fold) and were effective in blocking cocaine self-administration in the rats (FR2; 1–10 mg/kg, i.p.). Overall, these convincing behavioral data support the notion that moderately D₃R selective partial agonists/antagonists that are also partial agonists at D₂R, may be more effective than highly selective (>200-fold) D₃R antagonists in reducing drug-seeking behavior. Of course, additional testing will be needed to determine the suitability of **13a** and **13e** for further development. For example, the extrapyramidal side effects of our lead compounds will need to be examined as well as their efficacy in animal models of affective disorders, such as BD-I.^{66, 67} Nonetheless, the cariprazine analogs described herein demonstrate high potential for treating PSUD that may be dual diagnosed with affective disorders.

EXPERIMENTAL METHODS

Chemistry

General Information.—Chemicals and solvents were purchased from commercial suppliers and used as received. Unless stated otherwise, reactions were performed under ambient conditions and monitored by thin-layer chromatography using Analtech silica gel GHLF (250 microns) coated glass plates, which were visualized with either phosphomolybdic acid, potassium permanganate, or vanillin stain. Normal phase column chromatography was conducted with a Teledyne Isco Combiflash Rf or EZ-Prep purification system (ELS detector associated). All nuclear magnetic resonance (NMR) spectra (¹H and ¹³C) were acquired in deuterated solvents (CDCl₃ or CD₃OD) on a Varian Mercury Plus 400 spectrometer. Chemical shifts are reported in parts per million (ppm) and were adjusted

using the residual solvents (CDCl_3 : 7.26 ppm for ^1H NMR, 77.2 ppm for ^{13}C NMR; CD_3OD : 3.31 ppm for ^1H NMR, 49.0 ppm for ^{13}C NMR) as an internal reference. Coupling constants are reported in Hertz (Hz) and peak multiplicities as either a singlet (s), doublet (d), triplet (t), quartet (q), or multiplet (m). Infrared (IR) spectra were acquired on a Perkin Elmer Spectrum Two FT-IR spectrometer. Melting points were determined on an OptiMelt MPA100 instrument and are uncorrected. High-resolution mass spectrometry (HRMS) data were collected on a Thermo Scientific LTQ-Orbitrap Velos spectrometer using either electrospray ionization (ESI) or matrix-assisted laser desorption/ionization (MALDI). High-performance liquid chromatography (HPLC) was conducted on an Agilent Technologies 1260 Infinity system coupled to a diode-array detector. A Phenomenex Gemini C18 100 Å LC column (50×4.6 mm, 3 μm particle size) was used as the stationary phase. For basic conditions, the mobile phase consisted of H_2O with 0.1% diethylamine (solvent A) and MeCN with 0.1% diethylamine (solvent B). For acidic conditions, solvents contained 0.1% TFA instead of diethylamine. All samples were prepared at a concentration of ca. 1 mg/mL in MeOH, and 20 μL of each solution was injected onto the column, which was maintained at 40 $^\circ\text{C}$. Using a flow rate of 1.0 mL/min, the solvent gradient was as follows: 10% B held for 10 min, 10–40% B ramped over 10 min, 40% B held for 10 min, 40–80% B over 10 min, 80% B held for 20 min. Compound purity was determined based on peak integration (area under the curve) of the absorbance signals at 254 and 214 nm. Elemental analysis was performed by Atlantic Microlab, Inc. (Norcross, GA). All tested compounds were >95% pure by either HPLC or elemental analysis.

General Procedure A.—Using oven-dried glassware under an Ar atmosphere, a 0.60 M solution of $(\text{COCl})_2$ in anhydrous DCM (1.5 equiv) was cooled to -78 $^\circ\text{C}$. Then, anhydrous DMSO (3.0 equiv) was added over ca. 5 min, and the reaction was stirred for 30 min. Next, a 0.30 M solution of the alcohol in anhydrous DCM (1.0 equiv) was added over ca. 10 min, and the reaction was stirred for an additional 30 min. Finally, anhydrous NEt_3 (6.0 equiv) was added over ca. 5 min, and the mixture was allowed to warm to rt. When TLC analysis suggested the complete disappearance of starting material (ca. 2 h), the reaction was quenched with a 1.0 M aq solution of HCl, and the aq layer was extracted with DCM (2 \times). The combined organic layers were dried over Na_2SO_4 , filtered, and concentrated. The crude product was purified by chromatography as described.

General Procedure B.—To a 0.08–0.13 M solution of **3** in anhydrous DCE (1.0 equiv) was added AcOH (1.0 equiv) followed by the appropriate aryl piperazine (1.1 equiv). The mixture was stirred for 30 min, and $\text{NaBH}(\text{OAc})_3$ (1.5 equiv) was added in one portion. After stirring overnight, the reaction was quenched with a saturated aq solution of NaHCO_3 , and the aq layer was extracted with DCM (2 \times). The combined organic layers were washed with brine, dried over Na_2SO_4 , filtered, and concentrated. The crude product was purified by chromatography as described.

General Procedure C.—TFA (27–144 equiv) was added to a 0.03–0.15 M solution of the appropriate Boc-protected amine in DCM (1.0 equiv). The reaction mixture was stirred for ca. 4 h and then concentrated. The resulting residue was suspended in a 1.0 M aq solution of

NaOH, and the aq layer was extracted with CHCl₃ (3 ×). The combined organic layers were dried over Na₂SO₄, filtered, and concentrated to afford the corresponding amine.

General Procedure D.—To a 0.07–0.10 M solution of the amine in DCM (1.0 equiv) was added DIPEA (1.5 equiv) followed by the appropriate carbamyl chloride (1.25 equiv) over 5 min. After stirring overnight, the reaction was quenched with a saturated aq solution of NaHCO₃, and the aq layer was extracted with CHCl₃ (3 ×). The combined organic layers were dried over Na₂SO₄, filtered, and concentrated. The crude product was purified by chromatography as described.

General Procedure E.—A 0.03–0.05 M mixture of the appropriate carboxylic acid (1.1 equiv) in CHCl₃ was cooled to 0 °C, and EDCI (1.3 equiv) followed by HOBt (1.2 equiv) were each added in one portion. After 30 min, the amine (1.0 equiv) was added followed by DIPEA (1.4 equiv). The mixture was allowed to warm to rt and stirred overnight. Then, a saturated aq solution of NaHCO₃ was added, and the aq layer was extracted with CHCl₃ (3 ×). The combined organic layers were dried over anhydrous Na₂SO₄, filtered, and concentrated. The crude product was purified by chromatography as described.

General Procedure F.—To a 0.10 M mixture of HCTU (1.2 equiv) in DCM was added 3-methoxypropanoic acid (1.1 equiv) in one portion. After stirring the mixture for 10 min, a solution of the amine (1.0 equiv) and DIPEA (1.2 equiv) in DCM (0.04 M with respect to the limiting reagent) was added over 5 min. The reaction was stirred overnight, quenched with a saturated aq solution of NaHCO₃, and the aq layer was extracted with DCM (3 ×). The combined organic layers were dried over anhydrous Na₂SO₄, filtered, and concentrated. The crude product was purified by chromatography as described to afford the corresponding amide.

tert-Butyl (trans-4-(2-hydroxyethyl)cyclohexyl)carbamate (2).—Using oven-dried glassware under an Ar atmosphere, a solution of 2-(trans-4-(tert-butoxycarbonyl)amino)cyclohexyl)acetic acid (6.01 g, 23.4 mmol) in anhydrous THF (30 mL) was cooled to 0 °C. Then, borane dimethylsulfide complex (3.4 mL, 36 mmol) was added dropwise over 5 min. The solution was allowed to warm to rt and stirred for 15 h. Afterward, the reaction was cooled back to 0 °C, quenched with a saturated aq solution of NaHCO₃ (60 mL), and the aq layer was extracted with EtOAc (2 × 60 mL). The organic layer was dried over anhydrous Na₂SO₄, filtered, and concentrated to afford **2** (5.18 g, 21.3 mmol, 91% yield) as a white solid. An analytical sample was prepared by recrystallization using Et₂O—hexanes (slow evaporation of solvent mixture). *R*_f = 0.4 (50% EtOAc/hexanes); ¹H NMR (400 MHz, CDCl₃) δ 4.44–4.27 (m, 1H), 3.71–3.64 (m, 2H), 3.43–3.28 (m, 1H), 2.04–1.96 (m, 2H), 1.81–1.73 (m, 2H), 1.51–1.26 (m, 4H), 1.43 (s, 9H), 1.15–0.96 (m, 4H); ¹³C NMR (101 MHz, CDCl₃) δ 155.4, 79.2, 60.9, 50.0, 39.8, 33.6 (3C), 32.0 (2C), 28.6 (3C); IR (neat) 3425, 3365, 1682, 1517 cm⁻¹; mp 102–103 °C (Et₂O—hexanes); HRMS (MALDI) *m/z* [M + Na]⁺ calcd for C₁₃H₂₅NNaO₃ 266.1727, found 266.1730.

tert-Butyl (trans-4-(2-oxoethyl)cyclohexyl)carbamate (3).—General Procedure A was followed using **2** (5.18 g, 21.3 mmol). After work-up, the crude product was purified by chromatography (120 g of silica gel, 0–40% EtOAc/hexanes) to afford **3** (3.04 g, 12.6

mmol, 59% yield) as a white solid. R_f = 0.5 (40% EtOAc/hexanes); ^1H NMR (400 MHz, CDCl_3) δ 9.78–9.73 (m, 1H), 4.47–4.29 (m, 1H), 3.45–3.26 (m, 1H), 2.35–2.29 (m, 2H), 2.06–1.95 (m, 2H), 1.90–1.74 (m, 3H), 1.44 (s, 9H), 1.20–1.03 (m, 4H); ^{13}C NMR (101 MHz, CDCl_3) δ 202.3, 155.3, 79.3, 50.8, 49.6, 33.3 (2C), 31.9 (2C), 31.8, 28.6 (3C); IR (neat) 3377, 1715, 1686 cm^{-1} ; mp 90–91 $^\circ\text{C}$; HRMS (MALDI) m/z [$\text{M} + \text{Na}$] $^+$ calcd for $\text{C}_{13}\text{H}_{23}\text{NNaO}_3$ 264.1570, found 264.1578.

***tert*-Butyl (*trans*-4-(2-(4-(2,3-dichlorophenyl)piperazin-1-**

yl)ethyl)cyclohexyl)carbamate (4a).—General procedure B was followed using **3** (2.00 g, 8.29 mmol) and 1-(2,3-dichlorophenyl)piperazine•HCl (2.44 g, 9.12 mmol) in DCE (56 mL). After work-up, the crude product was purified by chromatography (80 g of silica gel, 0–50% EtOAc/hexanes) to afford **4a** (1.79 g, 3.92 mmol, 47% yield) as a white solid. R_f = 0.2 (50% EtOAc/hexanes); ^1H NMR (400 MHz, CDCl_3) δ 7.16–7.08 (m, 2H), 6.98–6.91 (m, 1H), 4.44–4.24 (m, 1H), 3.44–3.27 (m, 1H), 3.14–2.97 (m, 4H), 2.71–2.52 (m, 4H), 2.46–2.36 (m, 2H), 2.05–1.92 (m, 2H), 1.81–1.71 (m, 2H), 1.49–1.37 (m, 2H), 1.44 (s, 9H), 1.29–1.15 (m, 1H), 1.14–0.95 (m, 4H); ^{13}C NMR (101 MHz, CDCl_3) δ 155.7, 151.8, 135.5, 128.0, 127.9, 125.0, 119.0, 79.5, 57.1, 53.9, 51.8, 50.4, 35.9, 34.4, 33.9 (2C), 32.5 (2C), 28.9 (3C); IR (neat) 3366, 1677 cm^{-1} ; mp 147–148 $^\circ\text{C}$; HRMS (MALDI) m/z [$\text{M} + \text{H}$] $^+$ calcd for $\text{C}_{23}\text{H}_{36}\text{Cl}_2\text{N}_3\text{O}_2$ 456.2179, found 456.2174; t_R = 39.4 min (HPLC, basic). The oxalate salt was precipitated from a 0.03 M solution of the free base in 50% CHCl_3 /acetone using oxalic acid (1.25 equiv). Dec >185 $^\circ\text{C}$. Anal. calcd for $\text{C}_{23}\text{H}_{35}\text{Cl}_2\text{N}_3\text{O}_2 \cdot 1.25\text{C}_2\text{H}_2\text{O}_4$: C, 53.83; H, 6.64; N, 7.39. Found: C, 54.06; H, 6.67; N, 7.48.

***tert*-Butyl (*trans*-4-(2-(4-(2-chloro-3-ethylphenyl)piperazin-1-**

yl)ethyl)cyclohexyl)carbamate (4b).—General procedure B was followed using **3** (0.710 g, 2.94 mmol) and 1-(2-chloro-3-ethylphenyl)piperazine (0.810 g, 3.60 mmol) in DCE (35 mL). After work-up, the crude product was purified by chromatography (silica gel, 0–70% EtOAc/hexanes) to afford **4b** (0.990 g, 2.20 mmol, 75% yield) as a white solid. ^1H NMR (400 MHz, CDCl_3) δ 7.15 (t, J = 7.7 Hz, 1H), 6.96–6.91 (m, 2H), 4.41–4.31 (m, 1H), 3.45–3.29 (m, 1H), 3.16–2.95 (m, 4H), 2.77 (q, J = 7.6 Hz, 2H), 2.72–2.48 (m, 4H), 2.46–2.38 (m, 2H), 2.02–1.95 (m, 2H), 1.82–1.73 (m, 2H), 1.48–1.40 (m, 2H), 1.44 (s, 9H), 1.27–1.19 (m, 1H), 1.22 (t, J = 7.5 Hz, 3H), 1.13–0.99 (m, 4H).

***tert*-Butyl (*trans*-4-(2-(4-(2-fluoro-3-methoxyphenyl)piperazin-1-**

yl)ethyl)cyclohexyl)carbamate (4c).—General procedure B was followed using **3** (0.725 g, 3.00 mmol) and 1-(2-fluoro-3-methoxyphenyl)piperazine•HCl (0.816 g, 3.31 mmol) in DCE (25 mL). After work-up, the crude product was purified by chromatography (40 g of silica gel, 0–80% EtOAc/hexanes) to afford **4c** (0.695 g, 1.60 mmol, 53% yield) as a light orange solid. R_f = 0.4 (80% EtOAc/hexanes); ^1H NMR (400 MHz, CDCl_3) δ 6.95 (dt, J = 8.3, 1.9 Hz, 1H), 6.66–6.53 (m, 2H), 4.43–4.26 (m, 1H), 3.86 (s, 3H), 3.43–3.25 (m, 1H), 3.19–2.98 (m, 4H), 2.68–2.47 (m, 4H), 2.43–2.35 (m, 2H), 2.03–1.92 (m, 2H), 1.82–1.69 (m, 2H), 1.48–1.36 (m, 2H), 1.43 (s, 9H), 1.29–1.15 (m, 1H), 1.12–0.95 (m, 4H); ^{13}C NMR (101 MHz, CDCl_3) δ 155.4, 148.7 (d, J = 10 Hz), 145.8 (d, J = 245 Hz), 141.2 (d, J = 6 Hz), 123.6 (d, J = 5 Hz), 111.2 (d, J = 2 Hz), 107.2, 79.2, 56.8, 56.6, 53.6 (2C), 50.8 (d, J = 3 Hz, 2C), 50.0, 35.6, 34.0, 33.6 (2C), 32.1 (2C), 28.6 (3C); IR (neat) 3370, 1685

cm^{-1} ; mp 118–119 °C; HRMS (ESI) m/z $[M + H]^+$ calcd for $\text{C}_{24}\text{H}_{39}\text{FN}_3\text{O}_3$ 436.2970, found 436.2964.

tert-Butyl (trans-4-(2-(4-(6-(trifluoromethyl)pyridin-2-yl)piperazin-1-yl)ethyl)cyclohexyl)carbamate (4d).—General procedure B was followed using **3** (1.00 g, 4.16 mmol) and 1-(6-(trifluoromethyl)pyridin-2-yl)piperazine (1.06 g, 4.58 mmol) in DCE (28 mL). Note: **3** was added to a solution of the aryl piperazine. After work-up, the crude product was purified by chromatography (40 g of silica gel, 0–80% EtOAc/hexanes) to afford **4d** (1.23 g, 2.69 mmol, 65% yield) as a white solid. R_f = 0.3 (80% EtOAc/hexanes); ^1H NMR (400 MHz, CDCl_3) δ 7.55 (t, J = 8.0 Hz, 1H), 6.92 (d, J = 7.3 Hz, 1H), 6.75 (d, J = 8.7 Hz, 1H), 4.44–4.28 (m, 1H), 3.60 (t, J = 5.1 Hz, 4H), 3.43–3.27 (m, 1H), 2.51 (t, J = 5.1 Hz, 4H), 2.42–2.35 (m, 2H), 2.03–1.93 (m, 2H), 1.81–1.68 (m, 2H), 1.50–1.38 (m, 2H), 1.43 (s, 9H), 1.30–1.16 (m, 1H), 1.14–0.97 (m, 4H); ^{13}C NMR (101 MHz, CDCl_3) δ 159.0, 155.4, 146.6 (q, J = 34 Hz), 138.3, 121.8 (q, J = 274 Hz), 109.5, 108.9 (q, J = 3 Hz), 79.2, 56.8, 53.1 (2C), 50.0, 44.9 (2C), 35.6, 34.0 (2C), 33.6, 32.1 (2C), 28.6 (3C); IR (neat) 3369, 1678 cm^{-1} ; mp 131–132 °C; HRMS (ESI) m/z $[M + H]^+$ calcd for $\text{C}_{23}\text{H}_{36}\text{F}_3\text{N}_4\text{O}_2$ 457.2785, found 457.2777.

tert-Butyl (trans-4-(2-(4-(3-chloro-5-ethyl-2-methoxyphenyl)piperazin-1-yl)ethyl)cyclohexyl)carbamate (4e).—General procedure B was followed using **3** (1.00 g, 4.16 mmol) and 1-(3-chloro-5-ethyl-2-methoxyphenyl)piperazine•HCl (1.33 g, 4.57 mmol) in DCE (27 mL). After work-up, the crude product was purified by chromatography (40 g of silica gel, 0–50% EtOAc/hexanes) to afford **4e** (1.10 g, 2.29 mmol, 55% yield) as a yellow solid. R_f = 0.5 (50% MeOH/DCM); ^1H NMR (400 MHz, CDCl_3) δ 6.84 (s, 1H), 6.61 (s, 1H), 4.44–4.26 (m, 1H), 3.83 (s, 3H), 3.44–3.26 (m, 1H), 3.23–3.02 (m, 4H), 2.68–2.49 (m, 6H), 2.45–2.35 (m, 2H), 2.03–1.94 (m, 2H), 1.81–1.71 (m, 2H), 1.50–1.37 (m, 2H), 1.43 (s, 9H), 1.30–1.15 (m, 4H), 1.14–0.97 (m, 4H); ^{13}C NMR (101 MHz, CDCl_3) δ 155.1, 146.2, 146.0, 140.6, 128.0, 122.0, 116.5, 78.90, 58.8, 56.5, 53.7 (2C), 50.1 (2C), 49.7, 35.3, 33.7, 33.3 (2C), 31.8 (2C), 28.30, 28.27 (3C), 15.2; IR (neat) 3364, 1681 cm^{-1} ; mp 86–88 °C; HRMS (MALDI) m/z $[M + H]^+$ calcd for $\text{C}_{26}\text{H}_{43}\text{ClN}_3\text{O}_3$ 480.2987, found 480.2985. The oxalate salt was precipitated from a 0.02 M solution of the free base in 50% CHCl_3 /acetone using oxalic acid (1.25 equiv). mp 132–135 °C. Anal. calcd for $\text{C}_{26}\text{H}_{42}\text{ClN}_3\text{O}_3 \cdot \text{C}_2\text{H}_2\text{O}_4$: C, 58.99; H, 7.78; N, 7.37. Found: C, 58.70; H, 7.81; N, 7.30.

trans-4-(2-(4-(2,3-Dichlorophenyl)piperazin-1-yl)ethyl)cyclohexan-1-amine (5a).—General procedure C was followed using **4a** (1.33 g, 2.91 mmol) and TFA (9.0 mL, 0.12 mol) in DCM (20 mL). After work-up, **5a** (1.00 g, 2.81 mmol, 96% yield) was isolated as a white solid. R_f = 0.1 (10% MeOH/DCM); ^1H NMR (400 MHz, CDCl_3) δ 7.17–7.09 (m, 2H), 6.95 (dd, J = 6.4, 3.1 Hz, 1H), 3.15–2.96 (m, 4H), 2.72–2.51 (m, 5H), 2.47–2.37 (m, 2H), 1.84 (d, J = 12.2 Hz, 2H), 1.76 (d, J = 12.3 Hz, 2H), 1.48–1.32 (m, 4H), 1.32–1.17 (m, 1H), 1.14–0.92 (m, 4H); ^{13}C NMR (101 MHz, CDCl_3) δ 151.5, 134.2, 127.7, 127.6, 124.6, 118.7, 56.9, 53.6 (2C), 51.5 (2C), 50.9, 36.9 (2C), 35.8, 34.2, 32.3 (2C); IR (neat) 1578 cm^{-1} ; mp 72–74 °C; HRMS (MALDI) m/z $[M + H]^+$ calcd for $\text{C}_{18}\text{H}_{28}\text{Cl}_2\text{N}_3$ 356.1655, found 356.1660.

trans-4-(2-(4-(2-Chloro-3-ethylphenyl)piperazin-1-yl)ethyl)cyclohexan-1-amine (5b).—General procedure C was followed using **4b** (0.990 g, 2.20 mmol) and TFA (5.0 mL, 60 mmol) in DCM (15 mL). After work-up, **5b** (0.775 g, 2.20 mmol, 100% yield) was isolated as a beige solid. ¹H NMR (400 MHz, CDCl₃) δ 7.15 (t, *J* = 7.8 Hz, 1H), 6.97–6.91 (m, 2H), 3.13–2.98 (m, 4H), 2.77 (q, *J* = 7.5 Hz, 2H), 2.72–2.54 (m, 5H), 2.47–2.40 (m, 2H), 1.88–1.81 (m, 2H), 1.80–1.73 (m, 2H), 1.48–1.40 (m, 2H), 1.28–1.18 (m, 1H), 1.22 (t, *J* = 7.5 Hz, 3H), 1.14–0.94 (m, 4H).

trans-4-(2-(4-(2-Fluoro-3-methoxyphenyl)piperazin-1-yl)ethyl)cyclohexan-1-amine (5c).—General procedure C was followed using **4c** (0.251 g, 0.577 mmol) and TFA (1.8 mL, 24 mmol) in DCM (4.0 mL). After work-up, **5c** (0.191 g, 0.569 mmol, 99% yield) was isolated as a tan solid. *R_f* = 0.1 (10% MeOH/DCM); ¹H NMR (400 MHz, CDCl₃) δ 6.95 (dt, *J* = 8.3, 1.9 Hz, 1H), 6.66–6.53 (m, 2H), 3.85 (s, 3H), 3.18–3.01 (m, 4H), 2.69–2.52 (m, 5H), 2.44–2.37 (m, 2H), 1.88–1.80 (m, 2H), 1.79–1.70 (m, 2H), 1.48–1.16 (m, 5H), 1.12–0.91 (m, 4H); ¹³C NMR (101 MHz, CDCl₃) δ 148.7 (d, *J* = 10 Hz), 145.8 (d, *J* = 245 Hz), 141.2 (d, *J* = 6 Hz), 123.6 (d, *J* = 5 Hz), 111.2 (d, *J* = 2 Hz), 107.1, 56.9, 56.6, 50.9, 50.8 (d, *J* = 3 Hz, 2C), 36.9, 35.8, 34.2, 32.3; IR (film) 1611, 1576 cm⁻¹; mp 59–60 °C; HRMS (ESI) *m/z* [M + H]⁺ calcd for C₁₉H₃₁FN₃O 336.2446, found 336.2442.

trans-4-(2-(4-(6-(Trifluoromethyl)pyridin-2-yl)piperazin-1-yl)ethyl)cyclohexan-1-amine (5d).—General procedure C was followed using **4d** (0.301 g, 0.659 mmol) and TFA (2.0 mL, 26 mmol) in DCM (4.0 mL). After work-up, **5d** (0.234 g, 0.656 mmol, 100% yield) was isolated as a clear, colorless oil. *R_f* = 0.1 (10% MeOH/DCM); ¹H NMR (400 MHz, CDCl₃) δ 7.55 (t, *J* = 8.0 Hz, 1H), 6.92 (d, *J* = 7.3 Hz, 1H), 6.75 (d, *J* = 8.7 Hz, 1H), 3.60 (t, *J* = 5.1 Hz, 4H), 2.63–2.55 (m, 1H), 2.52 (t, *J* = 5.1 Hz, 4H), 2.42–2.35 (m, 2H), 1.88–1.81 (m, 2H), 1.79–1.71 (m, 2H), 1.47–1.38 (m, 2H), 1.34–1.16 (m, 3H), 1.13–0.93 (m, 4H); ¹³C NMR (101 MHz, CDCl₃) δ 159.0, 146.6 (q, *J* = 34 Hz), 138.3, 121.8 (q, *J* = 274 Hz), 117.7, 108.9 (q, *J* = 3 Hz), 56.9, 53.1 (2C), 50.9, 44.9 (2C), 36.5 (2C), 35.7, 34.1, 32.2 (2C); IR (neat) 1604 cm⁻¹; HRMS (ESI) *m/z* [M + H]⁺ calcd for C₁₈H₂₈F₃N₄ 357.2261, found 357.2255.

trans-4-(2-(4-(3-Chloro-5-ethyl-2-methoxyphenyl)piperazin-1-yl)ethyl)cyclohexan-1-amine (5e).—General procedure C was followed using **4e** (1.10 g, 2.29 mmol) and TFA (7.0 mL, 91 mmol) in DCM (16 mL). After work-up, **5e** (0.87 g, 2.3 mmol, 100% yield) was isolated as a clear, orange oil. *R_f* = 0.1 (10% MeOH/DCM); ¹H NMR (400 MHz, CDCl₃) δ 6.83 (d, *J* = 1.9 Hz, 1H), 6.61 (d, *J* = 2.0 Hz, 1H), 3.83 (s, 3H), 3.20–3.04 (m, 4H), 2.65–2.49 (m, 6H), 2.44–2.37 (m, 2H), 1.84 (d, *J* = 11.9 Hz, 2H), 1.76 (d, *J* = 12.0 Hz, 2H), 1.47–1.33 (m, 4H), 1.30–1.15 (m, 5H), 1.13–0.93 (m, 4H); ¹³C NMR (101 MHz, CDCl₃) δ 146.5, 146.3, 140.9, 128.3, 122.3, 116.8, 59.1, 57.0, 54.0 (2C), 50.9, 50.4 (2C), 36.9 (2C), 35.8, 34.2, 32.3 (2C), 28.6, 15.6; IR (neat) 1593, 1565 cm⁻¹; HRMS (MALDI) *m/z* [M + H]⁺ calcd for C₂₁H₃₅ClN₃O 380.2463, found 380.2467.

3-(trans-4-(2-(4-(2,3-Dichlorophenyl)piperazin-1-yl)ethyl)cyclohexyl)-1,1-dimethylurea (cariprazine).—General procedure D was followed using **5a** (1.00 g, 2.81 mmol) and *N,N*-dimethylcarbonyl chloride (0.33 mL, 3.6 mmol) in DCM

(28 mL). After work-up, the crude product was purified by chromatography (40 g of silica gel, 0–60% EtOAc/hexanes) to afford cariprazine (1.02 g, 2.39 mmol, 85% yield) as a white solid. R_f = 0.5 (10% MeOH/DCM); $^1\text{H NMR}$ (400 MHz, CDCl_3) δ 7.17–7.10 (m, 2H), 6.95 (dd, J = 6.3, 3.2 Hz, 1H), 4.11 (d, J = 7.6 Hz, 1H), 3.64–3.52 (m, 1H), 3.15–2.98 (m, 4H), 2.88 (s, 6H), 2.71–2.53 (m, 4H), 2.47–2.38 (m, 2H), 2.07–1.96 (m, 2H), 1.83–1.70 (m, 2H), 1.49–1.39 (m, 2H), 1.30–1.18 (m, 1H), 1.16–1.01 (m, 4H); $^{13}\text{C NMR}$ (101 MHz, CDCl_3) δ 158.0, 151.5, 134.2, 127.7, 127.6, 124.6, 118.7, 56.8, 53.6 (2C), 51.5 (2C), 50.0, 36.3 (2C), 35.8, 34.2 (2C), 34.1, 32.3 (2C); IR (neat) 3338, 1622 cm^{-1} ; mp 212–213 °C (dec); HRMS (MALDI) m/z $[\text{M} + \text{H}]^+$ calcd for $\text{C}_{21}\text{H}_{33}\text{Cl}_2\text{N}_4\text{O}$ 427.2026, found 427.2023; t_R = 32.1 min (HPLC, basic). The HCl salt was precipitated from 0.03 M solution of the free base in 50% CHCl_3 /acetone using a 2.0 M solution of HCl in Et_2O (5.0 equiv). Dec >200 °C. Anal. calcd for $\text{C}_{21}\text{H}_{32}\text{Cl}_2\text{N}_4\text{O}\cdot 2\text{HCl}$: C, 50.41; H, 6.85; N, 11.20. Found: C, 50.43; H, 6.84; N, 11.01.

3-(trans-4-(2-(4-(2-Chloro-3-ethylphenyl)piperazin-1-yl)ethyl)cyclohexyl)-1,1-dimethylurea (6b).—General procedure D was followed using **5b** (0.500 g, 1.43 mmol) and *N,N*-dimethylcarbonyl chloride (0.16 mL, 1.8 mmol) in DCM (20 mL). After work-up, the crude product was purified by chromatography (silica gel, 0–10% MeOH/ CHCl_3) to afford **6b** (0.414 g, 0.983 mmol, 69% yield) as a yellow solid. $^1\text{H NMR}$ (400 MHz, CDCl_3) δ 7.15 (t, J = 7.7 Hz, 1H), 6.97–6.89 (m, 2H), 4.11 (d, J = 7.6 Hz, 1H), 3.63–3.53 (m, 1H), 3.14–2.98 (m, 4H), 2.88 (s, 6H), 2.77 (q, J = 7.6 Hz, 2H), 2.72–2.54 (m, 4H), 2.46–2.38 (m, 2H), 2.07–1.97 (m, 2H), 1.83–1.72 (m, 2H), 1.48–1.40 (m, 2H), 1.30–1.18 (m, 1H), 1.22 (t, J = 7.5 Hz, 3H), 1.15–1.01 (m, 4H); $^{13}\text{C NMR}$ (101 MHz, CDCl_3) δ 158.0, 149.8, 143.4, 128.8, 127.0, 124.1, 118.1, 56.9, 53.7 (2C), 51.7 (2C), 50.0, 36.3 (2C), 35.8, 34.2 (2C), 34.1, 32.3, 27.6, 14.2; t_R = 20.3 min (HPLC, acidic). The HCl salt was precipitated from 50% acetone/ CHCl_3 using a 2.0 M solution of HCl in Et_2O . Dec >200 °C. Anal. calcd for $\text{C}_{23}\text{H}_{37}\text{ClN}_4\text{O}\cdot\text{HCl}\cdot\text{H}_2\text{O}$: C, 58.10; H, 8.48; N, 11.78. Found: C, 58.32; H, 8.24; N, 11.56.

3-(trans-4-(2-(4-(2-Fluoro-3-methoxyphenyl)piperazin-1-yl)ethyl)cyclohexyl)-1,1-dimethylurea (6c).—General procedure D was followed using **5c** (0.189 g, 0.565 mmol) and *N,N*-dimethylcarbonyl chloride (66 μL , 0.72 mmol) in DCM (5.6 mL). After work-up, the crude product was purified by chromatography (12 g of silica gel, 0–10% MeOH/DCM) to afford **6c** (0.179 g, 0.440 mmol, 78% yield) as a white solid. R_f = 0.5 (10% MeOH/DCM); $^1\text{H NMR}$ (400 MHz, CDCl_3) δ 6.95 (dt, J = 8.3, 1.8 Hz, 1H), 6.66–6.52 (m, 2H), 4.12 (d, J = 7.6 Hz, 1H), 3.85 (s, 3H), 3.63–3.50 (m, 1H), 3.18–3.01 (m, 4H), 2.87 (s, 6H), 2.68–2.50 (m, 4H), 2.44–2.35 (m, 2H), 2.05–1.94 (m, 2H), 1.82–1.70 (m, 2H), 1.47–1.38 (m, 2H), 1.30–1.16 (m, 1H), 1.14–0.99 (m, 4H); $^{13}\text{C NMR}$ (101 MHz, CDCl_3) δ 157.9, 148.7 (d, J = 10 Hz), 145.8 (d, J = 245 Hz), 141.2 (d, J = 6 Hz), 123.6 (d, J = 5 Hz), 111.2 (d, J = 2 Hz), 107.1, 56.8, 56.6, 53.6 (2C), 50.8 (d, J = 3 Hz, 2C), 50.0, 36.3 (2C), 35.8, 34.2 (2C), 34.1, 32.2 (2C); IR (film) 3342, 1626 cm^{-1} ; mp 159–160 °C (dec); HRMS (ESI) m/z $[\text{M} + \text{H}]^+$ calcd for $\text{C}_{22}\text{H}_{36}\text{FN}_4\text{O}_2$ 407.2817, found 407.2811; t_R = 22.2 min (HPLC, basic). The HCl salt was precipitated from a 0.03 M solution of the free base in 50% CHCl_3 /acetone using a 2.0 M solution of HCl in Et_2O (5.0 equiv). mp 175–177 °C (dec). Anal. calcd for $\text{C}_{22}\text{H}_{35}\text{FN}_4\text{O}_2\cdot 2\text{HCl}\cdot 1.25\text{H}_2\text{O}$: C, 52.64; H, 7.93; N, 11.16. Found: C, 52.50; H, 7.79; N, 11.01.

1,1-Dimethyl-3-(trans-4-(2-(4-(6-(trifluoromethyl)pyridine-2-yl)piperazin-1-yl)ethyl)cyclohexyl)urea (6d).—General procedure D was followed using **5d** (0.232 g, 0.651 mmol) and *N,N*-dimethylcarbonyl chloride (80 μ L, 0.81 mmol) in DCM (9.5 mL). After work-up, the crude product was purified by chromatography (silica gel, 0–10% MeOH/CHCl₃) to afford **6d** (0.107 g, 0.249 mmol, 38% yield) as a white solid. ¹H NMR (400 MHz, CDCl₃) δ 7.55 (t, *J* = 8.2 Hz, 1H), 6.92 (d, *J* = 7.7 Hz, 1H), 6.75 (d, *J* = 8.5 Hz, 1H), 4.11 (d, *J* = 7.7 Hz, 1H), 3.65–3.52 (m, 5H), 2.88 (s, 6H), 2.57–2.46 (m, 4H), 2.43–2.35 (m, 2H), 2.05–1.96 (m, 2H), 1.83–1.72 (m, 2H), 1.47–1.39 (m, 2H), 1.32–1.18 (m, 1H), 1.16–1.00 (m, 4H); ¹³C NMR (101 MHz, CDCl₃) δ 159.0, 158.0, 146.6 (q, *J* = 34 Hz), 138.3, 121.8 (q, *J* = 274 Hz), 109.5, 108.9 (q, *J* = 3 Hz), 56.8, 53.1 (2C), 50.0, 44.9 (2C), 36.3 (2C), 35.8, 34.2 (2C), 34.0, 32.2 (2C); HRMS (MALDI) *m/z* [M + H]⁺ calcd for C₂₁H₃₃F₃N₅O 428.2632, found 428.2629; *t*_R = 18.5 min (HPLC, acidic).

3-(trans-4-(2-(4-(3-Chloro-5-ethyl-2-methoxyphenyl)piperazin-1-yl)ethyl)cyclohexyl)-1,1-dimethylurea (6e).—General procedure D was followed using **5e** (0.275 g, 0.723 mmol) and *N,N*-dimethylcarbonyl chloride (82 μ L, 0.90 mmol) in DCM (10 mL). After work-up, the crude product was purified by chromatography (silica gel, 0–10% MeOH/CHCl₃) to afford **6e** (0.215 g, 0.477 mmol, 66% yield) as an off-white solid. ¹H NMR (400 MHz, CDCl₃) δ 6.87 (d, *J* = 1.9 Hz, 1H), 6.63 (d, *J* = 2.0 Hz, 1H), 4.13 (d, *J* = 7.6 Hz, 1H), 3.82 (s, 3H), 3.64–3.49 (m, 1H), 3.46–3.21 (m, 4H), 3.06–2.77 (m, 4H), 2.87 (s, 6H), 2.76–2.60 (m, 2H), 2.54 (q, *J* = 7.6 Hz, 2H), 2.08–1.97 (m, 2H), 1.83–1.72 (m, 2H), 1.67–1.54 (m, 2H), 1.39–1.25 (m, 1H), 1.19 (t, *J* = 7.6 Hz, 3H), 1.16–1.02 (m, 4H); ¹³C NMR (101 MHz, CDCl₃) δ 158.0, 146.6, 146.4, 140.9, 128.4, 122.3, 116.8, 66.0, 59.1, 56.9, 54.0 (2C), 50.4 (2C), 50.0, 36.3 (2C), 35.8, 34.2 (2C), 32.2 (2C), 28.6, 15.4. The HCl salt was precipitated from 50% CHCl₃/acetone using a 2.0 M solution of HCl in Et₂O. Dec >189 °C. Anal. calcd for C₂₄H₃₉ClN₄O₂•2HCl: C, 55.02; H, 7.89; N, 10.69. Found: C, 54.96; H, 7.88; N, 10.54.

1-(trans-4-(2-(4-(2,3-Dichlorophenyl)piperazin-1-yl)ethyl)cyclohexyl)-3-methylurea (7a).—General procedure D was followed using **5a** (0.250 g, 0.702 mmol) and *N*-methylcarbonyl chloride (83.0 mg, 0.456 mmol) in DCM (10 mL). After work-up, the crude product was purified by chromatography (silica gel, 0–10% MeOH/CHCl₃) to afford **7a** (0.141 g, 0.341 mmol, 49% yield) as a white solid. ¹H NMR (400 MHz, CDCl₃) δ 7.19–7.13 (m, 2H), 6.97 (dd, *J* = 5.7, 3.9 Hz, 1H), 5.11–5.05 (m, 1H), 5.00 (d, *J* = 8.0 Hz, 1H), 3.53–3.40 (m, 1H), 3.18–2.94 (m, 4H), 2.72 (d, *J* = 4.7 Hz, 3H), 2.68–2.55 (m, 4H), 2.47–2.38 (m, 2H), 2.04–1.92 (m, 2H), 1.82–1.70 (m, 2H), 1.49–1.39 (m, 2H), 1.30–1.19 (m, 1H), 1.14–1.00 (m, 4H); ¹³C NMR (101 MHz, CDCl₃) δ 158.6, 151.1, 133.6, 127.3, 127.1, 124.3, 118.5, 56.4, 53.1 (2C), 51.1 (2C), 48.9, 35.3, 33.7 (3C), 31.9 (2C), 26.5. The HCl salt was precipitated from a 0.02 M solution of the free base in 50% CHCl₃/acetone using a 2.0 M solution of HCl in Et₂O (35 equiv). Dec >175 °C. Anal. calcd for C₂₀H₃₀Cl₂N₄O•HCl•1.25H₂O: C, 50.85; H, 7.15; N, 11.86. Found: C, 50.86; H, 6.86; N, 11.60.

1-(trans-4-(2-(4-(2-Chloro-3-ethylphenyl)piperazin-1-yl)ethyl)cyclohexyl)-3-methylurea (7b).—General procedure D was followed using **5b** (0.172

g, 0.491 mmol) and *N*-methylcarbonyl chloride (0.139 g, 1.47 mmol) in DCM (15 mL). After work-up, the crude product was purified by chromatography (silica gel, 0–10% MeOH/CHCl₃) to afford **7b** (0.150 g, 0.368 mmol, 75% yield) as a white solid. ¹H NMR (400 MHz, CDCl₃) δ 7.15 (t, *J* = 7.7 Hz, 1H), 6.96–6.90 (m, 2H), 4.28–4.21 (m, 1H), 4.15 (d, *J* = 8.0 Hz, 1H), 3.51–3.39 (m, 1H), 3.16–2.94 (m, 4H), 2.81–2.73 (m, 5H), 2.72–2.52 (m, 4H), 2.46–2.36 (m, 2H), 2.06–1.94 (m, 2H), 1.85–1.69 (m, 2H), 1.49–1.41 (m, 2H), 1.22 (t, *J* = 7.5 Hz, 3H), 1.31–1.17 (m, 1H), 1.15–1.01 (m, 4H); ¹³C NMR (101 MHz, CDCl₃) δ 158.3, 149.8, 143.4, 128.8, 127.0, 124.1, 118.1, 56.8, 53.7 (2C), 51.7 (2C), 49.8, 35.7, 34.09, 34.06 (2C), 32.2 (2C), 27.6, 27.4, 14.2. The HCl salt was precipitated from a 0.03 M solution of the free base in 50% CHCl₃/acetone using a 2.0 M solution of HCl in Et₂O (29 equiv). Dec >199 °C. Anal. calcd for C₂₂H₃₅ClN₄O•HCl•1.25H₂O: C, 56.71; H, 8.33; N, 12.02. Found: C, 56.54; H, 7.92; N, 11.94.

1-(trans-4-(2-(4-(3-Chloro-5-ethyl-2-methoxyphenyl)piperazin-1-yl)ethyl)cyclohexyl)-3-methylurea (7e).—General procedure

D was followed using **5e** (0.420 g, 1.11 mmol) and *N*-methylcarbonyl chloride (0.130 g, 1.38 mmol) in DCM (15 mL). After work-up, the crude product was purified by chromatography (silica gel, 0–10% MeOH/CHCl₃) to afford **7e** (0.416 g, 0.952 mmol, 86% yield) as a white solid. ¹H NMR (400 MHz, CDCl₃) δ 6.84 (d, *J* = 2.0 Hz, 1H), 6.61 (d, *J* = 2.0 Hz, 1H), 4.16 (d, *J* = 5.1 Hz, 1H), 4.08 (d, *J* = 8.0 Hz, 1H), 3.83 (s, 3H), 3.52–3.40 (m, 1H), 3.22–3.05 (m, 4H), 2.77 (d, *J* = 4.9 Hz, 3H), 2.66–2.49 (m, 6H), 2.44–2.36 (m, 2H), 2.06–1.95 (m, 2H), 1.84–1.73 (m, 2H), 1.48–1.40 (m, 2H), 1.31–1.23 (m, 1H), 1.20 (t, *J* = 7.6 Hz, 3H), 1.15–1.01 (m, 4H); ¹³C NMR (101 MHz, CDCl₃) δ 158.3, 146.5, 146.3, 141.0, 128.4, 122.3, 116.8, 59.2, 56.9, 54.0 (2C), 50.4 (2C), 49.9, 35.7, 34.1 (2C), 34.0, 32.2 (2C), 28.6, 27.4, 15.6. The HCl salt was precipitated from a 0.04 M solution of the free base in 50% CHCl₃/acetone using a 2.0 M solution of HCl in Et₂O (27 equiv). Dec >220 °C. Anal. calcd for C₂₃H₃₇ClN₄O₂•2HCl•1.25H₂O: C, 51.88; H, 7.86; N, 10.52. Found: C, 51.89; H, 7.60; N, 10.36.

1-(trans-4-(2-(4-(2,3-Dichlorophenyl)piperazin-1-yl)ethyl)cyclohexyl)urea (8a).

—To a solution of **5a** (0.108 g, 0.303 mmol) and KOCN (0.256 g, 3.16 mmol) in H₂O (1.5 mL) and THF (3.0 mL) was added a 1.0 M aq solution of HCl (1.5 mL, 1.5 mmol) over 3 min. After stirring overnight, the reaction was quenched with a saturated aq solution of NaHCO₃ (20 mL), and the aq layer was extracted with EtOAc (2 × 20 mL). The combined organic layers were dried over Na₂SO₄, filtered, and concentrated. The crude product was purified by chromatography (12 g of silica gel, 0–10% MeOH/DCM) to afford **8a** (71.3 mg, 0.179 mmol, 59% yield) as a white solid. *R*_f = 0.3 (10% MeOH/DCM); ¹H NMR (400 MHz, CDCl₃) δ 7.18–7.10 (m, 2H), 6.95 (dd, *J* = 6.5, 3.1 Hz, 1H), 4.38–4.23 (m, 3H), 3.50–3.37 (m, 1H), 3.16–2.97 (m, 4H), 2.72–2.52 (m, 4H), 2.42 (t, *J* = 8.0 Hz, 2H), 2.08–1.96 (m, 2H), 1.85–1.64 (m, 3H), 1.51–1.39 (m, 2H), 1.17–0.99 (m, 4H); ¹³C NMR (101 MHz, CDCl₃) δ 157.8, 151.5, 134.2, 127.7, 127.6, 124.7, 118.7, 56.7, 53.6 (2C), 51.5 (2C), 50.2, 35.6, 34.1, 33.8 (2C), 32.1 (2C); IR (neat) 3477, 3329, 1645 cm⁻¹; mp 212–213 °C (dec); HRMS (MALDI) *m/z* [M + H]⁺ calcd for C₁₉H₂₉Cl₂N₄O 399.1713, found 399.1711; *t*_R = 24.9 min (HPLC, basic).

1-(trans-4-(2-(4-(3-Chloro-5-ethyl-2-methoxyphenyl)piperazin-1-yl)ethyl)cyclohexyl)urea (8e).—The same procedure as the one described for **8a** was followed starting from **5e** (0.203 g, 0.534 mmol). After work-up, the crude product was purified by chromatography (12 g of silica gel, 0–10% MeOH/DCM) to afford **8e** (93.0 mg, 0.220 mmol, 41% yield) as a tan solid. R_f = 0.3 (10% MeOH/DCM); $^1\text{H NMR}$ (400 MHz, CDCl_3) δ 6.83 (d, J = 2.0 Hz, 1H), 6.61 (d, J = 2.0 Hz, 1H), 4.58–4.33 (m, 3H), 3.83 (s, 3H), 3.49–3.34 (m, 1H), 3.26–2.99 (m, 4H), 2.68–2.48 (m, 6H), 2.45–2.34 (m, 2H), 2.06–1.94 (m, 2H), 1.85–1.70 (m, 2H), 1.48–1.38 (m, 2H), 1.30–1.22 (m, 1H), 1.19 (t, J = 7.6 Hz, 3H), 1.16–1.00 (m, 4H); $^{13}\text{C NMR}$ (101 MHz, CDCl_3) δ 158.2, 146.5, 146.3, 140.9, 128.3, 122.3, 116.8, 59.1, 56.8, 54.0 (2C), 50.4 (2C), 50.0, 35.6, 34.0, 33.8 (2C), 32.1 (2C), 28.6, 15.6; IR (neat) 3492, 3348, 1647 cm^{-1} ; mp 163–166 °C (dec); HRMS (MALDI) m/z $[\text{M} + \text{H}]^+$ calcd for $\text{C}_{22}\text{H}_{36}\text{ClN}_4\text{O}_2$ 423.2521, found 423.2518; t_R = 32.0 min (HPLC, basic).

N-(trans-4-(2-(4-(2,3-Dichlorophenyl)piperazin-1-yl)ethyl)cyclohexyl)-7,8-dihydro-1,6-naphthyridine-6(5H)-carboxamide (9a).—Using oven-dried glassware under an Ar atmosphere, a solution of NEt_3 (0.21 mL, 1.5 mmol) in anhydrous THF (3.5 mL) was cooled to 0 °C, and a 15 wt% solution of phosgene in toluene (0.40 mL, 0.56 mmol) was added over 3 min. Next, a solution of **5a** (0.179 g, 0.502 mmol) in anhydrous THF (3.5 mL) was added over 3 min, and the reaction was stirred for 1 h. Then, a solution of 5,6,7,8-tetrahydro-1,6-naphthyridine (80.5 mg, 0.600 mmol) in anhydrous THF (3.5 mL) was added over 3 min, and the reaction was allowed to warm to rt. After stirring for 19 h, the reaction was quenched with a saturated aq solution of NaHCO_3 (40 mL), and the aq layer was extracted with EtOAc (40 mL). The organic layer was dried over anhydrous Na_2SO_4 , filtered, and concentrated. The crude product was purified by chromatography (12 g of silica gel, 0–10% MeOH/DCM) to afford **9a** (35.1 mg, 68.0 μmol , 14% yield) as a white solid. R_f = 0.4 (10% MeOH/DCM); $^1\text{H NMR}$ (400 MHz, CDCl_3) δ 8.42 (d, J = 4.2 Hz, 1H), 7.42 (d, J = 7.6 Hz, 1H), 7.17–7.10 (m, 3H), 6.95 (dd, J = 6.4, 3.2 Hz, 1H), 4.57 (s, 2H), 4.32 (d, J = 7.6 Hz, 1H), 3.71–3.57 (m, 3H), 3.14–2.96 (m, 6H), 2.76–2.52 (m, 4H), 2.47–2.39 (m, 2H), 2.08–2.00 (m, 2H), 1.83–1.75 (m, 2H), 1.48–1.39 (m, 2H), 1.30–1.20 (m, 1H), 1.18–1.03 (m, 4H); $^{13}\text{C NMR}$ (101 MHz, CDCl_3) δ 156.9, 155.0, 151.4, 148.0, 134.2, 134.1, 129.1, 127.62, 127.56, 124.6, 121.7, 118.7, 56.8, 53.5 (2C), 51.5 (2C), 50.1, 45.0, 41.6, 35.8, 34.08 (2C), 34.05, 32.2 (3C); IR (neat) 3326, 1620 cm^{-1} ; mp 163–164 °C (dec); HRMS (MALDI) m/z $[\text{M} + \text{H}]^+$ calcd for $\text{C}_{27}\text{H}_{36}\text{Cl}_2\text{N}_5\text{O}$ 516.2291, found 516.2283; t_R = 33.8 min (HPLC, basic).

N-(trans-4-(2-(4-(2-Chloro-3-ethylphenyl)piperazin-1-yl)ethyl)cyclohexyl)-7,8-dihydro-1,6-naphthyridine-6(5H)-carboxamide (9b).—The same procedure as the one described for **9a** was followed starting from **5b** (0.205 g, 0.586 mmol). After work-up, the crude product was purified by chromatography (12 g of silica gel, 0–10% MeOH/DCM) to afford **9b** (0.192 g, 0.376 mmol, 64% yield) as a white solid. R_f = 0.4 (10% MeOH/DCM); $^1\text{H NMR}$ (400 MHz, CDCl_3) δ 8.42 (d, J = 4.7 Hz, 1H), 7.43 (d, J = 7.7 Hz, 1H), 7.18–7.10 (m, 2H), 6.93 (t, J = 7.2 Hz, 2H), 4.57 (s, 2H), 4.32 (d, J = 7.5 Hz, 1H), 3.71–3.59 (m, 3H), 3.12–2.98 (m, 6H), 2.77 (q, J = 7.5 Hz, 2H), 2.71–2.54 (m, 4H), 2.47–2.39 (m, 2H), 2.10–2.01 (m, 2H), 1.84–1.74 (m, 2H), 1.50–1.40 (m, 2H), 1.30–1.18 (m, 1H), 1.22 (t, J = 7.5 Hz, 3H), 1.15–1.04

(m, 4H); ^{13}C NMR (101 MHz, CDCl_3) δ 156.9, 155.1, 149.8, 148.0, 143.4, 134.2, 129.1, 128.8, 127.0, 124.1, 121.7, 118.1, 56.9, 53.7 (2C), 51.7 (2C), 50.2, 45.0, 41.6, 35.8, 34.1 (3C), 32.2 (3C), 27.6, 14.4; IR (neat) 3323, 1619 cm^{-1} ; mp 58–60 °C; HRMS (MALDI) m/z $[\text{M} + \text{H}]^+$ calcd for $\text{C}_{29}\text{H}_{41}\text{ClN}_5\text{O}$ 510.2994, found 510.2988; $t_{\text{R}} = 35.2$ min (HPLC, basic).

***N*-(*trans*-4-(2-(4-(2,3-Dichlorophenyl)piperazin-1-yl)ethyl)cyclohexyl)-1*H*-indole-2-carboxamide (10a).**—General procedure E was followed

using **5a** (0.101 g, 0.283 mmol) and 1*H*-indole-2-carboxylic acid (62.0 mg, 0.385 mmol) in CHCl_3 (8.0 mL). After work-up, the crude product was purified by chromatography (12 g of silica gel, 0–10% MeOH/DCM) to afford **10a** (20.2 mg, 40.2 μmol , 14% yield) as a white solid. $R_f = 0.5$ (10% MeOH/DCM); ^1H NMR (400 MHz, CDCl_3) δ 9.22 (s, 1H), 7.64 (d, $J = 8.0$ Hz, 1H), 7.43 (d, $J = 8.3$ Hz, 1H), 7.32–7.28 (m, 1H), 7.19–7.10 (m, 3H), 6.97 (dd, $J = 6.5, 3.1$ Hz, 1H), 6.80 (s, 1H), 5.95 (d, $J = 8.2$ Hz, 1H), 4.03–3.89 (m, 1H), 3.17–2.00 (m, 4H), 2.76–2.55 (m, 4H), 2.47 (t, $J = 7.9$ Hz, 2H), 2.13 (d, $J = 11.8$ Hz, 2H), 1.86 (d, $J = 12.4$ Hz, 2H), 1.54–1.42 (m, 2H), 1.37–1.10 (m, 5H); ^{13}C NMR (101 MHz, CDCl_3) δ 160.8, 151.4, 136.2, 134.2, 131.2, 127.9, 127.7, 127.6, 124.7, 124.6, 122.0, 120.8, 118.7, 112.0, 101.6, 56.7, 53.6 (2C), 51.5 (2C), 49.1, 35.6, 34.0, 33.4 (2C), 32.1 (2C); IR (neat) 3616, 3268, 1624 cm^{-1} ; mp 240–241 °C (dec); HRMS (MALDI) m/z $[\text{M} + \text{H}]^+$ calcd for $\text{C}_{27}\text{H}_{33}\text{Cl}_2\text{N}_4\text{O}$ 499.2026, found 499.2025; $t_{\text{R}} = 37.8$ min (HPLC, basic).

***N*-(*trans*-4-(2-(4-(2-Chloro-3-ethylphenyl)piperazin-1-yl)ethyl)cyclohexyl)indole-2-carboxamide (10b).**—General

procedure E was followed using **5b** (0.100 g, 0.286 mmol) and 1*H*-indole-2-carboxylic acid (58.0 mg, 0.360 mmol) in CHCl_3 (10 mL). After work-up, the crude product was purified by chromatography (silica gel, 0–50% EtOAc/hexanes) to afford **10b** (70 mg, 0.142 mmol, 50% yield) as an off-white solid. ^1H NMR (400 MHz, CDCl_3) δ 9.16 (s, 1H), 7.64 (d, $J = 8.0$ Hz, 1H), 7.43 (d, $J = 8.4$ Hz, 1H), 7.31–7.26 (m, 1H), 7.18–7.11 (m, 2H), 6.97–6.92 (m, 2H), 6.80 (dd, $J = 2.1, 0.9$ Hz, 1H), 5.94 (d, $J = 8.2$ Hz, 1H), 4.00–3.89 (m, 1H), 3.16–2.98 (m, 4H), 2.78 (q, $J = 7.5$ Hz, 2H), 2.73–2.55 (m, 4H), 2.50–2.41 (m, 2H), 2.17–2.08 (m, 2H), 1.90–1.82 (m, 2H), 1.53–1.45 (m, 2H), 1.38–1.10 (m, 7H); ^{13}C NMR (101 MHz, CDCl_3) δ 160.8, 149.8, 143.4, 136.2, 131.2, 128.9, 127.9, 127.0, 124.6, 124.1, 122.0, 120.8, 118.2, 112.0, 101.6, 56.8, 53.8 (2C), 51.8 (2C), 49.1, 35.7, 34.1, 33.4 (2C), 32.1 (2C), 27.6, 14.3. The HCl salt was precipitated from 50% CHCl_3 /acetone using a 2.0 M solution of HCl in Et_2O . Anal. calcd for $\text{C}_{29}\text{H}_{37}\text{ClN}_4\text{O} \cdot \text{HCl} \cdot 0.75\text{H}_2\text{O}$: C, 64.14; H, 7.33; N, 10.32. Found: C, 64.11; H, 7.09; N, 10.04.

***N*-(*trans*-4-(2-(4-(3-Chloro-5-ethyl-2-methoxyphenyl)piperazin-1-yl)ethyl)cyclohexyl)indole-2-carboxamide (10e).**—General procedure

E was followed using **5e** (0.125 g, 0.329 mmol) and 1*H*-indole-2-carboxylic acid (58.3 mg, 0.362 mmol) in CHCl_3 (8.0 mL). After work-up, the crude product was purified by chromatography (silica gel, 0–10% MeOH/ CHCl_3) to afford **10e** (0.133 g, 0.254 mmol, 77% yield) as a white solid. ^1H NMR (400 MHz, CDCl_3) δ 9.33 (s, 1H), 7.64 (d, $J = 8.0$ Hz, 1H), 7.44 (d, $J = 8.3$ Hz, 1H), 7.33–7.24 (m, 1H), 7.14 (t, $J = 7.5$ Hz, 1H), 6.85 (s, 1H), 6.81 (s, 1H), 6.62 (s, 1H), 5.97 (d, $J = 8.2$ Hz, 1H), 4.02–3.90 (m, 1H), 3.85 (s, 3H), 3.25–3.06 (m, 4H), 2.69–2.51 (m, 6H), 2.47–2.40 (m, 2H), 2.17–2.08 (m, 2H),

1.90–1.81 (m, 2H), 1.53–1.44 (m, 2H), 1.39–1.09 (m, 8H). The HCl salt was precipitated from a 0.06 M solution of the free base in 50% CHCl₃/acetone using a 2.0 M solution of HCl in Et₂O (20 equiv). Dec >220 °C. Anal. calcd for C₃₀H₃₉ClN₄O₂•2HCl•0.25H₂O: C, 60.00; H, 6.97; N, 9.33. Found: C, 60.16; H, 7.10; N, 9.12.

***N*-(*trans*-4-(2-(4-(2,3-Dichlorophenyl)piperazin-1-yl)ethyl)cyclohexyl)quinoline-4-carboxamide (11a).**—General procedure E was followed using **5a** (0.221 g, 0.620 mmol) and quinoline-4-carboxylic acid (0.118 g, 0.680 mmol) in CHCl₃ (15 mL). Note: The reaction mixture was washed with a 1.0 M aq solution of NaOH. After work-up, the crude product was purified by chromatography (24 g of silica gel, 0–10% MeOH/DCM) to afford **11a** (0.231 g, 0.451 mmol, 73% yield) as a white solid. *R*_f = 0.5 (10% MeOH/DCM); ¹H NMR (400 MHz, CDCl₃) δ 8.89 (d, *J* = 4.3 Hz, 1H), 8.18 (d, *J* = 8.4 Hz, 1H), 8.12 (d, *J* = 8.4 Hz, 1H), 7.75 (ddd, *J* = 8.4, 6.8, 1.2 Hz, 1H), 7.60 (ddd, *J* = 8.3, 6.9, 1.2 Hz, 1H), 7.38 (d, *J* = 4.3 Hz, 1H), 7.17–7.11 (m, 2H), 6.96 (dd, *J* = 6.4, 3.1 Hz, 1H), 5.96 (d, *J* = 8.2 Hz, 1H), 4.10–3.98 (m, 1H), 3.18–2.94 (m, 4H), 2.75–2.51 (m, 4H), 2.50–2.38 (m, 2H), 2.24–2.12 (m, 2H), 1.92–1.81 (m, 2H), 1.54–1.43 (m, 2H), 1.37–1.11 (m, 5H); ¹³C NMR (101 MHz, CDCl₃) δ 166.7, 151.4, 150.0, 148.8, 142.5, 134.2, 130.1, 130.0, 127.8, 127.64, 127.57, 125.3, 124.7, 124.6, 118.7, 118.4, 56.7, 53.6 (2C), 51.5 (2C), 49.6, 35.6, 34.0, 33.2 (2C), 32.0 (2C); IR (neat) 3274, 1633 cm⁻¹; mp 222–223 °C (dec); HRMS (ESI) *m/z* [M + H]⁺ calcd for C₂₈H₃₃Cl₂N₄O 511.2026, found 511.2024; *t*_R = 36.0 min (HPLC, basic). The HCl salt was precipitated from 1 0.03 M solution of the free base in 50% CHCl₃/acetone using a 2.0 M solution of HCl in Et₂O (14 equiv). Dec >270 °C. Anal. calcd for C₂₈H₃₂Cl₂N₄O•2HCl•0.5H₂O: C, 56.67; H, 5.95; N, 9.44. Found: C, 56.68; H, 5.81; N, 9.34.

***N*-(*trans*-4-(2-(4-(2-Chloro-3-ethylphenyl)piperazin-1-yl)ethyl)cyclohexyl)quinoline-4-carboxamide (11b).**—General procedure E was followed using **5b** (0.125 g, 0.358 mmol) and quinoline-4-carboxylic acid (68.0 mg, 0.393 mmol) in CHCl₃ (9.0 mL). After work-up, the crude product was purified by chromatography (silica gel, 0–8% MeOH/CHCl₃) to afford **11b** (0.185 g, mmol, ~100% yield) as a white solid, which was purified further by HCl salt formation. ¹H NMR (400 MHz, CDCl₃) δ 8.90 (d, *J* = 4.3, 1H), 8.19 (d, *J* = 8.5 Hz, 1H), 8.13 (d, *J* = 8.5 Hz, 1H), 7.75 (t, *J* = 7.7 Hz, 1H), 7.60 (t, *J* = 7.7 Hz, 1H), 7.39 (d, *J* = 4.3, 1H), 7.18–1.7.12 (m, 1H), 6.94 (t, *J* = 7.6 Hz, 2H), 5.94 (d, *J* = 8.3 Hz, 1H), 4.11–3.98 (m, 1H), 3.19–2.95 (m, 4H), 2.77 (q, *J* = 7.3 Hz, 2H), 2.72–2.51 (m, 4H), 2.50–2.41 (m, 2H), 2.23–2.15 (m, 2H), 1.91–1.83 (m, 2H), 1.54–1.45 (m, 2H), 1.41–1.11 (m, 8H); ¹³C NMR (101 MHz, CDCl₃) δ 166.7, 150.0, 149.8, 148.8, 143.4, 142.5, 130.2, 130.1, 128.8, 127.8, 127.0, 125.3, 124.6, 124.1, 118.5, 118.1, 56.8, 53.7 (2C), 51.7 (2C), 49.6, 35.6, 34.0, 33.2 (2C), 32.0 (2C), 27.6, 14.3. The HCl salt was precipitated from 50% CHCl₃/acetone using a 2.0 M solution of HCl in Et₂O. Dec >250 °C. Anal. calcd for C₃₀H₃₇ClN₄O•2HCl•2H₂O: C, 58.68; H, 7.06; N, 9.12. Found: C, 58.74; H, 6.97; N, 8.94.

***N*-(*trans*-4-(2-(4-(6-(Trifluoromethyl)pyridin-2-yl)piperazin-1-yl)ethyl)cyclohexyl)quinoline-4-carboxamide (11d).**—General procedure E was followed using

5d (0.234 g, 0.656 mmol) and quinoline-4-carboxylic acid (0.125 g, 0.720 mmol) in CHCl_3 (16 mL). Note: The reaction mixture was washed with a 1.0 M aq solution of NaOH. After work-up, the crude product was purified by chromatography (24 g of silica gel, 0–10% MeOH/DCM) to afford **11d** (0.234 g, 0.458 mmol, 70% yield) as a white solid. $R_f = 0.2$ (5% MeOH/DCM); $^1\text{H NMR}$ (400 MHz, CDCl_3) δ 8.88 (d, $J = 4.3$ Hz, 1H), 8.18 (d, $J = 8.5$ Hz, 1H), 8.11 (d, $J = 8.4$ Hz, 1H), 7.74 (ddd, $J = 8.4, 6.9, 1.4$ Hz, 1H), 7.63–7.52 (m, 2H), 7.37 (d, $J = 4.3$ Hz, 1H), 6.93 (d, $J = 7.3$ Hz, 1H), 6.76 (d, $J = 8.7$ Hz, 1H), 5.98 (d, $J = 8.2$ Hz, 1H), 4.10–3.97 (m, 1H), 3.61–3.53 (m, 4H), 2.60–2.47 (m, 4H), 2.46–2.35 (m, 2H), 2.23–2.14 (m, 2H), 1.91–1.82 (m, 2H), 1.53–1.43 (m, 2H), 1.38–1.10 (m, 5H); $^{13}\text{C NMR}$ (101 MHz, CDCl_3) δ 166.7, 159.0, 150.0, 148.8, 146.5 (q, $J = 34$ Hz), 142.5, 138.4, 130.1, 130.0, 127.8, 125.3, 124.6, 121.8 (q, $J = 274$ Hz), 118.4, 109.5, 109.0 (q, $J = 3$ Hz), 56.7, 53.1 (2C), 49.6, 44.9 (2C), 35.5, 33.9, 33.2 (2C), 32.0 (2C); IR (neat) 3328, 1635 cm^{-1} ; mp 187–188 °C (dec); HRMS (ESI) m/z $[\text{M} + \text{H}]^+$ calcd for $\text{C}_{28}\text{H}_{33}\text{F}_3\text{N}_5\text{O}$ 512.2632, found 512.2627; $t_R = 34.3$ min (HPLC, basic). The HCl salt was precipitated from a 0.03 M solution of the free base in 50% CHCl_3 /acetone using a 2.0 M solution of HCl in Et_2O (14 equiv). mp 292–294 °C (dec). Anal. calcd for $\text{C}_{28}\text{H}_{32}\text{F}_3\text{N}_5\text{O} \cdot 2\text{HCl} \cdot 0.25\text{H}_2\text{O}$: C, 57.10; H, 5.90; N, 11.89. Found: C, 57.06; H, 5.93; N, 11.78.

***N*-trans-4-(2-(4-(2,3-Dichlorophenyl)piperazin-1-yl)ethyl)cyclohexyl)-4-(pyridin-3-yl)benzamide (12a).**—General procedure E was followed

using **5a** (0.101 g, 0.284 mmol) and 4-(pyridin-3-yl)benzoic acid•HCl (73.1 mg, 0.310 mmol) in CHCl_3 (8.0 mL). After work-up, the crude product was purified by chromatography (12 g of silica gel, 0–10% MeOH/DCM) to afford **12a** (0.120 g, 0.224 mmol, 79% yield) as a white solid. $R_f = 0.5$ (10% MeOH/DCM); $^1\text{H NMR}$ (400 MHz, CDCl_3) δ 8.88–8.84 (m, 1H), 8.63 (d, $J = 4.9$ Hz, 1H), 7.92–7.83 (m, 3H), 7.67–7.61 (m, 2H), 7.39 (dd, $J = 7.9, 4.8$ Hz, 1H), 7.18–7.10 (m, 1H), 6.96 (dd, $J = 6.3, 3.2$ Hz, 1H), 5.98 (d, $J = 8.1$ Hz, 1H), 4.02–3.90 (m, 1H), 3.16–2.97 (m, 4H), 2.74–2.53 (m, 4H), 2.49–2.40 (m, 2H), 4.02–3.90 (m, 2H), 2.18–2.09 (m, 2H), 1.89–1.80 (m, 2H), 1.54–1.42 (m, 2H), 1.37–1.00 (m, 5H); $^{13}\text{C NMR}$ (101 MHz, CDCl_3) δ 166.3, 151.5, 149.3, 148.5, 140.9, 135.7, 134.7, 134.5, 134.5, 134.2, 127.8 (2C), 127.7, 127.6, 127.4 (2C), 123.8, 118.7, 56.7, 53.6 (2C), 51.5 (2C), 49.4, 35.7, 34.1 (2C), 33.3, 32.1 (2C); IR (neat) 3269, 1629 cm^{-1} ; mp 257–258 °C (dec); HRMS (MALDI) m/z $[\text{M} + \text{H}]^+$ calcd for $\text{C}_{30}\text{H}_{35}\text{Cl}_2\text{N}_4\text{O}$ 537.2182, found 537.2185; $t_R = 36.9$ min (HPLC, basic).

***N*-(trans-4-(2-(4-(2-Chloro-3-ethylphenyl)piperazin-1-yl)ethyl)cyclohexyl)-4-(pyridine-3-yl)benzamide (12b).**—General procedure E was followed using

5b (101 mg, 0.289 mmol) and 4-(pyridine-3-yl)benzoic acid•HCl (74.8 mg, 0.317 mmol) in CHCl_3 (8.0 mL). After work-up, the crude product was purified by chromatography (silica gel, 0–10% MeOH/ CHCl_3) to afford **12b** (0.150 g, 0.282 mmol, 98% yield) as a white solid. $^1\text{H NMR}$ (400 MHz, CDCl_3) δ 8.86 (s, 1H), 8.63 (s, 1H), 7.94–7.81 (m, 3H), 7.69–7.61 (m, 2H), 7.43–7.34 (m, 1H), 7.19–7.11 (m, 1H), 6.98–6.90 (m, 2H), 5.95 (d, $J = 8.0$ Hz, 1H), 4.03–3.90 (m, 1H), 3.19–2.96 (m, 4H), 2.78 (q, $J = 7.6$ Hz, 2H), 2.73–2.52 (m, 4H), 2.51–2.40 (m, 2H), 2.19–2.08 (m, 2H), 1.92–1.81 (m, 2H), 1.54–1.45 (m, 2H), 1.37–1.11 (m, 8H); $^{13}\text{C NMR}$ (101 MHz, CDCl_3) δ 166.3, 149.8, 149.3, 148.5, 143.4, 140.9, 135.8, 134.7, 134.6, 128.9, 127.8, 127.4, 127.0, 124.1, 123.8, 118.2, 56.8, 53.8 (2C),

51.7 (2C), 49.4, 35.7, 34.1, 33.4 (2C), 32.1 (2C), 27.6, 14.3. The HCl salt was precipitated from a 0.02 M solution of the free base in 50% CHCl₃/acetone using a 2.0 M solution of HCl in Et₂O (44 equiv). Dec >223 °C. Anal. calcd for C₃₂H₃₉ClN₄O•2HCl•2.25H₂O: C, 59.63; H, 7.12; N, 8.69. Found: C, 59.24; H, 6.82; N, 8.54.

***N*-(*trans*-4-(2-(4-(2,3-Dichlorophenyl)piperazin-1-yl)ethyl)cyclohexyl)-3-methoxypropanamide (13a).**—General procedure F was followed using **5a**

(0.85 g, 2.4 mmol). After work-up, the crude product was purified by chromatography (40 g of silica gel, 0–5% MeOH/DCM) to afford **13a** (1.04 g, 2.35 mmol, 99% yield) as a white solid. *R*_f = 0.5 (10% MeOH/DCM); ¹H NMR (400 MHz, CDCl₃) δ 7.17–7.11 (m, 2H), 6.95 (dd, *J* = 6.4, 3.2 Hz, 1H), 5.95 (d, *J* = 8.2 Hz, 1H), 3.77–3.66 (m, 1H), 3.62 (t, *J* = 5.8 Hz, 2H), 3.36 (s, 3H), 3.17–2.98 (m, 4H), 2.73–2.52 (m, 4H), 2.47–2.37 (m, 4H), 2.04–1.92 (m, 2H), 1.82–1.72 (m, 2H), 1.47–1.38 (m, 2H), 1.31–1.18 (m, 1H), 1.17–1.01 (m, 4H); ¹³C NMR (101 MHz, CDCl₃) δ 170.7, 151.4, 134.2, 127.65, 127.57, 124.7, 118.7, 69.0, 58.9, 56.7, 53.6 (2C), 51.5 (2C), 48.6, 37.4, 35.6, 34.0, 33.2 (2C), 32.0 (2C); IR (neat) 3279, 1635 cm⁻¹; mp 180–181 °C (dec); HRMS (MALDI) *m/z* [M + H]⁺ calcd for C₂₂H₃₄Cl₂N₃O₂ 442.2023, found 442.2023; *t*_R = 30.3 min (HPLC, basic). The HCl salt was precipitated from a 0.03 M solution of the free base in 50% CHCl₃/acetone using a 2.0 M solution of HCl in Et₂O (5.0 equiv). Dec >235 °C. Anal. calcd for C₂₂H₃₃Cl₂N₃O₂•HCl•0.75H₂O: C, 53.66; H, 7.27; N, 8.53. Found: C, 53.54; H, 6.95; N, 8.49.

***N*-(*trans*-4-(2-(4-(2-Chloro-3-ethylphenyl)piperazin-1-yl)ethyl)cyclohexyl)-3-methoxypropanamide (13b).**—General procedure F was followed using **5b**

(0.197 g, 0.563 mmol). After work-up, the crude product was purified by chromatography (silica gel, 0–5% MeOH/CHCl₃) to afford **13b** (0.245 g, 0.562 mmol, 100% yield) as an off-white solid. ¹H NMR (400 MHz, CDCl₃) δ 7.15 (t, *J* = 7.8 Hz, 1H), 6.96–6.91 (m, 2H), 5.93 (d, *J* = 8.2 Hz, 1H), 3.77–3.66 (m, 1H), 3.63 (t, *J* = 5.8 Hz, 2H), 3.36 (s, 3H), 3.13–2.98 (m, 4H), 2.77 (q, *J* = 7.5 Hz, 2H), 2.71–2.53 (m, 4H), 2.46–2.39 (m, 4H), 2.03–1.95 (m, 2H), 1.82–1.73 (m, 2H), 1.48–1.41 (m, 2H), 1.32–1.25 (m, 1H), 1.22 (t, *J* = 7.5 Hz, 3H), 1.17–1.02 (m, 4H); ¹³C NMR (101 MHz, CDCl₃) δ 170.7, 149.8, 143.4, 128.9, 127.0, 124.1, 118.2, 69.0, 58.9, 56.8, 53.7 (2C), 51.8 (2C), 48.6, 37.4, 35.7, 34.1, 33.2 (2C), 32.0 (2C), 27.6, 14.3. The HCl salt was precipitated from a 0.04 M solution of the free base in 50% CHCl₃/acetone using a 2.0 M solution of HCl in Et₂O (22 equiv). Dec >240 °C. Anal. calcd for C₂₈H₃₈ClN₃O₂•HCl: C, 61.01; H, 8.32; N, 8.89. Found: C, 60.82; H, 8.21; N, 8.81.

***N*-(*trans*-4-(2-(4-(2-Fluoro-3-methoxyphenyl)piperazin-1-yl)ethyl)cyclohexyl)-3-methoxypropanamide (13c).**—General procedure F was followed using **5c** (0.243 g,

0.724 mmol). After work-up, the crude product was purified by chromatography (24 g of silica gel, 0–5% MeOH/DCM) to afford **13c** (0.159 g, 0.377 mmol, 52% yield) as a tan solid. *R*_f = 0.2 (5% MeOH/DCM); ¹H NMR (400 MHz, CDCl₃) δ 6.96 (td, *J* = 8.3, 1.8 Hz, 1H), 6.66–6.54 (m, 2H), 5.95 (d, *J* = 8.2 Hz, 1H), 3.86 (s, 3H), 3.76–3.65 (m, 1H), 3.61 (t, *J* = 5.8 Hz, 2H), 3.35 (s, 3H), 3.15–3.03 (m, 4H), 2.66–2.53 (m, 4H), 2.45–2.35 (m, 4H), 2.03–1.92 (m, 2H), 1.81–1.72 (m, 2H), 1.48–1.38 (m, 2H), 1.30–1.18 (m, 1H), 1.16–1.00 (m, 4H); ¹³C NMR (101 MHz, CDCl₃) δ 170.6, 148.7 (d, *J* = 10 Hz), 145.8 (d, *J* = 245 Hz), 141.2 (d, *J* = 6 Hz), 123.6 (d, *J* = 5 Hz), 111.2 (d, *J* =

2 Hz), 107.2, 69.0, 58.9, 56.8, 56.6, 53.6 (2C), 50.8 (d, $J = 3$ Hz, 2C), 48.5, 37.4, 35.6, 34.0, 33.2 (2C), 32.0 (2C); IR (neat) 3275, 1635 cm^{-1} ; mp 156–157 °C (dec); HRMS (ESI) m/z $[\text{M} + \text{H}]^+$ calcd for $\text{C}_{23}\text{H}_{37}\text{FN}_3\text{O}_3$ 422.2813, found 422.2807; $t_{\text{R}} = 21.6$ min (HPLC, basic). The HCl salt was precipitated from a 0.03 M solution of the free base in 50% CHCl_3 /acetone using a 2.0 M solution of HCl in Et_2O (5.0 equiv). mp 211–213 °C (dec). Anal. calcd for $\text{C}_{23}\text{H}_{36}\text{FN}_3\text{O}_3 \cdot 2\text{HCl} \cdot 2\text{H}_2\text{O}$: C, 52.07; H, 7.98; N, 7.92. Found: C, 51.96; H, 7.64; N, 7.78.

3-Methoxy-*N*-(*trans*-4-(2-(4-(6-(trifluoromethyl)pyridin-2-yl)piperazin-1-yl)ethyl)cyclohexyl)propenamide (13d).—General procedure F was

followed using **5d** (0.424 g, 1.19 mmol). After work-up, the crude product was purified by chromatography (40 g of silica gel, 0–5% MeOH/ CHCl_3) to afford **13d** (0.289 g, 0.654 mmol, 55% yield) as a white solid. $R_f = 0.2$ (5% MeOH/DCM); ^1H NMR (400 MHz, CDCl_3) δ 7.56 (t, $J = 8.1$ Hz, 1H), 6.93 (d, $J = 6.8$ Hz, 1H), 6.76 (d, $J = 8.6$ Hz, 1H), 5.95 (d, $J = 8.2$ Hz, 1H), 3.77–3.66 (m, 1H), 3.65–3.54 (m, 6H), 3.36 (s, 3H), 2.58–2.47 (m, 4H), 2.44–2.33 (m, 4H), 2.04–1.92 (m, 2H), 1.83–1.73 (m, 2H), 1.48–1.39 (m, 2H), 1.32–1.21 (m, 1H), 1.17–1.01 (m, 4H); ^{13}C NMR (101 MHz, CDCl_3) δ 170.6, 159.0, 146.6 (q, $J = 35$ Hz), 138.4, 121.8 (q, $J = 274$ Hz), 109.5, 108.9, 69.0, 58.9, 56.8, 53.1 (2C), 48.5, 44.9 (2C), 37.4, 35.6, 33.9, 33.2 (2C), 32.0 (2C); IR (film) 3277, 1634 cm^{-1} ; mp 167–168 °C (dec); HRMS (ESI) m/z $[\text{M} + \text{H}]^+$ calcd for $\text{C}_{22}\text{H}_{34}\text{F}_3\text{N}_4\text{O}_2$ 443.2628, found 443.2625; $t_{\text{R}} = 14.5$ min (HPLC, acidic). The HCl salt was precipitated from a 0.04 M solution of the free base in 50% CHCl_3 /acetone using a 2.0 M solution of HCl in Et_2O (3.0 equiv). Note: Et_2O was added to initiate precipitation. Dec >229 °C. Anal. calcd for $\text{C}_{22}\text{H}_{33}\text{F}_3\text{N}_4\text{O}_2 \cdot \text{HCl} \cdot 0.5\text{H}_2\text{O}$: C, 54.15; H, 7.23; N, 11.48. Found: C, 53.96; H, 6.99; N, 11.50.

***N*-(*trans*-4-(2-(4-(3-Chloro-5-ethyl-2-methoxyphenyl)piperazin-1-yl)ethyl)cyclohexyl)-3-methoxypropanamide (13e).**—General procedure

F was followed using **5e** (0.87 g, 2.3 mmol). After work-up, the crude product was purified by chromatography (40 g of silica gel, 0–5% MeOH/DCM) to afford **13e** (0.89 g, 1.9 mmol, 83% yield) as a white solid. $R_f = 0.2$ (5% MeOH/DCM); ^1H NMR (400 MHz, CDCl_3) δ 6.85 (d, $J = 2.0$ Hz, 1H), 6.61 (d, $J = 2.0$ Hz, 1H), 6.02 (d, $J = 8.1$ Hz, 1H), 3.83 (s, 3H), 3.75–3.65 (m, 1H), 3.62 (t, $J = 5.8$ Hz, 2H), 3.36 (s, 3H), 3.24–3.10 (m, 4H), 2.77–2.62 (m, 4H), 2.58–2.46 (m, 4H), 2.41 (t, $J = 5.8$ Hz, 2H), 1.97 (d, $J = 9.7$ Hz, 2H), 1.78 (d, $J = 10.2$ Hz, 2H), 1.15–1.42 (m, 2H), 1.33–1.22 (m, 1H), 1.19 (t, $J = 7.6$ Hz, 3H), 1.15–1.01 (m, 4H); ^{13}C NMR (101 MHz, CDCl_3) δ 170.6, 146.4, 146.0, 140.8, 128.2, 122.3, 116.7, 68.8, 59.0, 58.7, 56.6, 53.8 (2C), 50.0 (2C), 48.4, 37.2, 35.4, 33.6, 33.0 (2C), 31.8 (2C), 28.4, 15.4; IR (neat) 3303, 1634 cm^{-1} ; mp 118–120 °C; HRMS (MALDI) m/z $[\text{M} + \text{H}]^+$ calcd for $\text{C}_{25}\text{H}_{41}\text{ClN}_3\text{O}_3$ 466.2831, found 466.2824; $t_{\text{R}} = 35.1$ min (HPLC, basic). The HCl salt was precipitated from a 0.03 M solution of the free base in 50% CHCl_3 /acetone using a 2.0 M solution of HCl in Et_2O (5.0 equiv). Dec >240 °C. Anal. calcd for $\text{C}_{25}\text{H}_{40}\text{ClN}_3\text{O}_3 \cdot 2\text{HCl} \cdot 0.25\text{H}_2\text{O}$: C, 55.25; H, 7.88; N, 7.73. Found: C, 55.06; H, 7.69; N, 7.62.

***tert*-Butyl 4-(2-methoxy-2-oxoethylidene)piperidine-1-carboxylate (15).**—Using oven-dried glassware under an Ar atmosphere, a mixture of 90 wt% NaH (0.521 g, 19.5 mmol) in anhydrous THF (76 mL) was cooled to 0 °C, and methyl 2-

(dimethoxyphosphoryl)acetate (3.2 mL, 20 mmol) was added over 10 min. After stirring the mixture vigorously for 30 min, a solution of *tert*-butyl 4-oxopiperidine-1-carboxylate (3.01 g, 15.1 mmol) in anhydrous THF (38 mL) was added over 10 min. The reaction was allowed to warm to rt and stirred for an additional 18 h. Then, H₂O (50 mL) was added, and the aq layer was extracted with EtOAc (2 × 50 mL). The combined organic layers were washed with brine (50 mL), dried over anhydrous Na₂SO₄, filtered, and concentrated. The crude product was purified by chromatography (80 g of silica gel, 0–20% EtOAc/hexanes) to afford **15** (3.69 g, 14.5 mmol, 96% yield) as a white solid. *R_f* = 0.4 (20% EtOAc/hexanes); ¹H NMR (400 MHz, CDCl₃) δ 5.71 (s, 1H), 3.69 (s, 3H), 3.54–3.43 (m, 4H), 2.97–2.89 (m, 2H), 2.31–2.23 (m, 2H), 1.47 (s, 9H); ¹³C NMR (101 MHz, CDCl₃) δ 166.9, 158.4, 154.7, 115.0, 80.0, 51.2, 44.7 (2C), 36.6, 29.7, 28.6 (3C); IR (neat) 1711, 1680, 1655 cm⁻¹; mp 64–65 °C; HRMS (MALDI) *m/z* [M + Na]⁺ calcd for C₁₃H₂₁NNaO₄ 278.1363, found 278.1367.

***tert*-Butyl 4-(2-methoxy-2-oxoethyl)piperidine-1-carboxylate (16).**—Using a Parr shaker, a mixture of **15** (2.00 g, 7.84 mmol), 10 wt% Pd/C (0.839 g, 0.787 mmol), and MeOH (60 mL) was agitated under H₂ (50 psi) for 5 h. Afterward, the mixture was passed through a pad of Celite (ca. 30 g) using EtOAc (3 × 50 mL), and the filtrate was concentrated. The crude product was purified by chromatography (40 g of silica gel, 0–20% EtOAc/hexanes) to afford **16** (1.81 g, 7.03 mmol, 90% yield) as a clear, colorless oil. *R_f* = 0.3 (20% EtOAc/hexanes); ¹H NMR (400 MHz, CDCl₃) δ 4.21–3.96 (m, 2H), 3.67 (s, 3H), 2.71 (t, *J* = 12.9 Hz, 2H), 2.24 (d, *J* = 7.1 Hz, 2H), 1.98–1.86 (m, 1H), 1.68 (d, *J* = 13.1 Hz, 2H), 1.44 (s, 9H), 1.22–1.07 (m, 2H); ¹³C NMR (101 MHz, CDCl₃) δ 173.0, 154.9, 79.5, 51.6, 43.8 (2C), 41.0, 33.2, 32.0 (2C), 28.6 (3C); IR (neat) 1737, 1688 cm⁻¹; HRMS (MALDI) *m/z* [M + Na]⁺ calcd for C₁₃H₂₃NNaO₄ 280.1519, found 280.1525.

***tert*-Butyl 4-(2-oxoethyl)piperidine-1-carboxylate (17a).**—Using oven-dried glassware under an Ar atmosphere, a solution of **16** (1.10 g, 4.27 mmol) in anhydrous DCM (33 mL) was cooled to –78 °C, and a 1.0 M solution of DIBALH in toluene (5.4 mL, 5.4 mmol) was added over 5 min. The reaction was stirred for 3 h and allowed to warm to rt. Then, a saturated aq solution of Rochelle salt (60 mL) was added, and the aq layer was extracted with DCM (3 × 30 mL). The combined organic layers were dried over Na₂SO₄, filtered, and concentrated. The crude product was purified by chromatography (80 g of silica gel, 0–40% EtOAc/hexanes) to afford **17a** (0.492 g, 2.17 mmol, 51% yield) as a clear, colorless oil. *R_f* = 0.5 (40% EtOAc/hexanes); ¹H NMR (400 MHz, CDCl₃) δ 9.80–9.76 (m, 1H), 4.21–3.96 (m, 2H), 2.73 (t, *J* = 12.8 Hz, 2H), 2.38 (d, *J* = 6.7 Hz, 2H), 2.11–1.98 (m, 1H), 1.68 (d, *J* = 13.2 Hz, 2H), 1.45 (s, 9H), 1.24–1.09 (m, 2H); ¹³C NMR (101 MHz, CDCl₃) δ 201.6, 154.9, 79.6, 50.3, 43.9 (2C), 32.1 (2C), 30.8, 28.6 (3C); IR (neat) 1722, 1686 cm⁻¹; HRMS (MALDI) *m/z* [M + Na]⁺ calcd for C₁₂H₂₁NNaO₃ 250.1414, found 250.1416.

***tert*-Butyl 4-(3-oxopropyl)piperidine-1-carboxylate (17b).**—General procedure A was followed using *tert*-butyl 4-(3-hydroxypropyl)piperidine-1-carboxylate (1.02 g, 4.18 mmol). After work-up, the crude product was purified by chromatography (40 g of silica gel, 0–30% EtOAc/hexanes) to afford **17b** (0.769 g, 3.19 mmol, 76% yield) as a clear, colorless

oil. R_f = 0.4 (30% EtOAc/hexanes); ^1H NMR (400 MHz, CDCl_3) δ 9.77 (t, J = 1.3 Hz, 1H), 4.22–3.94 (m, 2H), 2.65 (t, J = 13.1 Hz, 2H), 2.46 (td, J = 7.5, 1.7 Hz, 2H), 1.68–1.54 (m, 4H), 1.44 (s, 9H), 1.42–1.33 (m, 1H), 1.15–1.02 (m, 2H); ^{13}C NMR (101 MHz, CDCl_3) δ 202.4, 154.9, 79.4, 44.0 (2C), 41.3, 35.6, 32.0 (2C), 28.58 (3C), 28.55; IR (neat) 1724, 1686 cm^{-1} ; HRMS (MALDI) m/z [$\text{M} + \text{Na}$] $^+$ calcd for $\text{C}_{13}\text{H}_{23}\text{NNaO}_3$ 264.1570, found 264.1575.

tert-Butyl 4-(2-(4-(2,3-dichlorophenyl)piperazin-1-yl)ethyl)piperidine-1-carboxylate (19a).—General procedure B was followed using **17a** (0.486 g, 2.14 mmol) and 1-(2,3-dichlorophenyl)piperazine•HCl (0.688 g, 3.22 mmol) in DCE (14 mL). After work-up, the crude product was purified by chromatography (40 g of silica gel, 0–80% EtOAc/hexanes) to afford **19a** (0.61 g, 1.4 mmol, 64% yield) as a white solid. R_f = 0.3 (80% EtOAc/hexanes); ^1H NMR (400 MHz, CDCl_3) δ 7.18–7.10 (m, 2H), 6.95 (dd, J = 6.5, 3.1 Hz, 1H), 4.18–3.94 (m, 2H), 3.15–2.96 (m, 4H), 2.78–2.52 (m, 6H), 2.49–2.40 (m, 2H), 1.67 (d, J = 13.0 Hz, 2H), 1.52–1.39 (m, 3H), 1.45 (s, 9H), 1.20–1.05 (m, 2H); ^{13}C NMR (101 MHz, CDCl_3) δ 155.0, 151.4, 134.2, 127.7, 127.6, 124.7, 118.7, 79.4, 56.3, 53.6 (2C), 51.5 (2C), 44.2 (2C), 34.7, 33.7, 32.4 (2C), 28.6 (3C); IR (neat) 1682 cm^{-1} ; mp 116–117 °C; HRMS (MALDI) m/z [$\text{M} + \text{H}$] $^+$ calcd for $\text{C}_{22}\text{H}_{34}\text{Cl}_2\text{N}_3\text{O}_2$ 442.2023, found 442.2021.

tert-Butyl 4-(3-(4-(2,3-dichlorophenyl)piperazin-1-yl)propyl)piperidine-1-carboxylate (19b).—General procedure B was followed using **17b** (0.764 g, 3.17 mmol) and 1-(2,3-dichlorophenyl)piperazine•HCl (0.933 g, 3.49 mmol) in DCE (31 mL). After work-up, the crude product was purified by chromatography (40 g of silica gel, 0–100% EtOAc/hexanes) to afford **19b** (0.884 g, 1.94 mmol, 61% yield) as a clear, orange oil. R_f = 0.2 (EtOAc); ^1H NMR (400 MHz, CDCl_3) δ 7.19–7.07 (m, 2H), 6.95 (dd, J = 6.4, 3.1 Hz, 1H), 4.19–3.95 (m, 2H), 3.17–2.96 (m, 4H), 2.78–2.48 (m, 6H), 2.43–2.35 (m, 2H), 1.71–1.62 (m, 2H), 1.61–1.49 (m, 2H), 1.45 (s, 9H), 1.42–1.33 (m, 1H), 1.30–1.22 (m, 2H), 1.15–1.01 (m, 2H); ^{13}C NMR (101 MHz, CDCl_3) δ 155.0, 151.4, 134.2, 127.7, 127.6, 124.7, 118.7, 79.3, 59.0, 53.5 (2C), 51.5 (2C), 44.2 (2C), 36.2, 34.5, 32.4 (2C), 28.6 (3C), 24.2; IR (film) 1692 cm^{-1} ; HRMS (ESI) m/z [$\text{M} + \text{H}$] $^+$ calcd for $\text{C}_{23}\text{H}_{36}\text{Cl}_2\text{N}_3\text{O}_2$ 456.2179, found 456.2175.

1-(2,3-Dichlorophenyl)-4-(2-(piperidin-4-yl)ethyl)piperazine (20a).—General procedure C was followed using **19a** (0.250 g, 0.566 mmol) and TFA (7.0 mL, 91 mmol) in DCM (37 mL). After work-up, **20a** (0.191 g, 0.558 mmol, 99% yield) was isolated as a tan solid. R_f = 0.1 (10% MeOH/DCM); ^1H NMR (400 MHz, CDCl_3) δ 7.16–7.10 (m, 2H), 6.95 (dd, J = 6.4, 3.2 Hz, 1H), 3.14–2.94 (m, 6H), 2.73–2.49 (m, 6H), 2.47–2.38 (m, 2H), 1.73–1.55 (m, 3H), 1.51–1.34 (m, 3H), 1.00–1.06 (m, 2H); ^{13}C NMR (101 MHz, CDCl_3) δ 151.5, 134.1, 127.64, 127.56, 124.6, 118.7, 56.3, 53.6 (2C), 51.5 (2C), 47.0 (2C), 35.0, 34.5, 34.0 (2C); IR (neat) 1577 cm^{-1} ; mp 78–80 °C; HRMS (MALDI) m/z [$\text{M} + \text{H}$] $^+$ calcd for $\text{C}_{17}\text{H}_{26}\text{Cl}_2\text{N}_3$ 342.1498, found 342.1500.

1-(2,3-Dichlorophenyl)-4-(3-(piperidin-4-yl)propyl)piperazine (20b).—General procedure C was followed using **19b** (0.244 g, 0.535 mmol) and TFA (1.6 mL, 21 mmol) in DCM (3.7 mL). After work-up, **20b** (0.188 g, 0.527 mmol, 99% yield) was isolated as a clear, yellow oil. R_f = 0.1 (10% MeOH/DCM); ^1H NMR (400 MHz, CDCl_3) δ 7.16–7.08

(m, 2H), 6.98–6.90 (m, 1H), 2.17–2.92 (m, 6H), 2.74–2.49 (m, 6H), 2.42–2.31 (m, 2H), 1.95–1.77 (m, 1H), 1.72–1.60 (m, 2H), 1.59–1.43 (m, 2H), 1.42–1.16 (m, 3H), 1.15–0.98 (m, 2H); ^{13}C NMR (101 MHz, CDCl_3) δ 151.5, 134.2, 127.7, 127.6, 124.7, 118.7, 59.0, 53.5 (2C), 51.5 (2C), 46.0 (2C), 35.8, 34.7, 32.2 (2C), 24.1; IR (neat) 1577 cm^{-1} ; HRMS (ESI) m/z $[\text{M} + \text{H}]^+$ calcd for $\text{C}_{18}\text{H}_{28}\text{Cl}_2\text{N}_3$ 356.1655, found 356.1652.

4-(2-(4-(2,3-Dichlorophenyl)piperazin-1-yl)ethyl)-*N,N*-dimethylpiperidine-1-carboxamide (21a).—General procedure D was followed using **20a**

(0.184 g, 0.538 mmol) and *N,N*-dimethylcarbonyl chloride (65 μL , 0.71 mmol) in DCM (5.4 mL). After work-up, the crude product was purified by chromatography (12 g of silica gel, 0–10% MeOH/DCM) to afford **21a** (0.159 g, 0.385 mmol, 71% yield) as a tan solid. $R_f = 0.5$ (10% MeOH/DCM); ^1H NMR (400 MHz, CDCl_3) δ 7.17–7.10 (m, 2H), 6.95 (dd, $J = 6.4, 3.1$ Hz, 1H), 3.68–3.60 (m, 2H), 3.14–2.94 (m, 4H), 2.80 (s, 6H), 2.72 (td, $J = 12.7, 2.3$ Hz, 2H), 2.67–2.52 (m, 4H), 2.48–2.40 (m, 2H), 1.73–1.65 (m, 2H), 1.53–1.40 (m, 3H), 1.28–1.13 (m, 2H); ^{13}C NMR (101 MHz, CDCl_3) δ 165.3, 151.4, 134.1, 127.64, 127.57, 124.7, 118.7, 56.3, 53.6 (2C), 51.5 (2C), 47.3 (2C), 38.7 (2C), 34.9, 33.8, 32.4 (2C); IR (neat) 1640 cm^{-1} ; mp 96–97 $^\circ\text{C}$; HRMS (MALDI) m/z $[\text{M} + \text{H}]^+$ calcd for $\text{C}_{20}\text{H}_{31}\text{Cl}_2\text{N}_4\text{O}$ 413.1869, found 413.1870; $t_R = 32.6$ min (HPLC, basic).

4-(3-(4-(2,3-Dichlorophenyl)piperazin-1-yl)propyl)-*N,N*-dimethylpiperidine-1-carboxamide (21b).—General procedure D was followed using **20b** (0.188

g, 0.527 mmol) and *N,N*-dimethylcarbonyl chloride (65 μL , 0.71 mmol) in DCM (5.5 mL). After work-up, the crude product was purified by chromatography (12 g of silica gel, 0–10% MeOH/DCM) to afford **21b** (0.176 g, 0.410 mmol, 78% yield) as a tan, amorphous solid. $R_f = 0.5$ (10% MeOH/DCM); ^1H NMR (400 MHz, CDCl_3) δ 7.17–7.10 (m, 2H), 6.95 (dd, $J = 6.3, 3.3$ Hz, 1H), 3.68–3.59 (m, 2H), 3.16–2.96 (m, 4H), 2.80 (s, 6H), 2.75–2.51 (m, 6H), 2.43–2.34 (m, 2H), 1.73–1.69 (m, 2H), 1.60–1.48 (m, 2H), 1.45–1.34 (m, 1H), 1.31–1.22 (m, 2H), 1.21–1.08 (m, 2H); ^{13}C NMR (101 MHz, CDCl_3) δ 165.3, 151.4, 134.1, 127.63, 127.56, 124.7, 118.7, 59.0, 53.5 (2C), 51.5 (2C), 47.3 (2C), 38.7 (2C), 36.4, 34.6, 32.3 (2C), 24.2; IR (film) 1643 cm^{-1} ; mp 71–73 $^\circ\text{C}$; HRMS (ESI) m/z $[\text{M} + \text{H}]^+$ calcd for $\text{C}_{21}\text{H}_{33}\text{Cl}_2\text{N}_4\text{O}$ 427.2026, found 427.2021; $t_R = 35.5$ min (HPLC, basic).

1-(4-(2-(4-(2,3-Dichlorophenyl)piperazin-1-yl)ethyl)piperidin-1-yl)-3-methoxypropan-1-one (22a).—General procedure F was

followed using **20a** (0.192 g, 0.560 mmol). After work-up, the crude product was purified by chromatography (12 g of silica gel, 0–10% MeOH/DCM) to afford **22a** (0.121 g, 0.283 mmol, 50% yield) as a tan solid. $R_f = 0.5$ (10% MeOH/DCM); ^1H NMR (400 MHz, CDCl_3) δ 7.19–7.11 (m, 2H), 6.96 (dd, $J = 7.0, 2.6$ Hz, 1H), 4.61 (d, $J = 13.3$ Hz, 1H), 3.87 (d, $J = 13.5$ Hz, 1H), 3.70 (t, $J = 6.7$ Hz, 2H), 3.36 (s, 3H), 3.18–2.95 (m, 5H), 2.82–2.64 (m, 4H), 2.60 (t, $J = 6.7$ Hz, 2H), 2.57–2.44 (m, 3H), 1.74 (t, $J = 12.1$ Hz, 2H), 1.64–1.45 (m, 3H), 1.23–1.07 (m, 2H); ^{13}C NMR (101 MHz, CDCl_3) δ 169.2, 151.3, 134.2, 127.7, 127.6, 124.8, 118.7, 69.0, 59.0, 56.2, 53.5 (2C), 51.3 (2C), 46.1, 42.0, 34.7, 33.7, 33.4, 33.0, 32.1; IR (neat) 1644 cm^{-1} ; mp 88–90 $^\circ\text{C}$; HRMS (MALDI) m/z $[\text{M} + \text{H}]^+$ calcd for $\text{C}_{21}\text{H}_{32}\text{Cl}_2\text{N}_3\text{O}_2$ 428.1866, found 428.1860; $t_R = 27.4$ min (HPLC, basic).

1-(4-(3-(4-(2,3-Dichlorophenyl)piperazin-1-yl)propyl)piperidin-1-yl)-3-methoxypropan-1-one (22b).—General procedure F was

followed using **20b** (0.183 g, 0.513 mmol). After work-up, the crude product was purified by chromatography (24 g of silica gel, 0–5% MeOH/DCM) to afford **22b** (0.175 g, 0.396 mmol, 77% yield) as a clear, orange oil. R_f = 0.2 (5% MeOH/DCM); $^1\text{H NMR}$ (400 MHz, CDCl_3) δ 7.21–7.11 (m, 2H), 7.01–6.94 (m, 1H), 4.69–4.55 (m, 1H), 3.95–3.83 (m, 1H), 3.76–3.64 (m, 2H), 3.36 (s, 3H), 3.21–3.04 (m, 4H), 3.03–2.93 (m, 1H), 2.85–2.66 (m, 4H), 2.65–2.42 (m, 5H), 1.82–1.68 (m, 2H), 1.66–1.42 (m, 3H), 1.36–1.21 (m, 2H), 1.18–1.01 (m, 2H); $^{13}\text{C NMR}$ (101 MHz, CDCl_3) δ 169.2, 151.1, 134.2, 127.7, 127.6, 125.0, 118.8, 69.0, 59.0, 58.9, 53.5 (2C), 51.1 (2C), 46.1, 42.1, 36.2, 34.2, 33.7, 32.9, 32.0, 23.8; IR (neat) 1634 cm^{-1} ; HRMS (ESI) m/z $[\text{M} + \text{H}]^+$ calcd for $\text{C}_{22}\text{H}_{34}\text{Cl}_2\text{N}_3\text{O}_2$ 442.2023, found 442.2019; t_R = 17.8 min (HPLC, acidic). The HCl salt was prepared from a 0.03 M solution of the free base in 50% CHCl_3 /acetone using a 2.0 M solution of HCl in Et_2O (15 equiv). The solution was concentrated, and the resulting residue was sonicated with hexanes to obtain a yellow solid, which was recrystallized from CHCl_3 —hexanes (slow evaporation of solvent mixture). Mp 193–194 °C (dec). Anal. calcd for $\text{C}_{22}\text{H}_{33}\text{Cl}_2\text{N}_3\text{O}_2 \cdot \text{HCl} \cdot 0.25\text{H}_2\text{O}$: C, 54.66; H, 7.19; N, 8.69. Found: C, 54.37; H, 7.04; N, 8.52.

tert-Butyl 3-allyl-3-hydroxypyrrolidine-1-carboxylate (24a).—Using oven-dried glassware under an Ar atmosphere, a solution of *tert*-butyl 3-oxopyrrolidine-1-carboxylate (1.52 g, 8.21 mmol) in anhydrous Et_2O (50 mL) was cooled to 0 °C. Then, a 1.0 M solution of allyl magnesium bromide in Et_2O (9.8 mL, 9.8 mmol) was added over 5 min, and the mixture was allowed to warm to rt. After stirring for 4 h, the reaction was quenched with a saturated aq solution of NH_4Cl (10 mL), and the aq layer was extracted with Et_2O (3 \times 10 mL). The combined organic layers were washed with brine, dried over Na_2SO_4 , filtered, and concentrated. The crude product was purified by chromatography (40 g of silica gel, 0–30% EtOAc/hexanes) to afford **24a** (1.11 g, 4.88 mmol, 60% yield) as a clear, yellow oil. R_f = 0.2 (30% EtOAc/hexanes); $^1\text{H NMR}$ (400 MHz, CDCl_3 , mixture of rotamers) δ 5.94–5.79 (m, 1H), 5.25–5.15 (m, 2H), 3.59–3.42 (m, 2H), 3.41–3.20 (m, 2H), 2.39 (d, J = 7.5 Hz, 2H), 1.90–1.80 (m, 3H), 1.46 (s, 9H); $^{13}\text{C NMR}$ (101 MHz, CDCl_3 , mixture of rotamers) δ 154.8, 133.0, 119.9, 79.5, 79.0, 78.2, 57.7, 57.5, 44.9, 44.4, 43.5, 37.8, 37.3, 28.7 (3C); IR (film) 3412, 1697, 1670 cm^{-1} ; mp 110–112 °C; HRMS (ESI) m/z $[\text{M} + \text{Na}]^+$ calcd for $\text{C}_{12}\text{H}_{21}\text{NO}_3\text{Na}$ 250.1414, found 250.1414.

tert-Butyl 4-allyl-4-hydroxypiperidine-1-carboxylate (24b).—The same procedure as the one described for **24a** was followed starting from *tert*-butyl 4-oxopiperidine-1-carboxylate (2.00 g, 10.0 mmol). After work-up, the crude product was purified by chromatography (silica gel, 0–40% EtOAc/hexanes) to afford **24b** (1.44 g, 6.00 mmol, 60% yield) as a clear, colorless oil. $^1\text{H NMR}$ (400 MHz, CDCl_3) δ 5.93–5.79 (m, 1H), 5.25–5.10 (m, 2H), 4.00–3.60 (m, 2H), 3.28–3.04 (m, 2H), 2.23 (d, J = 7.6 Hz, 2H), 1.74–1.34 (m, 5H), 1.45 (s, 9H).

tert-Butyl 3-hydroxy-3-(3-hydroxypropyl)pyrrolidine-1-carboxylate (25a).—A 1.0 M solution of $\text{BH}_3 \cdot \text{THF}$ in THF (15 mL, 15 mmol) was added over 5 min to a solution of **24a** (1.75 g, 7.72 mmol) in THF (15 mL) at 0 °C. The reaction mixture was stirred for 3

h, and a 2.0 M aq solution of NaOH (24 mL, 47 mmol) was added followed by 30 wt% H₂O₂ in H₂O (24 mL, 0.23 mol). The resulting mixture was stirred for an additional 3 h and allowed to warm to rt. The mixture was diluted with H₂O (30 mL) and extracted with EtOAc (3 × 150 mL). The combined organic extracts were dried over anhydrous Na₂SO₄, filtered, and concentrated. The crude product was purified by chromatography (120 g of silica gel, 0–100% hexanes/EtOAc) to afford **25a** (1.34 g, 5.48 mmol, 71% yield) as a clear, colorless oil. *R*_f = 0.3 (EtOAc); ¹H NMR (400 MHz, CDCl₃, mixture of rotamers) δ 3.79–3.61 (m, 2H), 3.55–3.32 (m, 3H), 3.26–3.16 (m, 1H), 1.97–1.89 (m, 1H), 1.86–1.66 (m, 5H), 1.45 (s, 9H); ¹³C NMR (101 MHz, CDCl₃, mixture of rotamers) δ 155.1, 154.9, 79.5, 79.4, 78.3, 63.1, 58.3, 57.9, 45.1, 44.5, 38.4, 37.7, 36.9, 36.6, 28.7 (3C), 28.1, 27.8; IR (film) 3374, 1668 cm⁻¹; HRMS (ESI) *m/z* [M + Na]⁺ calcd for C₁₂H₂₃NO₄Na 268.1519, found 268.1517.

tert-Butyl 4-hydroxy-4-(3-hydroxypropyl)piperidine-1-carboxylate (25b).—The same procedure as the one described for **25a** was followed starting from **24b** (2.60 g, 10.8 mmol). After work-up, the crude product was purified by chromatography (silica gel, 0–100% hexanes/EtOAc) to afford **25b** (1.14 g, 4.40 mmol, 41% yield) of a clear, colorless oil. ¹H NMR (400 MHz, CDCl₃) δ 3.80 (d, *J* = 12.9 Hz, 2H), 3.70 (t, *J* = 6.1 Hz, 2H), 3.16 (t, *J* = 12.3 Hz, 2H), 2.06–1.80 (m, 2H), 1.73–1.65 (m, 2H), 1.63–1.48 (m, 6H), 1.45 (s, 9H).

tert-Butyl 2-hydroxy-1-oxa-7-azaspiro[4.4]nonane-7-carboxylate (26a).—General procedure A was followed using **25a** (1.34 g, 5.46 mmol). After work-up, the crude product was purified by chromatography (80 g of silica gel, 0–50% EtOAc/hexanes) to afford **26a** (0.958 g, 3.94 mmol, 72% yield) as a white solid. *R*_f = 0.3 (50% EtOAc/hexanes); ¹H NMR (400 MHz, CDCl₃, mixture of rotamers and diastereomers) δ 5.53 (s, 1H), 3.67–2.99 (m, 5H), 2.27–1.67 (m, 6H), 1.44 (s, 9H); ¹³C NMR (101 MHz, CDCl₃, mixture of rotamers and diastereomers) δ 154.7, 98.9, 89.2, 89.1, 88.4, 88.3, 79.4, 57.9, 57.5, 57.0, 56.4, 45.3, 44.8, 38.6, 38.1, 37.8, 37.1, 33.7, 33.6, 32.1, 32.0, 31.9, 31.4, 28.7 (3C); IR (film) 3406, 1695, 1675 cm⁻¹; HRMS (ESI) *m/z* [M + Na]⁺ calcd for C₁₂H₂₁NO₄Na 266.1363, found 266.1362.

tert-Butyl 2-hydroxy-1-oxa-8-azaspiro[4.5]decane-8-carboxylate (26b).—General procedure A was followed using **25b** (1.14 g, 4.40 mmol). After work-up, the crude product was purified by chromatography (silica gel, 0–40% EtOAc/hexanes) to afford **26b** (0.450 g, 1.75 mmol, 40% yield) as a white solid. ¹H NMR (400 MHz, CDCl₃) δ 5.55–5.48 (m, 1H), 3.69–3.48 (m, 2H), 3.44–3.26 (m, 2H), 2.56–2.50 (m, 1H), 2.01–1.85 (m, 2H), 1.85–1.64 (m, 3H), 1.62–1.39 (m, 3H), 1.45 (s, 9H).

tert-Butyl 3-(3-(4-(2,3-dichlorophenyl)piperazin-1-yl)propyl)-3-hydroxypyrrolidine-1-carboxylate (27a).—General procedure B was followed using **26a** (0.958 g, 3.94 mmol) and 1-(2,3-dichlorophenyl)piperazine•HCl (1.16 g, 4.33 mmol) in DCE (38 mL). After work-up, the crude product was purified by chromatography (silica gel, 0–10% MeOH/DCM) to afford **27a** (0.754 g, 1.64 mmol, 42% yield) as a yellow solid. ¹H NMR (400 MHz, CDCl₃, mixture of rotamers) δ 7.19–7.10 (m, 2H), 6.98–6.93 (m, 1H),

3.60–3.38 (m, 2H), 3.35–3.18 (m, 2H), 3.17–2.97 (m, 4H), 2.90–2.58 (m, 4H), 2.56–2.47 (m, 2H), 1.92–1.69 (m, 6H), 1.48–1.41 (m, 9H).

tert-Butyl 4-(3-(4-(2,3-Dichlorophenyl)piperazin-1-yl)propyl)-4-hydroxypiperidine-1-carboxylate (27b).—General procedure B was followed using

26b (0.445 g, 1.73 mmol) and 1-(2,3-dichlorophenyl)piperazine•HCl (0.509 g, 1.90 mmol) in DCE (18 mL). After work-up, the crude product was purified by chromatography (silica gel, 0–10% MeOH/DCM) to afford **27b** (0.810 g, 1.71 mmol, 99% yield) as a clear, yellow oil. ¹H NMR (400 MHz, CDCl₃) δ 7.19–7.12 (m, 2H), 6.96 (dd, *J* = 7.1, 2.5 Hz, 1H), 3.89–3.64 (m, 2H), 3.24 (t, *J* = 11.8 Hz, 2H), 3.16–2.96 (m, 4H), 2.83–2.57 (m, 4H), 2.53–2.46 (m, 2H), 1.74–1.63 (m, 4H), 1.56–1.38 (m, 5H), 1.45 (s, 9H).

3-(3-(4-(2,3-Dichlorophenyl)piperazin-1-yl)propyl)pyrrolidin-3-ol (28a).—General procedure C was followed using **27a** (0.754 g, 1.64 mmol) and TFA (2.5 mL, 33 mmol) in DCM (12 mL). After work-up, **28a** (0.422 g, 1.18 mmol, 72% yield) was isolated and used immediately.

4-(3-(4-(2,3-Dichlorophenyl)piperazin-1-yl)propyl)piperidin-4-ol (28b).—General procedure C was followed using **27b** (0.814 g, 1.72 mmol) and TFA (2.6 mL, 34 mmol) in DCM (12 mL). After work-up, **28b** (0.500 g, 1.34 mmol, 78% yield) was isolated and used immediately.

3-(3-(4-(2,3-Dichlorophenyl)piperazin-1-yl)propyl)-3-hydroxy-*N,N*-dimethylpyrrolidine-1-carboxamide (29a).—General procedure

D was followed using **28a** (0.150 g, 0.419 mmol) and *N,N*-dimethylcarbonyl chloride (48 μL, 0.52 mmol) in DCM (6.0 mL). After work-up, the crude product was purified by chromatography (silica gel, 0–5% MeOH/DCM) to afford **29a** (68.0 mg, 0.158 mmol, 38% yield) as a clear, yellow oil. ¹H NMR (400 MHz, CDCl₃) δ 7.16–7.08 (m, 2H), 6.97–6.91 (m, 1H), 3.70–3.60 (m, 1H), 3.45–3.35 (m, 2H), 3.24–3.18 (m, 1H), 3.15–2.95 (m, 4H), 2.82–2.58 (m, 4H), 2.81 (s, 6H), 2.53–2.46 (m, 2H), 1.87–1.67 (m, 6H); HRMS (MALDI) *m/z* [M + H]⁺ calcd for C₂₀H₃₁Cl₂N₄O₂ 429.1819, found 429.1802. The HCl salt was precipitated from a 0.06 M solution of the free base in 50% acetone/CHCl₃ using a 2.0 M solution of HCl in Et₂O (4.0 equiv). Mp 184–186 °C. Anal. calcd for C₂₀H₃₀Cl₂N₄O₂•1.25HCl: C, 50.58; H, 6.63; N, 11.80. Found: C, 50.64; H, 6.39; N, 11.60.

4-(3-(4-(2,3-Dichlorophenyl)piperazin-1-yl)propyl)-4-hydroxy-*N,N*-dimethylpiperidine-1-carboxamide (29b).—General procedure D was

followed using **28b** (0.804 g, 2.16 mmol) and *N,N*-dimethylcarbonyl chloride (0.25 mL, 2.7 mmol) in DCM (42 mL). After work-up, the crude product was purified by chromatography (silica gel, 0–5% MeOH/DCM) to afford **29b** (0.272 g, 0.613 mmol, 28% yield) as a clear, yellow oil. ¹H NMR (400 MHz, CDCl₃) δ 7.18–7.11 (m, 2H), 6.99–6.92 (m, 1H), 3.45–3.37 (m, 2H), 3.31–3.19 (m, 2H), 3.18–2.96 (m, 4H), 2.87–2.57 (m, 4H), 2.80 (s, 6H), 2.53–2.44 (m, 2H), 1.74–1.63 (m, 4H), 1.58–1.48 (m, 4H); HRMS (MALDI) *m/z* [M + H]⁺ calcd for C₂₁H₃₃Cl₂N₄O₂ 443.1975, found 443.1971. The HCl salt was precipitated from a 0.06 M solution of the free base in 50% acetone/CHCl₃ using a 2.0 M solution

of HCl in Et₂O (2.5 equiv). mp 189–192 °C. Anal. calcd for C₂₁H₃₂Cl₂N₄O₂•HCl•0.25H₂O: C, 52.07; H, 6.97; N, 11.57. Found: C, 51.98; H, 7.01; N, 11.22.

1-(3-(3-(4-(2,3-Dichlorophenyl)piperazin-1-yl)propyl)-3-hydroxypyrrolidin-1-yl)-3-methoxypropan-1-one (30a).—General procedure F was followed using **28a** (0.422 g, 1.18 mmol). After work-up, the crude product was purified by chromatography (silica gel, 0–5% MeOH/DCM) to afford **30a** (0.137 g, 0.309 mmol, 26% yield) as a clear, yellow oil. ¹H NMR (400 MHz, CD₃OD) δ 7.31–7.24 (m, 2H), 7.16–7.10 (m, 1H), 3.76–3.60 (m, 4H), 3.59–3.45 (m, 2H), 3.35–3.32 (m, 3H), 3.28–3.15 (m, 4H), 3.14–2.96 (m, 4H), 2.94–2.82 (m, 2H), 2.68–2.51 (m, 2H), 2.04–1.70 (m, 6H); HRMS (MALDI) *m/z* [M + H]⁺ calcd for C₂₁H₃₂Cl₂N₃O₃ 444.1815, found 444.1814; *t*_R = 16.9 min (HPLC, acidic).

1-(4-(3-(4-(2,3-Dichlorophenyl)piperazin-1-yl)propyl)-4-hydroxypiperidin-1-yl)-3-methoxypropan-1-one (30b).—General procedure F was followed using **28b** (0.500 g, 1.34 mmol). After work-up, the crude product was purified by chromatography (silica gel, 0–5% MeOH/CHCl₃) to afford **30b** (0.313 g, 0.309 mmol, 50% yield) as a yellow solid. ¹H NMR (400 MHz, CDCl₃) δ 7.22–7.11 (m, 2H), 7.00–6.94 (m, 1H), 4.38–4.29 (m, 1H), 3.74–3.67 (m, 2H), 3.66–3.58 (m, 1H), 3.43 (t, *J* = 12.6 Hz, 1H), 3.35 (s, 3H), 3.27–3.03 (m, 5H), 2.95–2.69 (m, 4H), 2.61 (t, *J* = 6.9 Hz, 4H), 1.84–1.53 (m, 6H), 1.50–1.36 (m, 2H); HRMS (MALDI) *m/z* [M + H]⁺ calcd for C₂₂H₃₄Cl₂N₃O₃ 458.1972, found 458.1962. The HCl salt was precipitated from a 0.08 M solution of the free base in 50% acetone/CHCl₃ using a 2.0 M solution of HCl in Et₂O (10 equiv). Dec >160 °C. Anal. calcd for C₂₂H₃₃Cl₂N₃O₃•HCl•H₂O: C, 51.52; H, 7.08; N, 8.19. Found: C, 51.62; H, 6.81; N, 8.14.

hD₂R and hD₃R Radioligand Binding Studies

Radioligand binding assays were conducted similarly as previously described.⁴⁶ HEK293 cells stably expressing human D₂LR or D₃R were grown in a 50:50 mix of DMEM and Ham's F12 culture media, supplemented with 20 mM HEPES, 2 mM L-glutamine, 0.1 mM non-essential amino acids, 1X antibiotic/antimycotic, 10% heat-inactivated fetal bovine serum, and 200 µg/mL hygromycin (Life Technologies, Grand Island, NY) and kept in an incubator at 37 °C and 5% CO₂. Upon reaching 80–90% confluence, cells were harvested using premixed Earle's balanced salt solution with 5 mM EDTA (Life Technologies) and centrifuged at 3000 rpm for 10 min at 21 °C. The supernatant was removed, and the pellet was resuspended in 10 mL hypotonic lysis buffer (5 mM MgCl₂, 5 mM Tris, pH 7.4 at 4 °C) and centrifuged at 14500 rpm (~25000 *g*) for 30 min at 4 °C. The pellet was then resuspended in binding buffer. Bradford protein assay (Bio-Rad, Hercules, CA) was used to determine the protein concentration. For [³H]-*N*-methylspiperone binding studies membranes were diluted to 500 µg/mL, in fresh EBSS binding buffer made from 8.7 g/L Earle's Balanced Salts without phenol red (US Biological, Salem, MA), 2.2 g/L sodium bicarbonate, pH to 7.4, and stored in a –80 °C freezer for later use. For [³H]-(*R*)-(+)-7-OH-DPAT binding studies,⁵¹ membranes were harvested and used fresh; the binding buffer was made from 50 mM Tris, 10 mM MgCl₂, 1 mM EDTA, pH 7.4. On the test day, each test compound was diluted into half-log serial dilutions using the 30% dimethyl sulfoxide (DMSO) vehicle. When it was necessary to assist solubilization of the drugs at the highest tested concentration, 0.1% AcOH (final concentration v/v) was added alongside the vehicle.

Membranes were diluted in fresh binding buffer. Radioligand competition experiments were conducted in 96-well plates containing 300 μ L fresh binding buffer, 50 μ L of the diluted test compound, 100 μ L of membranes (for [3 H]-*N*-methylspiperone assays: 10–20 μ g/well total protein for hD_{2L}R and hD₃R; for [3 H]-(*R*)-(+)-7-OH-DPAT assays: 40–80, and 20–40 μ g/well total protein for hD_{2L}R, and hD₃R, respectively), and 50 μ L of radioligand diluted in binding buffer ([3 H]-*N*-methylspiperone: 0.4 nM final concentration for all the hD₂-like receptor subtypes; [3 H]-(*R*)-(+)-7-OH-DPAT: 1.5 nM final concentration for hD_{2L}, and 0.5 nM final concentration for hD₃; Perkin Elmer). Aliquots of radioligands solution were also quantified accurately in each experiment replicate, to determine how much radioactivity was added, taking in account the experimentally determined counter efficiency. Nonspecific binding was determined using 10 μ M (+)-butaclamol (Sigma-Aldrich, St. Louis, MO), and total binding was determined with the 30% DMSO vehicle. All compound dilutions were tested in triplicate, and the reaction incubated for 60 min ([3 H]-*N*-methylspiperone assays) or 90 min ([3 H]-(*R*)-(+)-7-OH-DPAT assays) at RT. The reaction was terminated by filtration through PerkinElmer Uni-Filter-96 GF/B, presoaked for the incubation time in 0.5% polyethylenimine, using a Brandel 96-Well Plates Harvester Manifold (Brandel Instruments, Gaithersburg, MD). The filters were washed thrice with 3 mL (3 X \sim 1 mL/well) of ice-cold binding buffer. PerkinElmer MicroScint 20 Scintillation Cocktail (65 μ L) was added to each well, and filters were counted using a PerkinElmer MicroBeta Microplate Counter. IC₅₀ values for each compound were determined from dose–response curves, and K_i values were calculated using the Cheng–Prusoff equation.⁵⁰ K_d values were determined via separate homologous competitive binding experiments. When a complete inhibition could not be achieved at the highest tested concentrations, K_i values have been extrapolated by constraining the bottom of the dose–response curves (=0% residual specific binding) in the nonlinear regression analysis. These analyses were performed using GraphPad Prism version 8 for Macintosh (GraphPad Software, San Diego, CA). All results were rounded to the third significant figure. K_i values were determined from at least three independent experiments, each performed in triplicate, and are reported as the mean \pm standard error of the mean (SEM).

BRET Studies of D₂R and D₃R Signaling

All reagents were purchased from Sigma Aldrich-Merck unless otherwise stated. BRET experiments were performed in transiently transfected human embryonic kidney 293 T (HEK 293T) cells, as described previously.^{53, 68} Briefly, cells were grown and maintained at 37 °C in 5% CO₂ in Dulbecco's modified eagle medium (DMEM) supplemented with 10% (v/v) fetal bovine serum (FBS). Cells were seeded in 10 cm Petri dishes (2.5 \times 10⁶ cells per dish) and allowed to grow overnight in media at 37 °C, 5% CO₂. The following day, cells were transiently transfected in full media supplemented with antibiotics (100 U/mL penicillin and 100 μ g/mL streptomycin, Gibco) using a 1:6 total DNA to PEI (PolySciences Inc) ratio. BRET constructs were as follows: 2 μ g of WT-G α_{oA} , 1 μ g of G β 1-Venus(156–239), 1 μ g of G γ 2-Venus(1–155), 1 μ g of masGRK3ct-Rluc8 and 1 μ g of receptor (D_{2L}R or D₃R) for GPA assays and 4 μ g of Venus-mG_{si} and 1 μ g of D₂LR-Rluc8 for mini G recruitment assays. Cells were then allowed to grow overnight at 37 °C, 5% CO₂. The next day, cells were plated in Greiner poly-D-lysine-coated 96-well plates (SLS) in media and allowed to grow overnight. On the day of the assay (48h post-transfection), cells were

washed once with D-PBS (Lonza, SLS) and incubated in D-PBS for 30 min at 37 °C, 5% CO₂. The Rluc substrate coelenterazine h (NanoLight) was added to each well (final concentration of 5 μM) and cells were incubated for 5 minutes at 37 °C. After 5 minutes, ligands (final concentration from 10 μM to 0.01 nM in D-PBS) were added to the plate and cells were incubated for a further 10 minutes at 37 °C. For the antagonist-mode assays that require co-addition, quinpirole was added together with the ligands (final concentration of 3 nM) to generate 50–70% of the signal that can then be displaced by an antagonist. The plate was then read in a PHERAstar FSX microplate reader (Venus and Rluc emission signals at 535 and 475 nm respectively, BMG Labtech). The ratio of Venus:Rluc counts was used to quantify the BRET signal in each well. Data were normalized to the maximal response of dopamine/quinpirole or no drug for the 100% or 0% response, respectively and as indicated in the figure axes titles. All experiments were performed in duplicate and at least three times independently. All data points represent the mean value and error bars represent the standard error of the mean (SEM). Data were fitted using the built-in log(agonist) vs. response (three parameters) model in Prism 9.0 (GraphPad software Inc., San Diego, CA). For agonist-mode assays, data were fitted to a three-parameter concentration-response model where EC₅₀ is the concentration of the agonist needed to elicit half the maximal response of the particular agonist, defined as E_{max} . For the antagonist-mode assays, data points were fitted using a three-parameter concentration-response model where IC₅₀ is the concentration required to inhibit half the maximum response of the agonist used at a particular concentration. Values of pEC₅₀ or pIC₅₀ plus/minus error are given as the error has a gaussian distribution whereas the error associated with the antilog value does not.

Cocaine Self Administration

Animals.—Male Long–Evans rats 275–325 g (Charles River Laboratories) were used in the experiments. All animals were housed individually in a climate-controlled animal room on a reversed light–dark cycle with free access to food and water. All experimental procedures were conducted in accordance with the Guide for the Care and Use of Laboratory Animals of the United States National Research Council and were approved by the National Institute on Drug Abuse Animal Care and Use Committee.

Surgery.—Rats used in cocaine self-administration experiments were implanted with a microrenathane intravenous (i.v.) catheter (Braintree Scientific Inc., Braintree, MA, USA). Each rat was first anaesthetized with ketamine (100 mg/kg i.p.) and xylazine (10 mg/kg, i.p.) and then a small incision was made to the right of the midline of the neck to expose the external jugular vein. One end of the i.v. catheter was next inserted into the vein with the catheter tip reaching the right atrium. The catheter was then secured to the vein with silk suture and the other end fed subcutaneously around the back of the neck to exit near the back of the skull, connected to a bent 24-gauge stainless steel cannula (Plastics One Inc., Roanoke, VA, USA) with a threaded head used to secure a dummy cannula and, during experimentation, an infusion line. The catheter and the guide cannula were secured to the skull with four stainless steel screws threaded into the skull and dental cement. After surgery, the catheters were flushed daily with gentamicin– and heparin–saline solutions (0.1 mg/ml gentamicin and 30 IU/ml heparin; ICN Biochemicals, Cleveland, OH, USA) as

precaution against catheter clogging and infection. The animals were allowed to recover for at least 7 days before behavioral training started.

Apparatus.—Standard MED associates operant test chambers were used for self-administration experiments. Each box was equipped with two levers (active and inactive) and a house light set to on at the beginning of each session. Presses on the active lever triggered a compound light and tone cue. Data were collected and analyzed using MED PC software.

Cocaine self-administration under Fixed Ratio (FR) reinforcement.—A total of 48 animals underwent intravenous catheterization surgery. Following recovery, subjects were trained to lever press for cocaine (1 mg/kg/infusion) under an FR1 reinforcement schedule for five sessions. Then cocaine self-administration continued under FR2 reinforcement at 0.5 mg/kg per infusion for approximately two weeks until stable responding was observed (more than 20 infusions, <20% variability in responding across three consecutive sessions and a ratio of at least 2:1 active to inactive lever presses). Each session was 3 h long with a cap of 50 infusions at a dose of 1 mg/kg/infusion to prevent overdose and a cap of 100 infusions at a dose of 0.5 mg/kg/infusion. Rats were randomly assigned to receive intraperitoneal injections of vehicle (25% 2-hydroxypropyl-beta-cyclodextrin; Onbio Inc., Ontario, Canada) or cariprazine (0.3, 1, and 3 mg/kg), **13a** (0.3, 1, and 3 mg/kg), **13e** (0.3, 1, 3, and 10 mg/kg), 30 min before cocaine self-administration testing. Each animal received 4 or 5 injections for the different drug doses. The sequence of the drug doses was counterbalanced. Between tests, subjects underwent an additional three to five sessions of cocaine self-administration until the baseline response was re-established.

Data analysis.—Behavioral experiments were analyzed with SigmaPlot 12.5 Software (Systat, Palo Alto, CA). All dose treatments groups were compared to vehicle group using One-way Repeated Measures ANOVA or One-way ANOVA tests followed by Dunnet's post-hoc test.

Supplementary Material

Refer to Web version on PubMed Central for supplementary material.

ACKNOWLEDGMENTS

This project was supported by the National Institute on Drug Abuse – Intramural Research Program (ZIADA000424) and the NIDA-IRP Medications Development Program. The authors thank Dr. Ning Sheng Cai from the Integrative Neurobiology Section at NIDA-IRP for assistance with cell lines and tissue culture protocols. We also acknowledge Dr. Shelley Jackson (Translational Analytical Core, NIDA-IRP) for providing all HRMS data. The ACUC approved animal protocol number is 22-BNRB-48.

ABBREVIATIONS

BD-I	bipolar 1 disorder
BMS	borane-dimethyl sulfide
BRET	bioluminescence resonance energy transfer

D₂R	dopamine D ₂ receptor
D₃R	dopamine D ₃ receptor
DIPEA	<i>N,N</i> -diisopropylethylamine
EDCI	1-ethyl-3-(3-dimethylaminopropyl)carbodiimide•HCl
GPA	G-protein Activation
HCTU	<i>O</i> -(1 <i>H</i> -6-chlorobenzotriazole-1-yl)-1,1,3,3-tetramethyluronium hexafluorophosphate
HEK 293 cells	human embryonic kidney 293 cells
HOBt	hydroxybenzotriazole
MPO	multiparameter optimization
PP	primary pharmacophore
PSUD	psychostimulant use disorders
SP	secondary pharmacophore
SUD	substance use disorders

REFERENCES

- Ahmad FB; Cisewski JA; Rossen LM; Sutton P Provisional drug overdose death counts. National Center for Health Statistics: 2022.
- Ciccarone D The rise of illicit fentanyls, stimulants and the fourth wave of the opioid overdose crisis. *Curr. Opin. Psychiatry* 2021, 34 (4), 344–350. [PubMed: 33965972]
- Angarita GA; Hadizadeh H; Cerdena I; Potenza MN Can pharmacotherapy improve treatment outcomes in people with co-occurring major depressive and cocaine use disorders? *Expert Opin. Pharmacother* 2021, 22 (13), 1669–1683. [PubMed: 34042556]
- Hellem TL; Lundberg KJ; Renshaw PF A Review of Treatment Options for Co-Occurring Methamphetamine Use Disorders and Depression. *J. Addict. Nurs* 2015, 26 (1), 14–23; quiz E11. [PubMed: 25761159]
- Murthy P; Mahadevan J; Chand PK Treatment of substance use disorders with co-occurring severe mental health disorders. *Curr. Opin. Psychiatry* 2019, 32 (4), 293–299. [PubMed: 31157674]
- Coles AS; Sasiadek J; George TP Pharmacotherapies for co-occurring substance use and bipolar disorders: A systematic review. *Bipolar Disord.* 2019, 21 (7), 595–610. [PubMed: 31077521]
- Peris L; Szman N Partial Agonists and Dual Disorders: Focus on Dual Schizophrenia. *Front. Psychiatry* 2021, 12, 769623. [PubMed: 34975572]
- Jordan CJ; Humburg B; Rice M; Bi GH; You ZB; Shaik AB; Cao J; Bonifazi A; Gadiano A; Rais R; Slusher B; Newman AH; Xi ZX The highly selective dopamine D₃R antagonist, *R*-VK4–40 attenuates oxycodone reward and augments analgesia in rodents. *Neuropharmacology* 2019, 158, 107597. [PubMed: 30974107]
- Prieto GA Abnormalities of Dopamine D₃ Receptor Signaling in the Diseased Brain. *J. Cent. Nerv. Syst. Dis* 2017, 9, 1179573517726335.
- Xi ZX; Gilbert J; Campos AC; Kline N; Ashby CR Jr.; Hagan JJ; Heidbreder CA; Gardner EL Blockade of mesolimbic dopamine D₃ receptors inhibits stress-induced reinstatement of cocaine-seeking in rats. *Psychopharmacology* 2004, 176 (1), 57–65. [PubMed: 15083257]

11. Xi ZX; Gilbert JG; Pak AC; Ashby CR Jr.; Heidbreder CA; Gardner EL Selective dopamine D₃ receptor antagonism by SB-277011A attenuates cocaine reinforcement as assessed by progressive-ratio and variable-cost-variable-payoff fixed-ratio cocaine self-administration in rats. *Eur. J. Neurosci* 2005, 21 (12), 3427–3438. [PubMed: 16026480]
12. Ashby CR Jr.; Paul M; Gardner EL; Heidbreder CA; Hagan JJ Acute Administration of the Selective D₃ Receptor Antagonist SB-277011A Blocks the Acquisition and Expression of the Conditioned Place Preference Response to Heroin in Male Rats. *Synapse* 2003, 48 (3), 154–156. [PubMed: 12645041]
13. Heidbreder CA; Newman AH Current perspectives on selective dopamine D₃ receptor antagonists as pharmacotherapeutics for addictions and related disorders. *Ann. N. Y. Acad. Sci* 2010, 1187 (1), 4–34. [PubMed: 20201845]
14. Payer D; Balasubramaniam G; Boileau I What is the role of the D₃ receptor in addiction? A mini review of PET studies with [¹¹C]-(+)-PHNO. *Prog. Neuro-Psychopharmacol. Biol. Psychiatry* 2014, 52, 4–8.
15. Ballon JS; Pajvani U; Freyberg Z; Leibel RL; Lieberman JA Molecular pathophysiology of metabolic effects of antipsychotic medications. *Trends Endocrinol. Metab* 2014, 25 (11), 593–600. [PubMed: 25190097]
16. Farino ZJ; Morgenstern TJ; Maffei A; Quick M; De Solis AJ; Wiriyasermkul P; Freyberg RJ; Aslanoglou D; Sorisio D; Inbar BP; Free RB; Donthamsetti P; Mosharov EV; Kellendonk C; Schwartz GJ; Sibley DR; Schmauss C; Zeltser LM; Moore H; Harris PE; Javitch JA; Freyberg Z New roles for dopamine D₂ and D₃ receptors in pancreatic beta cell insulin secretion. *Mol. Psychiatry* 2020, 25 (9), 2070–2085. [PubMed: 30626912]
17. Fyfe TJ; Kellam B; Sykes DA; Capuano B; Scammells PJ; Lane JR; Charlton SJ; Mistry SN Structure-Kinetic Profiling of Haloperidol Analogues at the Human Dopamine D₂ Receptor. *J. Med. Chem* 2019, 62 (21), 9488–9520. [PubMed: 31580666]
18. Keck TM; John WS; Czoty PW; Nader MA; Newman AH Identifying Medication Targets for Psychostimulant Addiction: Unraveling the Dopamine D₃ Receptor Hypothesis. *J. Med. Chem* 2015, 58 (14), 5361–5380. [PubMed: 25826710]
19. Meltzer HY Update on typical and atypical antipsychotic drugs. *Annu. Rev. Med* 2013, 64 (1), 393–406. [PubMed: 23020880]
20. Miyamoto S; Miyake N; Jarskog LF; Fleischhacker WW; Lieberman JA Pharmacological treatment of schizophrenia: a critical review of the pharmacology and clinical effects of current and future therapeutic agents. *Mol. Psychiatry* 2012, 17 (12), 1206–1227. [PubMed: 22584864]
21. Reavill C; Taylor SG; Wood MD; Ashmeade T; Austin NE; Avenell KY; Boyfield I; Branch CL; Cilia J; Coldwell MC; Hadley MS; Hunter AJ; Jeffrey P; Jewitt F; Johnson CN; Jones DN; Medhurst AD; Middlemiss DN; Nash DJ; Riley GJ; Routledge C; Stemp G; Thewlis KM; Trail B; Vong AK; Hagan JJ Pharmacological Actions of a Novel, High-Affinity, and Selective Human Dopamine D₃ Receptor Antagonist, SB-277011-A. *J. Pharmacol. Exp. Ther* 2000, 294 (3), 1154–1165. [PubMed: 10945872]
22. Grundt P; Carlson EE; Cao J; Bennett CJ; McElveen E; Taylor M; Luedtke RR; Newman AH Novel Heterocyclic Trans Olefin Analogues of *N*-{4-[4-(2,3-Dichlorophenyl)piperazin-1-yl]butyl}arylcarboxamides as Selective Probes with High Affinity for the Dopamine D₃ Receptor. *J. Med. Chem* 2005, 48 (3), 839–848. [PubMed: 15689168]
23. Kumar V; Bonifazi A; Ellenberger MP; Keck TM; Pommier E; Rais R; Slusher BS; Gardner E; You ZB; Xi ZX; Newman AH Highly Selective Dopamine D₃ Receptor (D₃R) Antagonists and Partial Agonists Based on Eticlopride and the D₃R Crystal Structure: New Leads for Opioid Dependence Treatment. *J. Med. Chem* 2016, 59 (16), 7634–7650. [PubMed: 27508895]
24. You ZB; Bi GH; Galaj E; Kumar V; Cao J; Gadiano A; Rais R; Slusher BS; Gardner EL; Xi ZX; Newman AH Dopamine D₃R antagonist VK4–116 attenuates oxycodone self-administration and reinstatement without compromising its antinociceptive effects. *Neuropsychopharmacology* 2019, 44 (8), 1415–1424. [PubMed: 30555159]
25. Shaik AB; Kumar V; Bonifazi A; Guerrero AM; Cemaj SL; Gadiano A; Lam J; Xi ZX; Rais R; Slusher BS; Newman AH Investigation of Novel Primary and Secondary Pharmacophores and 3-Substitution in the Linking Chain of a Series of Highly Selective and Bitopic Dopamine D₃

- Receptor Antagonists and Partial Agonists. *J. Med. Chem* 2019, 62 (20), 9061–9077. [PubMed: 31526003]
26. Di Ciano P; Mansouri E; Tong J; Wilson AA; Houle S; Boileau I; Duvauchelle T; Robert P; Schwartz JC; Le Foll B Occupancy of dopamine D₂ and D₃ receptors by a novel D₃ partial agonist BP1.4979: a [¹¹C]-(+)-PHNO PET study in humans. *Neuropsychopharmacology* 2019, 44 (7), 1284–1290. [PubMed: 30659274]
27. Chien EYT; Liu W; Zhao Q; Katritch V; Won Han G; Hanson MA; Shi L; Newman AH; Javitch JA; Cherezov V; Stevens RC Structure of the Human Dopamine D₃ Receptor in Complex with a D₂/D₃ Selective Antagonist. *Science* 2010, 330 (6007), 1091–1095. [PubMed: 21097933]
28. Keck TM; Burzynski C; Shi L; Newman AH Chapter Seven - Beyond Small-Molecule SAR: Using the Dopamine D₃ Receptor Crystal Structure to Guide Drug Design. In *Advances in Pharmacology*, Dvoskin LP Ed.; Vol. 69; Academic Press, 2014; pp 267–300. [PubMed: 24484980]
29. Newman AH; Xi Z-X; Heidbreder C Current Perspectives on Selective Dopamine D₃ Receptor Antagonists/Partial Agonists as Pharmacotherapeutics for Opioid and Psychostimulant Use Disorders. In *Current Topics in Behavioral Neurosciences*; Springer Berlin Heidelberg, 2022; pp 1–45. DOI: 10.1007/7854_2022_347.
30. Awad AG; Voruganti LN Neuroleptic dysphoria: revisiting the concept 50 years later. *Acta Psychiatr. Scand.*, Suppl 2005, 111 (427), 6–13.
31. Agai-Csongor E; Domany G; Nogradi K; Galambos J; Vago I; Keseru GM; Greiner I; Laszlovszky I; Gere A; Schmidt E; Kiss B; Vastag M; Tihanyi K; Saghy K; Laszy J; Gyertyan I; Zajer-Balazs M; Gemesi L; Kapas M; Szombathelyi Z Discovery of cariprazine (RGH-188): a novel antipsychotic acting on dopamine D₃/D₂ receptors. *Bioorg. Med. Chem. Lett* 2012, 22 (10), 3437–3440. [PubMed: 22537450]
32. Calabrese F; Tarazi FI; Racagni G; Riva MA The role of dopamine D₃ receptors in the mechanism of action of cariprazine. *CNS Spectr.* 2020, 25 (3), 343–351. [PubMed: 31010452]
33. Kiss B; Laszlovszky I; Kramos B; Visegrady A; Bobok A; Levay G; Lendvai B; Roman V Neuronal Dopamine D₃ Receptors: Translational Implications for Preclinical Research and CNS Disorders. *Biomolecules* 2021, 11 (1).
34. Laszlovszky I; Barabassy A; Nemeth G Cariprazine, A Broad-Spectrum Antipsychotic for the Treatment of Schizophrenia: Pharmacology, Efficacy, and Safety. *Adv. Ther* 2021, 38 (7), 3652–3673. [PubMed: 34091867]
35. Earley W; Burgess MV; Rekedal L; Dickinson R; Szatmári B; Németh G; McIntyre RS; Sachs GS; Yatham LN Cariprazine Treatment of Bipolar Depression: A Randomized Double-Blind Placebo-Controlled Phase 3 Study. *Am. J. Psychiatry* 2019, 176 (6), 439–448. [PubMed: 30845817]
36. Earley WR; Burgess MV; Khan B; Rekedal L; Suppes T; Tohen M; Calabrese JR Efficacy and safety of cariprazine in bipolar I depression: A double-blind, placebo-controlled phase 3 study. *Bipolar Disord.* 2020, 22 (4), 372–384. [PubMed: 31628698]
37. Guma E; Rocchetti J; Devenyi GA; Tanti A; Mathieu AP; Lerch JP; Elgbeili G; Courcot B; Mechawar N; Chakravarty MM; Giros B Role of D₃ dopamine receptors in modulating neuroanatomical changes in response to antipsychotic administration. *Sci. Rep* 2019, 9 (1), 7850. [PubMed: 31127135]
38. Huang M; He W; Kiss B; Farkas B; Adham N; Meltzer HY The Role of Dopamine D₃ Receptor Partial Agonism in Cariprazine-Induced Neurotransmitter Efflux in Rat Hippocampus and Nucleus Accumbens. *J. Pharmacol. Exp. Ther* 2019, 371 (2), 517–525. [PubMed: 31511365]
39. Michino M; Donthamsetti P; Beuming T; Banala A; Duan L; Roux T; Han Y; Trinquet E; Newman AH; Javitch JA; Shi L A Single Glycine in Extracellular Loop 1 Is the Critical Determinant for Pharmacological Specificity of Dopamine D₂ and D₃ Receptors. *Mol. Pharmacol* 2013, 84 (6), 854–864. [PubMed: 24061855]
40. Herenbrink CK; Verma R; Lim HD; Kopinathan A; Keen A; Shonberg J; Draper-Joyce CJ; Scammells PJ; Christopoulos A; Javitch JA; Capuano B; Shi L; Lane JR Molecular Determinants of the Intrinsic Efficacy of the Antipsychotic Aripiprazole. *ACS Chem. Biol* 2019, 14 (8), 1780–1792. [PubMed: 31339684]

41. Newman AH; Battiti FO; Bonifazi A 2016 Philip S. Portuguese Medicinal Chemistry Lectureship: Designing Bivalent or Bitopic Molecules for G-Protein Coupled Receptors. The Whole Is Greater Than the Sum of Its Parts. *J. Med. Chem* 2020, 63 (5), 1779–1797. [PubMed: 31499001]
42. Shonberg J; Herenbrink CK; Lopez L; Christopoulos A; Scammells PJ; Capuano B; Lane JR A Structure-Activity Analysis of Biased Agonism at the Dopamine D₂ Receptor. *J. Med. Chem* 2013, 56 (22), 9199–9221. [PubMed: 24138311]
43. Egyed A; Domany-Kovacs K; Kovanyi B; Horti F; Kurko D; Kiss DJ; Pandy-Szekeres G; Greiner I; Keseru GM Controlling receptor function from the extracellular vestibule of G-protein coupled receptors. *Chem. Commun* 2020, 56 (91), 14167–14170.
44. Egyed A; Kiss DJ; Keseru GM The Impact of the Secondary Binding Pocket on the Pharmacology of Class A GPCRs. *Front. Pharmacol* 2022, 13, 847788. [PubMed: 35355719]
45. Lim J; Kelley EH; Methot JL; Zhou H; Petrocchi A; Chen H; Hill SE; Hinton MC; Hruza A; Jung JO; Maclean JK; Mansueto M; Naumov GN; Philippar U; Raut S; Spacciopoli P; Sun D; Siliphaivanh P Discovery of 1-(1*H*-Pyrazolo[4,3-*c*]pyridin-6-yl)urea Inhibitors of Extracellular Signal-Regulated Kinase (ERK) for the Treatment of Cancers. *J. Med. Chem* 2016, 59 (13), 6501–6511. [PubMed: 27329786]
46. Bonifazi A; Battiti FO; Sanchez J; Zaidi SA; Bow E; Makarova M; Cao J; Shaik AB; Sulima A; Rice KC; Katritch V; Canals M; Lane JR; Newman AH Novel Dual-Target μ -Opioid Receptor and Dopamine D₃ Receptor Ligands as Potential Nonaddictive Pharmacotherapeutics for Pain Management. *J. Med. Chem* 2021, 64 (11), 7778–7808. [PubMed: 34011153]
47. Wager TT; Hou X; Verhoest PR; Villalobos A Moving beyond Rules: The Development of a Central Nervous System Multiparameter Optimization (CNS MPO) Approach To Enable Alignment of Druglike Properties. *ACS Chem. Neurosci* 2010, 1 (6), 435–449. [PubMed: 22778837]
48. Wager TT; Hou X; Verhoest PR; Villalobos A Central Nervous System Multiparameter Optimization Desirability: Application in Drug Discovery. *ACS Chem. Neurosci* 2016, 7 (6), 767–775. [PubMed: 26991242]
49. Kiss B; Nemethy Z; Fazekas K; Kurko D; Gyertyan I; Saghy K; Laszlovszky I; Farkas B; Kirschner N; Bolf-Terjeki E; Balazs O; Lendvai B Preclinical pharmacodynamic and pharmacokinetic characterization of the major metabolites of cariprazine. *Drug Des. Devel. Ther* 2019, 13, 3229–3248.
50. Yung-Chi C; Prusoff WH Relationship between the inhibition constant (K_i) and the concentration of inhibitor which causes 50 per cent inhibition (I_{50}) of an enzymatic reaction. *Biochem. Pharmacol* 1973, 22 (23), 3099–3108. [PubMed: 4202581]
51. Bonifazi A; Yano H; Ellenberger MP; Muller L; Kumar V; Zou M-F; Cai NS; Guerrero AM; Woods AS; Shi L; Newman AH Novel Bivalent Ligands Based on the Sumanirole Pharmacophore Reveal Dopamine D₂ Receptor (D₂R) Biased Agonism. *J. Med. Chem* 2017, 60 (7), 2890–2907. [PubMed: 28300398]
52. Zou M-F; Keck TM; Kumar V; Donthamsetti P; Michino M; Burzynski C; Schweppe C; Bonifazi A; Free RB; Sibley DR; Janowsky A; Shi L; Javitch JA; Newman AH Novel Analogues of (*R*)-5-(Methylamino)-5,6-dihydro-4*H*-imidazo[4,5,1-*i*]quinolin-2(1*H*)-one (Sumanirole) Provide Clues to Dopamine D₂/D₃ Receptor Agonist Selectivity. *J. Med. Chem* 2016, 59 (7), 2973–2988. [PubMed: 27035329]
53. Mann A; Keen AC; Mark H; Dasgupta P; Javitch JA; Canals M; Schulz S; Robert Lane J New phosphosite-specific antibodies to unravel the role of GRK phosphorylation in dopamine D₂ receptor regulation and signaling. *Sci. Rep* 2021, 11 (1), 8288. [PubMed: 33859231]
54. Masuho I; Martemyanov KA; Lambert NA Monitoring G Protein Activation in Cells with BRET. In *G Protein-Coupled Receptors in Drug Discovery: Methods and Protocols*, Filizola M Ed.; Springer New York, 2015; pp 107–113.
55. Nehme R; Carpenter B; Singhal A; Strege A; Edwards PC; White CF; Du H; Grishammer R; Tate CG Mini-G proteins: Novel tools for studying GPCRs in their active conformation. *PLoS One* 2017, 12 (4), e0175642. [PubMed: 28426733]
56. Lane JR; Powney B; Wise A; Rees S; Milligan G G Protein Coupling and Ligand Selectivity of the D_{2L} and D₃ Dopamine Receptors. *J. Pharmacol. Exp. Ther* 2008, 325 (1), 319–330. [PubMed: 18218829]

57. Newman-Tancredi A The importance of 5-HT_{1A} receptor agonism in antipsychotic drug action: rationale and perspectives. *Curr. Opin. Investig. Drugs* 2010, 11 (7), 802–812.
58. Newman-Tancredi A; Kleven MS Comparative pharmacology of antipsychotics possessing combined dopamine D₂ and serotonin 5-HT_{1A} receptor properties. *Psychopharmacology* 2011, 216 (4), 451–473. [PubMed: 21394633]
59. Rothman RB; Baumann MH; Savage JE; Rauser L; McBride A; Hufeisen SJ; Roth BL Evidence for Possible Involvement of 5-HT_{2B} Receptors in the Cardiac Valvulopathy Associated With Fenfluramine and Other Serotonergic Medications. *Circulation* 2000, 102 (23), 2836–2841. [PubMed: 11104741]
60. Roman V; Gyertyan I; Saghy K; Kiss B; Szombathelyi Z Cariprazine (RGH-188), a D₃-preferring dopamine D₃/D₂ receptor partial agonist antipsychotic candidate demonstrates anti-abuse potential in rats. *Psychopharmacology* 2013, 226 (2), 285–293. [PubMed: 23138433]
61. Yokel RA; Wise RA Attenuation of Intravenous Amphetamine Reinforcement by Central Dopamine Blockade in Rats. *Psychopharmacology* 1976, 48 (3), 311–318. [PubMed: 823588]
62. Galaj E; Newman AH; Xi ZX Dopamine D₃ receptor-based medication development for the treatment of opioid use disorder: Rationale, progress, and challenges. *Neurosci. Biobehav. Rev* 2020, 114, 38–52. [PubMed: 32376243]
63. de Guglielmo G; Kallupi M; Sedighim S; Newman AH; George O Dopamine D₃ Receptor Antagonism Reverses the Escalation of Oxycodone Self-administration and Decreases Withdrawal-Induced Hyperalgesia and Irritability-Like Behavior in Oxycodone-Dependent Heterogeneous Stock Rats. *Front. Behav. Neurosci* 2019, 13, 292. [PubMed: 31992976]
64. Galaj E; Bi G-H; Klein B; Hempel B; Shaik AB; Gogarnoiu ES; Friedman J; Lam J; Rais R; Reed JF; Bloom SH; Swanson TL; Schmachtenberg JL; Eshleman AJ; Janowsky A; Xi Z-X; Newman AH A highly D₃R-selective and efficacious partial agonist (*S*)-ABS01–113 compared to its D₃R-selective antagonist enantiomer (*R*)-ABS01–113 as potential treatments for opioid use disorder. *Neuropsychopharmacology* 2022.
65. Newman AH; Ku T; Jordan CJ; Bonifazi A; Xi ZX New Drugs, Old Targets: Tweaking the Dopamine System to Treat Psychostimulant Use Disorders. *Annu. Rev. Pharmacol. Toxicol* 2021, 61 (1), 609–628. [PubMed: 33411583]
66. Ozburn AR; Larson EB; Self DW; McClung CA Cocaine self-administration behaviors in *Clock* 19 mice. *Psychopharmacology* 2012, 223 (2), 169–177. [PubMed: 22535308]
67. Ozburn AR; Falcon E; Twaddle A; Nugent AL; Gillman AG; Spencer SM; Arey RN; Mukherjee S; Lyons-Weiler J; Self DW; McClung CA Direct Regulation of Diurnal *Drd3* Expression and Cocaine Reward by NPAS2. *Biol. Psychiatry* 2015, 77 (5), 425–433. [PubMed: 25444159]
68. Gillis A; Gondin AB; Kliewer A; Sanchez J; Lim HD; Alamein C; Manandhar P; Santiago M; Fritzwanker S; Schmiedel F; Katte TA; Reekie T; Grimsey NL; Kassiou M; Kellam B; Krasel C; Halls ML; Connor M; Lane JR; Schulz S; Christie MJ; Canals M Low intrinsic efficacy for G protein activation can explain the improved side effect profiles of new opioid agonists. *Sci. Signal* 2020, 13 (625), eaaz3140.

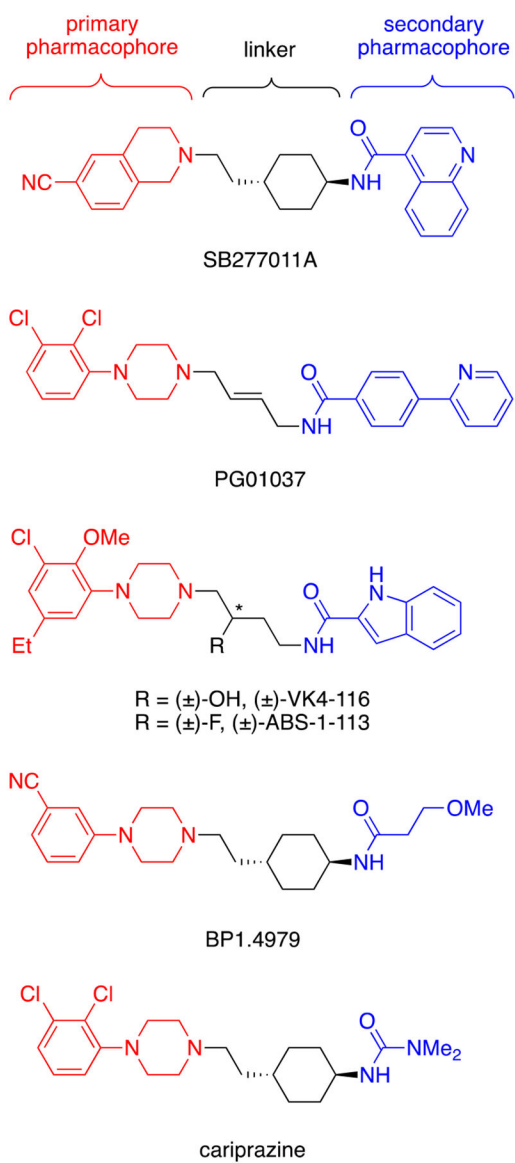


Figure 1.
Structures of representative D₃R-selective partial agonists/antagonists.

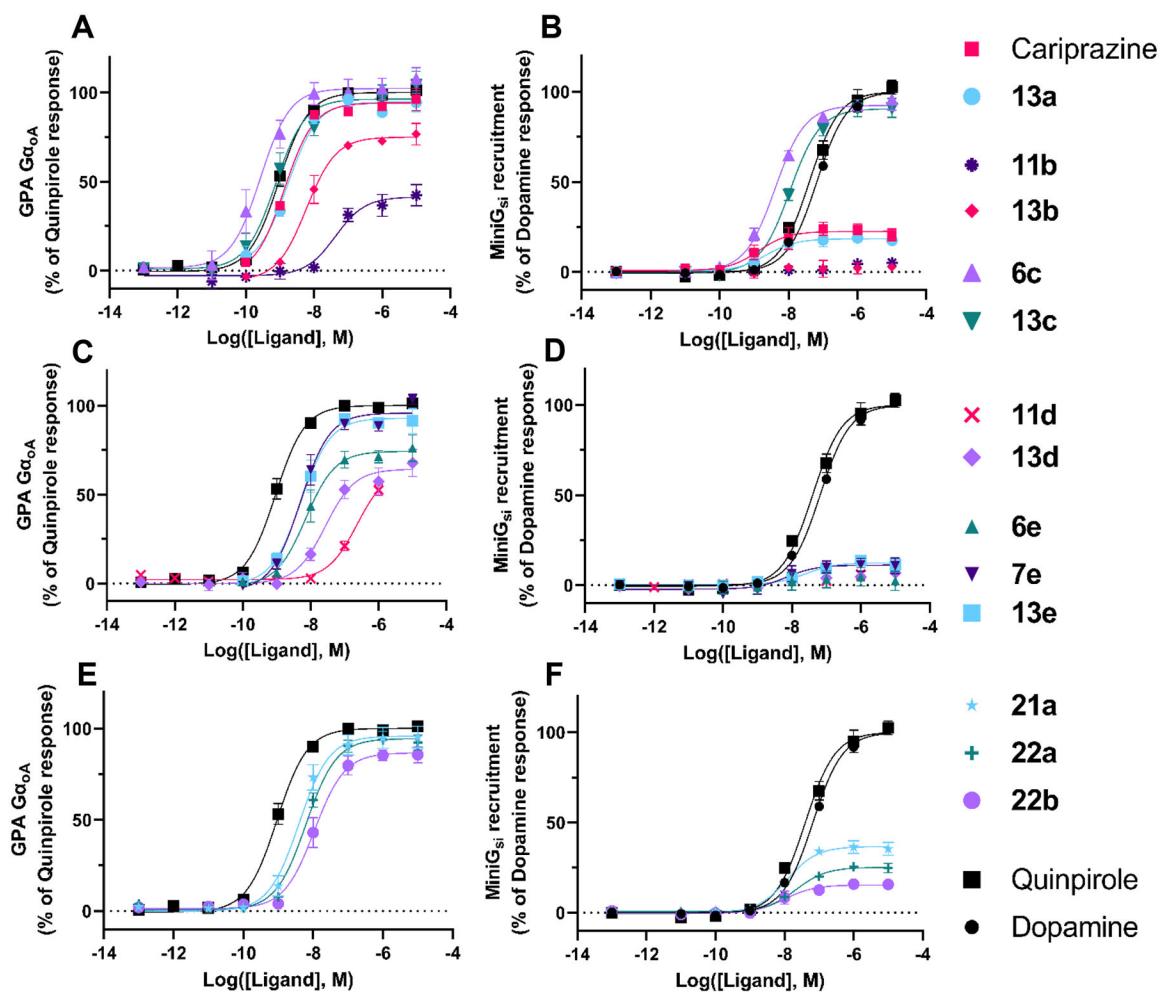


Figure 2. Agonism profiles at D₂R.

Two different BRET assays were used to assess D₂R activation: an amplified G α_{oA} G protein (GPA G α_{oA}) activation assay, shown on the left panels, and a less amplified miniG recruitment assay shown on the right panels. Each panel shows concentration response curves for a subset of the 14 selected ligands: 2,3-dichlorophenyl, 2-chloro-3-ethylphenyl, and 2-fluoro-3-methoxyphenyl compounds (A) GPA G α_{oA} and (B) miniG $_{Si}$; 2-trifluoromethyl substituted pyridine and 3-chloro-5-ethyl-2-methoxyphenyl compounds (C) GPA G α_{oA} and (D) miniG $_{Si}$; linker modified compounds (E) GPA G α_{oA} and (F) miniG $_{Si}$. Data points represent the mean \pm SEM of three independent experiments performed in duplicate.

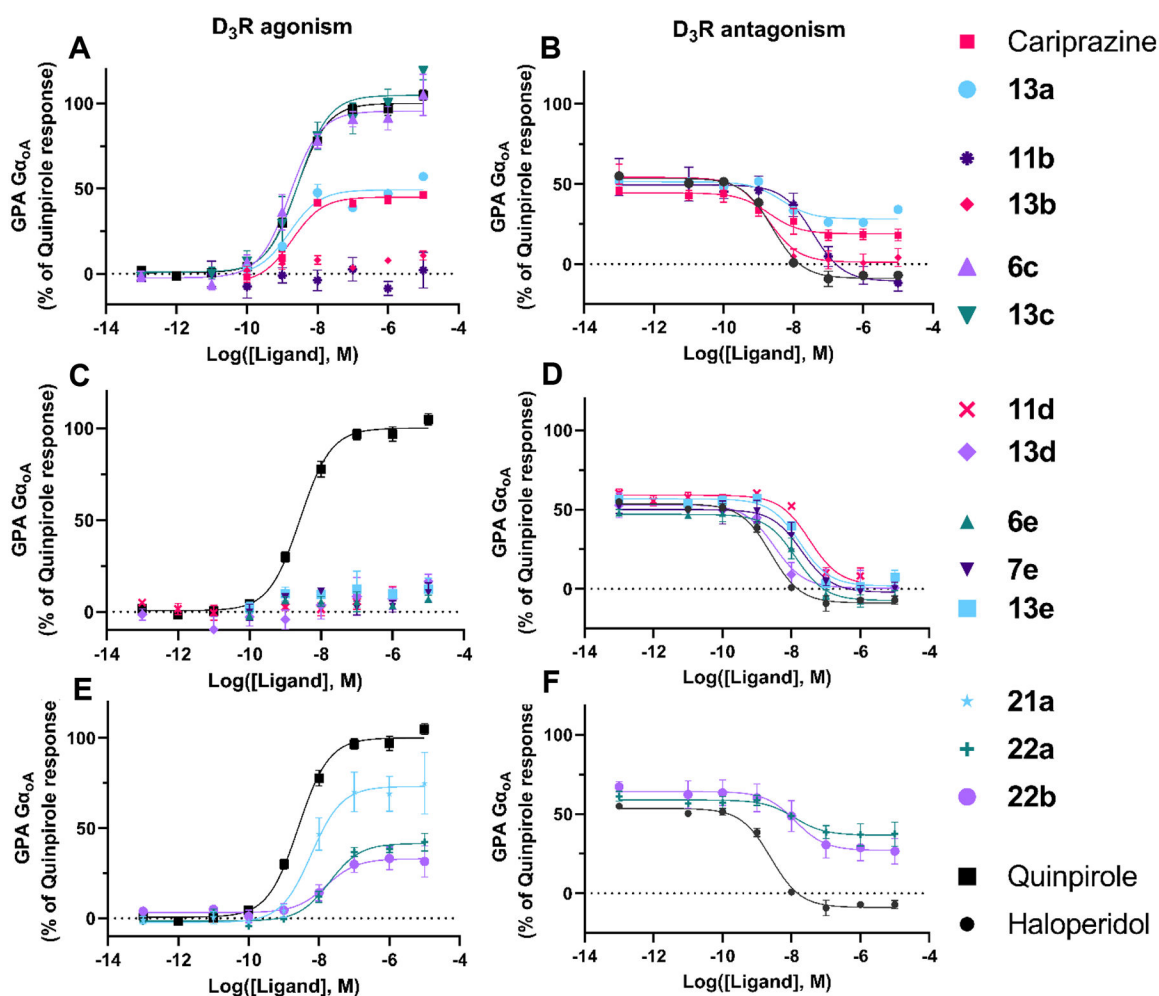


Figure 3. Functional profiles at the D₃R.

Using the $G\alpha_{oA}$ assay, all ligands were tested for D₃R agonism, shown on the left panels and 11 out of the 14 selected ligands were tested for D₃R antagonism (compounds were added to cells together with an EC₅₀ concentration (3 nM) of quinpirole), shown on the right panels. **6c**, **13c**, and **21a** signaled as robust D₃R agonists and were thus not tested as antagonists as they would not displace quinpirole signal. Each panel shows concentration response curves for a subset of the selected ligands: 2,3-dichlorophenyl, 2-chloro-3-ethylphenyl, and 2-fluoro-3-methoxyphenyl compounds (**A**) D₃R agonism and (**B**) D₃R antagonism; 2-trifluoromethyl substituted pyridine and 3-chloro-5-ethyl-2-methoxyphenyl compounds (**C**) D₃R agonism and (**D**) D₃R antagonism; linker modified compounds (**E**) D₃R agonism and (**F**) D₃R antagonism. Data points represent the mean \pm SEM of three independent experiments performed in duplicate.

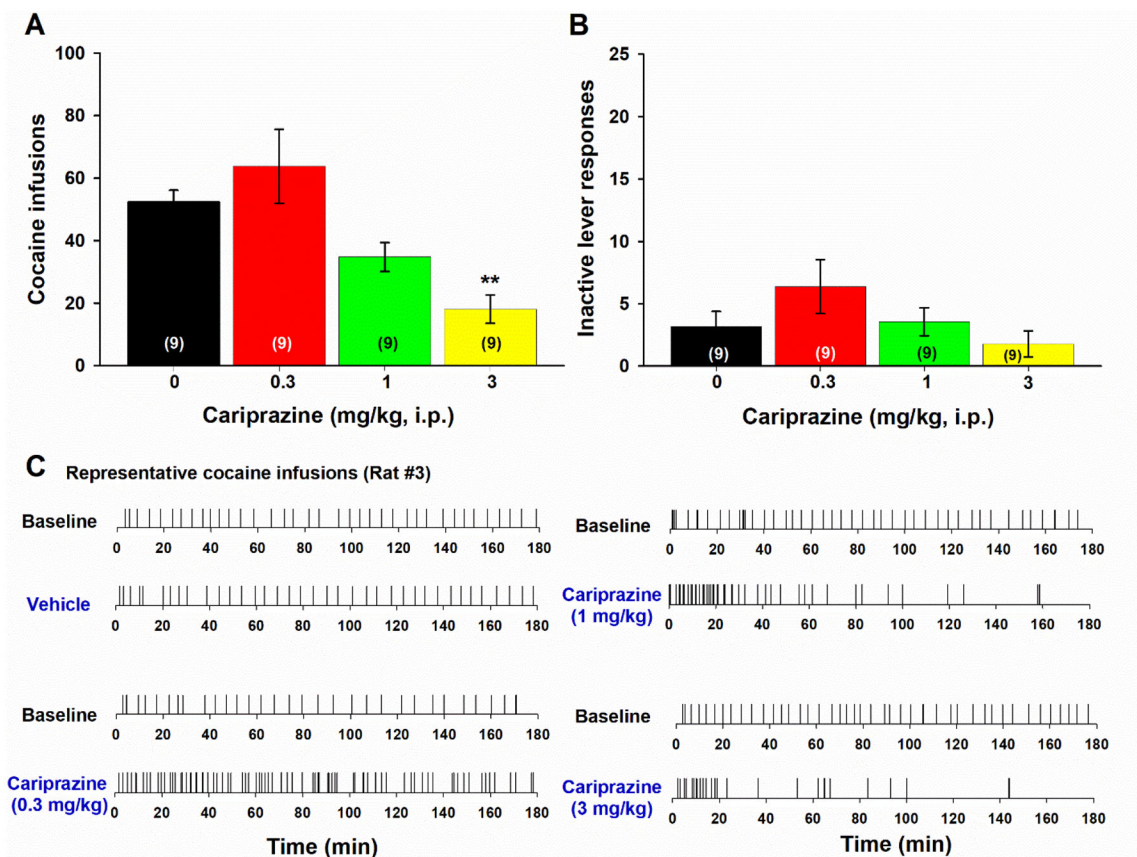


Figure 4. Dose-dependent effects of cariprazine on cocaine self-administration in rats. (A) The dose-dependent effects of cariprazine on cocaine self-administration (infusions). (B) Effects of cariprazine on inactive lever presses. (C) Representative cocaine self-administration (infusions) records, illustrating the typical extinction-like patterns of drug taking and drug seeking—lower doses of cariprazine (0.3 mg/kg) increased, while at higher doses it produced an initial burst-like drug infusions followed by cessation of drug self-administration. * $p < 0.05$, ** $p < 0.01$, compared to vehicle (0 mg/kg).

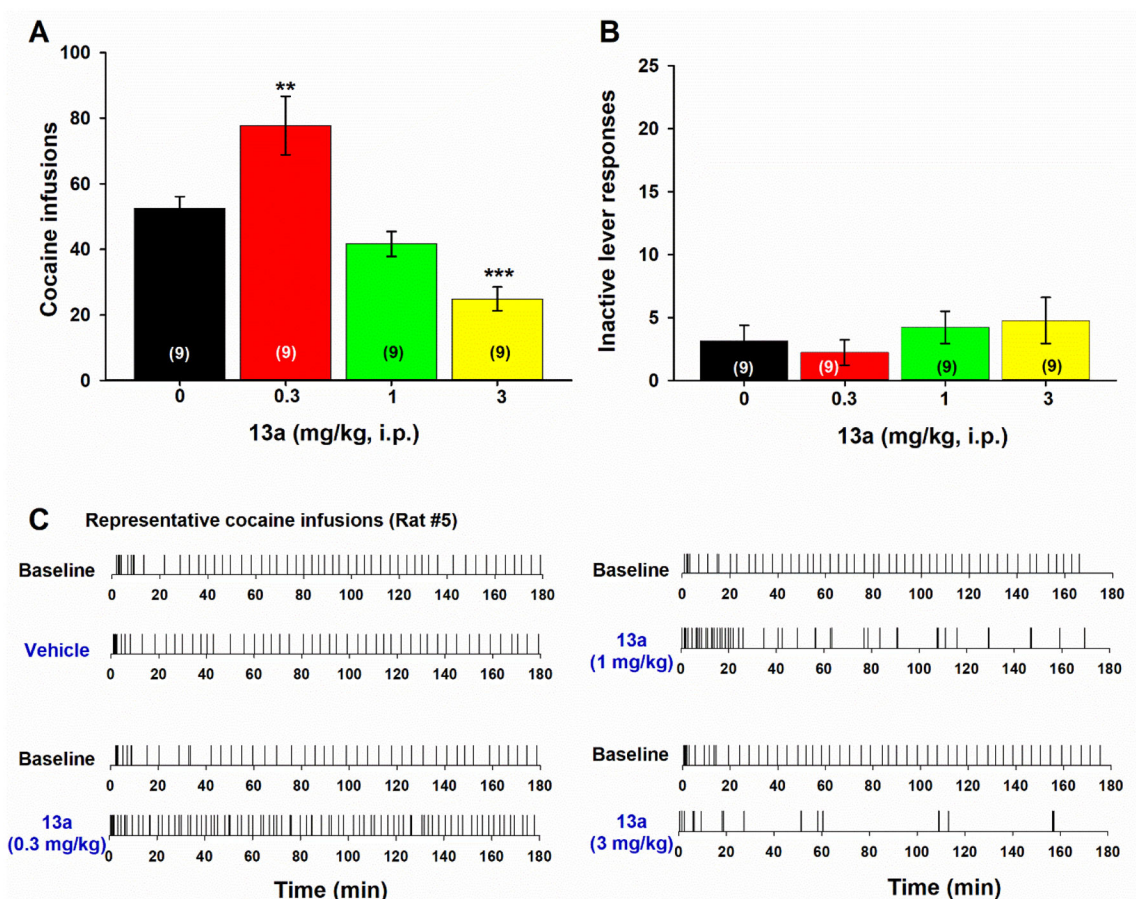


Figure 5. Dose-dependent effects of 13a on cocaine self-administration.

(A) Mean numbers after different doses of **13a** administration. (B) Mean numbers of inactive lever presses after different doses of **13a** pretreatments. (C) Representative cocaine infusions behavior indicating an extinction-like pattern of cocaine self-administration after **13a** administration in a way similar to cariprazine. (* $p < 0.05$, ** $p < 0.01$, *** $p < 0.001$, compared to the vehicle control group).

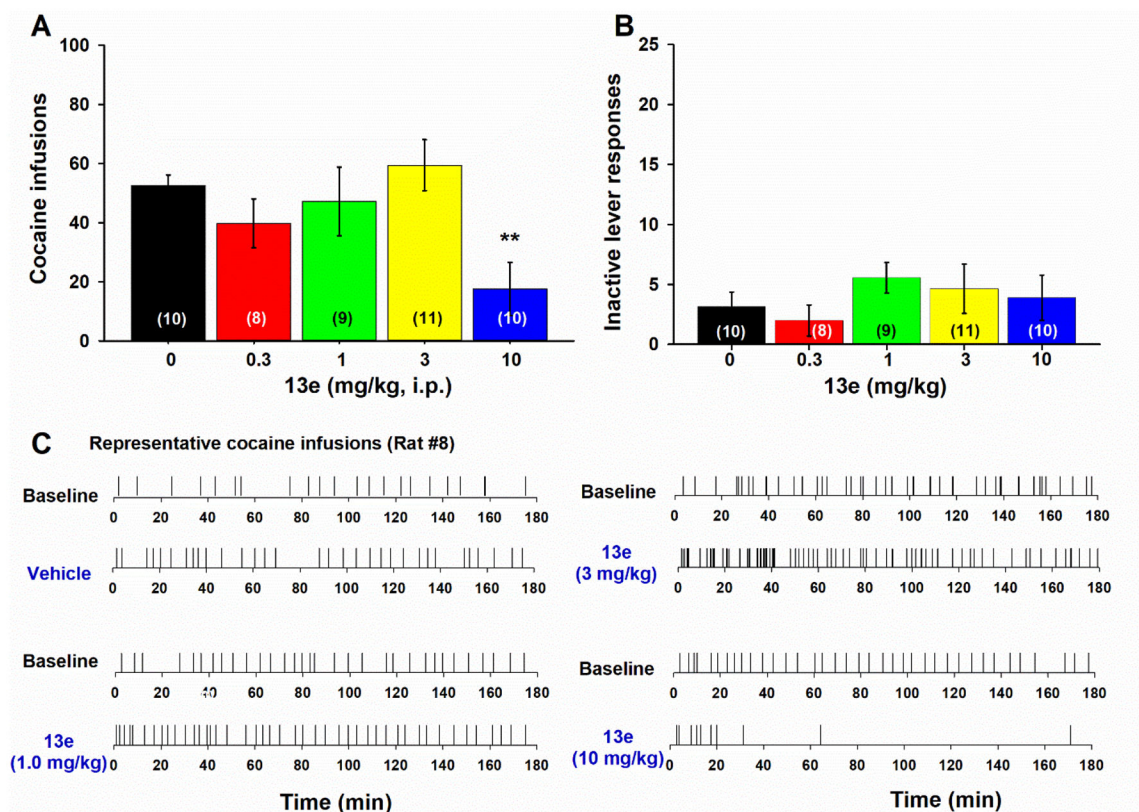
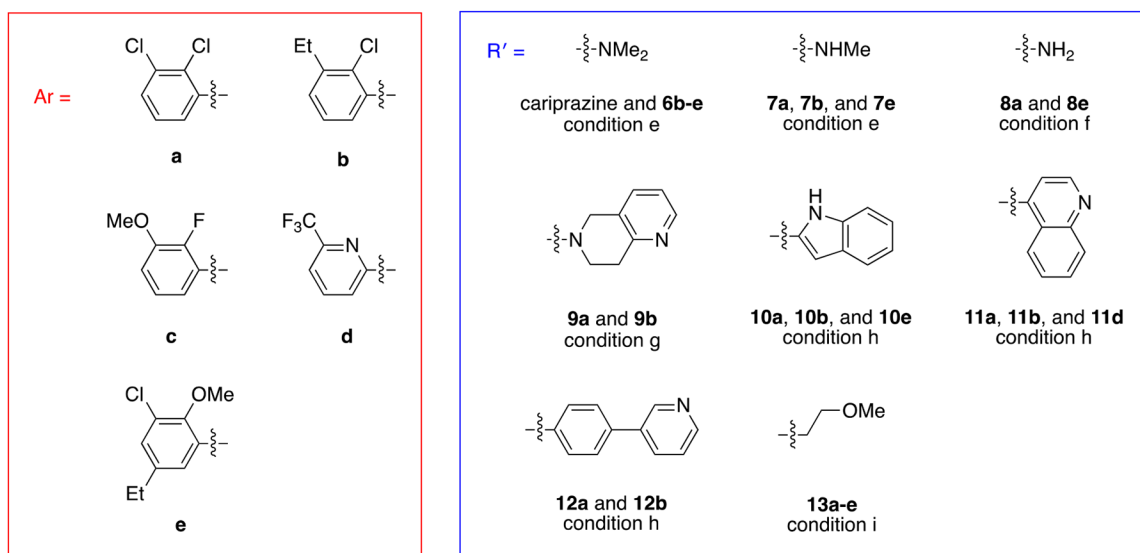
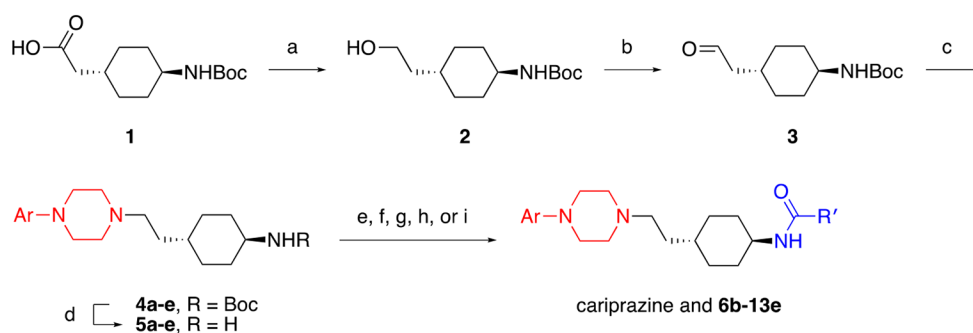
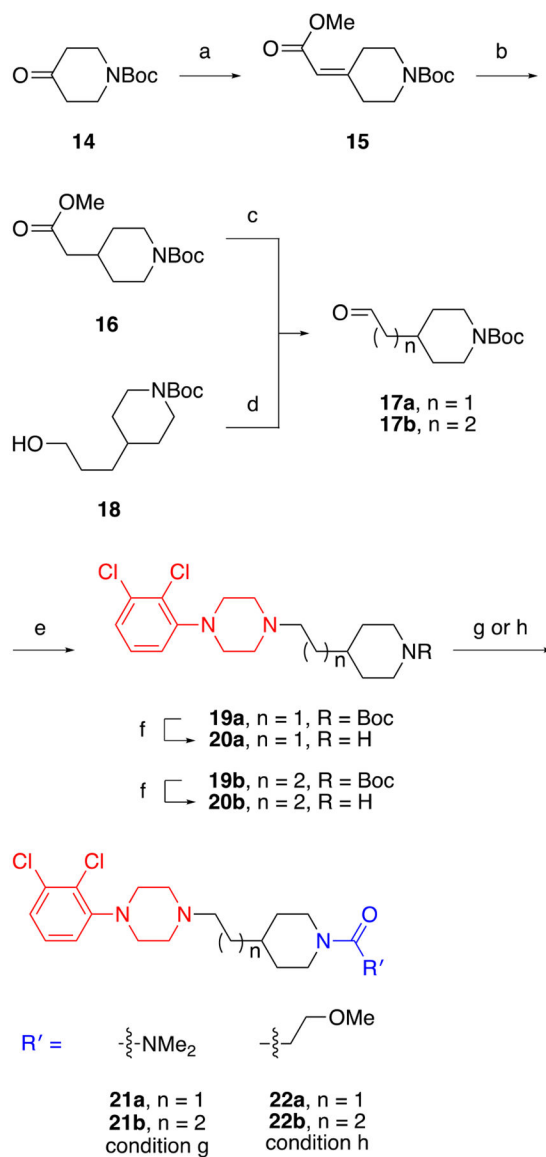


Figure 6. Dose-dependent effects of 13e on cocaine self-administration.

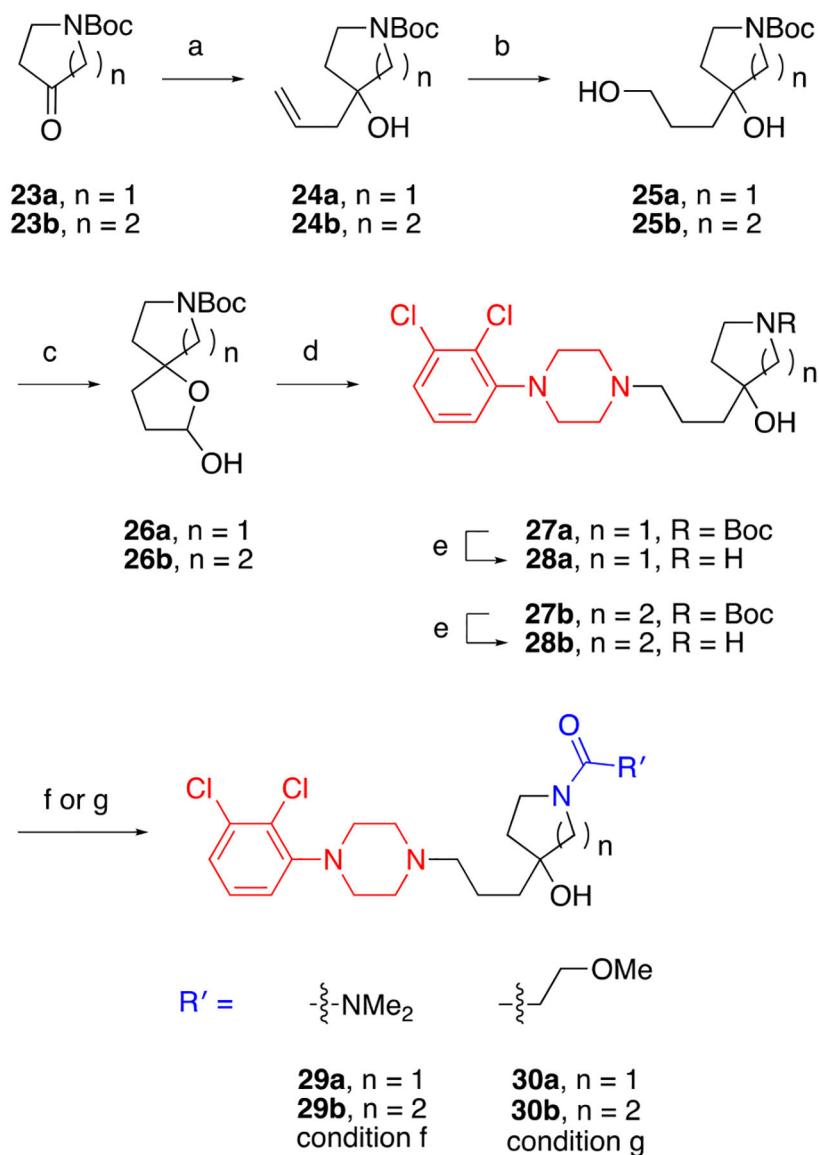
(A) Mean number of self-infusions after different doses of 13e. (B) Mean numbers of inactive lever presses 13e pretreatments. (C) Representative cocaine infusions illustrating the patterns of cocaine self-administration after vehicle or 13e administration. (* $p < 0.05$; ** $p < 0.01$, compared to the vehicle control group).

**Scheme 1.**Synthesis of cariprazine and its derivatives^a

^a Reagents and Conditions: (a) BMS, THF, 0 °C to rt; (b) DMSO, (COCl)₂, NEt₃, DCM, -78 °C to rt; (c) aryl piperazine, NaBH(OAc)₃, DCE, rt; (d) TFA, DCM, rt; (e) N,N-dimethyl- or N-methylcarbonyl chloride, DIPEA, DCM, rt; (f) KOCN, HCl, H₂O, THF, rt; (g) COCl₂, NEt₃, toluene, THF, 0 °C, then 5,6,7,8-tetrahydro-1,6-naphthyridine, THF, 0 °C to rt; (h) carboxylic acid, EDCI, HOBT, DIPEA, CHCl₃, rt; (i) 3-methoxypropionic acid, HCTU, DIPEA, DCM, rt.

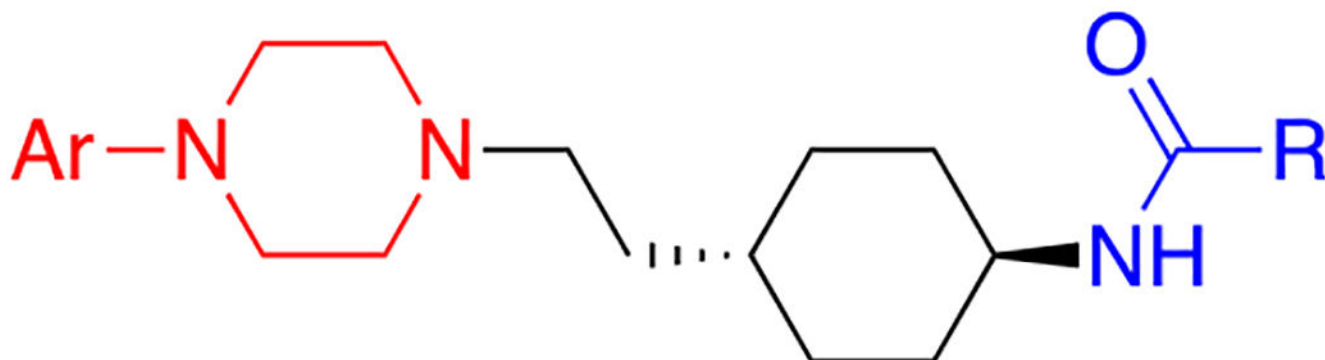
**Scheme 2.**Routes to linker modified cariprazine analogues^a

^a Reagents and Conditions: (a) NaH, methyl 2-(dimethoxyphosphoryl)acetate, THF, 0 °C to rt; (b) Pd/C, H₂ (50 psi), MeOH, rt; (c) DIBALH, toluene, DCM, -78 °C to rt; (d) DMSO, (COCl)₂, NEt₃, DCM, -78 °C to rt; (e) 1-(2,3-dichlorophenyl)piperazine•HCl, NaBH(OAc)₃, DCE, rt; (f) TFA, DCM, rt; (g) *N,N*-dimethylcarbamyl chloride, DIPEA, DCM, rt; (h) 3-methoxypropionic acid, HCTU, DIPEA, DCM, rt.

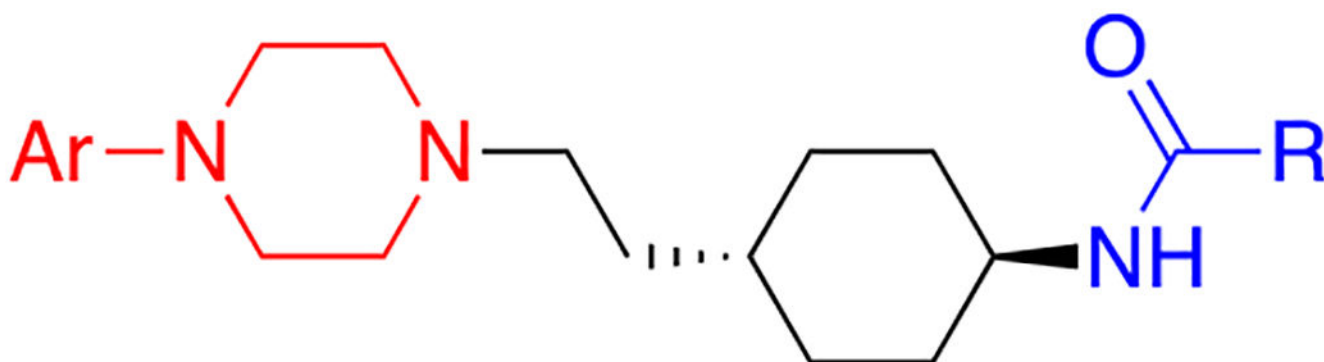
**Scheme 3.**Preparation of compounds bearing a hydroxyl group within the linker^a

^a Reagents and Conditions: (a) allyl magnesium bromide, Et₂O, 0 °C to rt; (b) BH₃•THF, THF, 0 °C to rt, then NaOH, H₂O₂, H₂O, 0 °C to rt; (c) DMSO, (COCl)₂, NEt₃, DCM, -78 °C to rt; (d) 1-(2,3-dichlorophenyl)piperazine•HCl, NaBH(OAc)₃, DCE, rt; (e) TFA, DCM, rt; (f) *N,N*-dimethylcarbamyl chloride, DIPEA, DCM, rt; (g) 3-methoxypropionic acid, HCTU, DIPEA, DCM, rt.

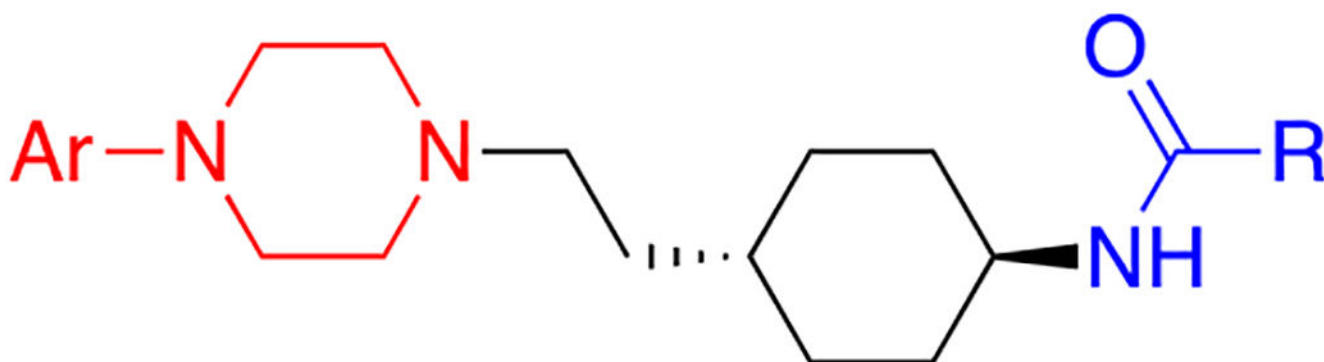
Table 1.

D₃R and D₂R binding affinities of cariprazine and its analogues.^a

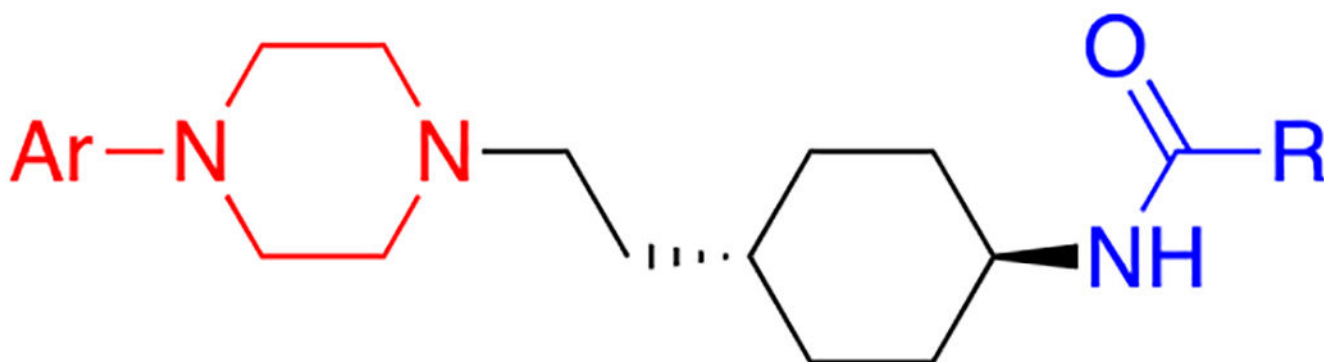
compound	Ar	R	MPO	$K_i \pm \text{SEM (nM)}$		$\text{D}_2\text{R } K_i / \text{D}_3\text{R } K_i$
				D_2R	D_3R	
4a		-Ot-Bu	2.8	8.2 ± 2.6	2.13 ± 0.85	3.8
cariprazine		-NMe ₂	3.6	0.78 ± 0.17	0.22 ± 0.06	3.6
7a		-NHMe	3.5	1.21 ± 0.06	0.21 ± 0.02	5.7
8a		-NH ₂	3.8	1.49 ± 0.03	0.26 ± 0.10	5.7
9a		-N-indole-2-yl	2.8	1.86 ± 0.06	0.36 ± 0.05	5.1
10a		-NH-indole-3-yl	2.5	6.5 ± 1.9	0.31 ± 0.10	21



compound	Ar	R	MPO	$K_i \pm \text{SEM (nM)}$		$\text{D}_2\text{R } K_i / \text{D}_3\text{R } K_i$
				D_2R	D_3R	
11a			2.8	29 ± 13	0.66 ± 0.28	44
12a			2.8	3.75 ± 0.65	0.59 ± 0.13	6.4
13a			3.6	2.85 ± 0.63	0.14 ± 0.05	20
6b			3.5	0.75 ± 0.07	0.26 ± 0.03	2.9
7b			3.4	0.48 ± 0.11	0.18 ± 0.01	2.6
9b			2.8	0.87 ± 0.08	0.29 ± 0.08	3.0
10b			2.5	7.8 ± 1.9	1.31 ± 0.46	6.0



compound	Ar	R	MPO	$K_i \pm \text{SEM (nM)}$		$D_2R K_i / D_3R K_i$
				D_2R	D_3R	
11b			2.8	5.76 ± 0.93	0.34 ± 0.06	17
12b			2.8	1.80 ± 0.34	0.58 ± 0.07	3.1
13b			3.5	1.78 ± 0.18	0.25 ± 0.04	7.1
6c			5.2	134 ± 17	9.4 ± 1.2	14
13c			5.1	479 ± 26	1.31 ± 0.02	370
6d			4.7	26.7 ± 5.4	2.38 ± 0.54	11
11d			2.6	162 ± 48	1.00 ± 0.08	160



compound	Ar	R	MPO	$K_i \pm \text{SEM}$ (nM)		$D_2R K_i / D_3R K_i$
				D_2R	D_3R	
13d			4.6	127 ± 14	1.06 ± 0.08	120
4e			3.1	68.1 ± 4.3	38.8 ± 3.0	1.8
6e			3.4	4.12 ± 0.17	1.76 ± 0.11	2.3
7e			3.3	5.8 ± 1.3	0.64 ± 0.10	9.1
8e			3.5	5.3 ± 1.8	0.78 ± 0.28	6.8
10e			2.3	114 ± 36	1.03 ± 0.26	110
13e			3.3	15.2 ± 2.0	0.73 ± 0.16	21

^a K_i values are derived from IC₅₀ values using the Cheng-Prusoff equation,⁵⁰ and calculated as the mean of at least three independent experiments.

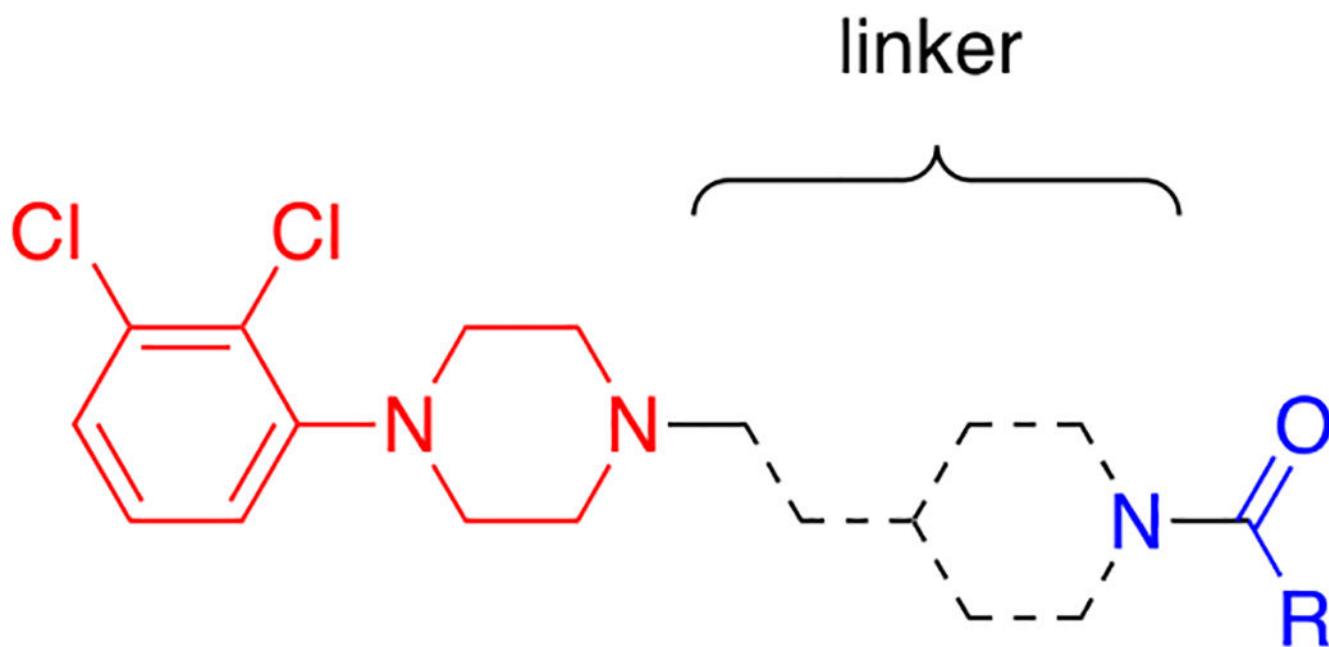
The radioligand used in these assays was [³H]-*N*-methylspiperone.

Table 2.

D₃R and D₂R binding affinities of linker modified compounds.^a

linker

compound	linker	R	MPO	$K_i \pm \text{SEM (nM)}$		$\frac{D_2R K_i}{D_3R K_i}$
				D ₂ R	D ₃ R	
21a			3.9	20.5 ± 2.1	1.02 ± 0.10	20
22a			4.4	86 ± 28	3.5 ± 1.3	25
21b			3.4	7.2 ± 1.1	1.86 ± 0.10	3.9
22b			3.7	19.4 ± 2.6	0.96 ± 0.05	20
29a			5.3	89.8 ± 5.9	29.5 ± 3.7	3.0



compound	linker	R	MPO	$K_i \pm \text{SEM (nM)}$		$\frac{D_2R K_i}{D_3R K_i}$
				D_2R	D_3R	
30a			5.1	175 ± 19	18.7 ± 2.5	9.4
29b			5.0	38.4 ± 5.2	50.7 ± 5.7	0.76
30b			5.1	125 ± 27	27.5 ± 3.3	4.5

^a K_i values are derived from IC_{50} values using the Cheng-Prusoff equation,⁵⁰ and calculated as the mean of at least three independent experiments. The radioligand used in these assays was [³H]-*N*-methylspiperone.

Table 3.

The maximal effects (E_{\max}) and potencies (EC_{50}) of compounds determined in two assays of D₂R activation.^a

compound	D ₂ R GPA Gα _{oA}			D ₂ R mini G _{si} recruitment		
	pEC ₅₀ ± SEM	EC ₅₀ (nM)	E _{max} ± SEM (%)	pEC ₅₀ ± SEM	EC ₅₀ (nM)	E _{max} ± SEM (%)
cariprazine	8.87 ± 0.08	1.35	94.2 ± 1.7	8.87 ± 0.28	1.34	22.5 ± 1.7
13a	8.77 ± 0.10	1.70	94.7 ± 2.2	8.65 ± 0.27	2.26	18.4 ± 1.4
11b	7.37 ± 0.19	42.60	41.4 ± 3.0	ND	ND	ND
13b	8.22 ± 0.10	5.98	75.0 ± 2.3	ND	ND	ND
6c	9.57 ± 0.15	0.27	102.3 ± 3.6	8.39 ± 0.06	4.10	92.4 ± 1.6
13c	9.13 ± 0.13	0.75	96.4 ± 3.3	7.96 ± 0.06	11.02	90.6 ± 2.0
11d	<7	>100	<60%	ND	ND	ND
13d	7.57 ± 0.15	27.12	64.3 ± 3.2	ND	ND	ND
6e	8.14 ± 0.14	7.18	74.3 ± 3.1	ND	ND	ND
7e	8.30 ± 0.11	5.00	95.9 ± 2.9	8.15 ± 0.43	7.08	11.1 ± 1.9
13e	8.28 ± 0.11	5.22	93.0 ± 2.9	7.58 ± 0.21	26.21	12.5 ± 0.9
21a	8.40 ± 0.10	3.97	95.9 ± 2.8	7.93 ± 0.12	11.86	36.7 ± 1.5
22a	8.20 ± 0.06	6.28	94.5 ± 1.9	7.66 ± 0.11	21.85	25.1 ± 0.9
22b	7.96 ± 0.08	10.89	86.7 ± 2.4	8.00 ± 0.18	9.92	15.4 ± 1.0
Quinpirole	9.03 ± 0.05	0.93	100.1 ± 1.3	7.40 ± 0.08	39.78	100.0 ± 2.7
Dopamine	-	-	-	7.18 ± 0.03	66.25	99.9 ± 1.1

^aCompounds were tested in an amplified Gα_{oA} G protein (GPA Gα_{oA}) activation assay, shown on the left columns, and a less amplified miniG recruitment assay, shown on the right columns. ND indicates no agonist response detected, '-' indicates compound not tested. Data represent the mean ± SEM of three independent experiments performed in duplicate.

Table 4.

The maximal effects (E_{\max}) and potencies (EC_{50} and IC_{50}) of compounds determined in an assay of D_3R activation.^a

compound	D ₃ R GPA Gα _{oA} agonism			D ₃ R GPA Gα _{oA} antagonism	
	pEC ₅₀ ± SEM	EC ₅₀ (nM)	E _{max} ± SEM (%)	pIC ₅₀ ± SEM	IC ₅₀ (nM)
cariprazine	8.72 ± 0.14	1.89	45.1 ± 1.6	8.70 ± 0.32	2.02
13a	8.80 ± 0.20	1.60	49.3 ± 2.3	8.34 ± 0.23	4.62
11b	ND	ND	ND	7.44 ± 0.25	36.00
13b	ND	ND	ND	8.73 ± 0.16	1.87
6c	8.79 ± 0.14	1.64	95.4 ± 3.8	-	-
13c	8.54 ± 0.16	2.87	104.8 ± 4.8	-	-
11d	ND	ND	ND	7.47 ± 0.15	33.63
13d	ND	ND	ND	8.49 ± 0.24	3.21
6e	ND	ND	ND	7.87 ± 0.13	13.41
7e	ND	ND	ND	7.70 ± 0.19	19.85
13e	ND	ND	ND	7.76 ± 0.13	17.45
21a	8.22 ± 0.20	6.07	73.2 ± 4.9	-	-
22a	7.70 ± 0.13	19.91	41.5 ± 1.9	7.92 ± 0.35	12.12
22b	7.80 ± 0.28	16.02	33.0 ± 2.9	7.89 ± 0.37	12.93
Quinpirole	8.59 ± 0.06	2.59	100.1 ± 1.7	-	-
Haloperidol	-	-	-	8.60 ± 0.08	2.54

^aCompounds were tested in an amplified Gα_{oA} G protein (GPA Gα_{oA}) activation assay as agonists and antagonists. ND indicates no agonist response detected, '-' indicates compound not tested. Data represent the mean ± SEM of three independent experiments performed in duplicate.

Table 5.Off-target binding affinities of cariprazine-based analogues.^a

compound	$K_i \pm \text{SEM}$ (nM)					
	D_1R^b	D_4R^c	5-HT _{1A} ^d	5-HT _{2A} ^e	5-HT _{2B} ^e	5-HT _{2C} ^e
cariprazine	2920 ± 300	233 ± 20	1.81 ± 0.46	568 ± 72	0.151 ± 0.023	221.1 ± 8.0
11a	>3160	1390 ± 480	184 ± 25	1810 ± 640	1.99 ± 0.62	644 ± 58
13a	4600 ± 400	756 ± 63	6.0 ± 1.8	54 ± 15	1.47 ± 0.36	252 ± 64
11b	5390 ± 730	417 ± 40	75 ± 25	15.1 ± 4.8	1.27 ± 0.39	253 ± 86
13b	6800 ± 480	342 ± 15	7.7 ± 1.8	20.8 ± 6.9	1.71 ± 0.43	34.0 ± 8.1
6c	>10000	1257 ± 23	33.8 ± 5.9	>10000	34.2 ± 9.3	>10000
13c	>10000	734 ± 16	69.9 ± 1.7	>10000	29.6 ± 9.5	>10000
11d	>3160	1790 ± 430	22.3 ± 6.4	1450 ± 340	18.8 ± 6.2	5800 ± 1300
13d	>10000	2520 ± 170	9.6 ± 2.6	4420 ± 340	11.3 ± 2.2	3170 ± 200
6e	>10,000	2434 ± 87	45.4 ± 9.0	680 ± 200	7.3 ± 1.9	1062 ± 86
7e	8000 ± 1100	1346 ± 29	54.9 ± 4.2	207 ± 74	6.2 ± 1.5	162 ± 48
13e	>10,000	1870 ± 240	108 ± 11	158 ± 45	5.8 ± 1.7	800 ± 280

^aData were obtained through the NIDA Addiction Treatment Discovery Program Contract (ADA12013) with Oregon Health & Science University. The radioligands used in these assays were

^b[³H]-SCH23390,

^c[³H]-spiperone,

^d[³H]-8-OH-DPAT, and

^e[³H]5-HT.